



SCHOOL of
GRADUATE STUDIES
EAST TENNESSEE STATE UNIVERSITY

East Tennessee State University
**Digital Commons @ East
Tennessee State University**

Electronic Theses and Dissertations

Student Works

12-2011

Using Geographical Information Systems to Investigate Spatial Patterns in Fossils of *Tapirus polkenis* from the Gray Fossil Site, Washington County, Tennessee

Winn Addison Ketchum
East Tennessee State University

Follow this and additional works at: <https://dc.etsu.edu/etd>

 Part of the [Earth Sciences Commons](#)

Recommended Citation

Ketchum, Winn Addison, "Using Geographical Information Systems to Investigate Spatial Patterns in Fossils of *Tapirus polkenis* from the Gray Fossil Site, Washington County, Tennessee" (2011). *Electronic Theses and Dissertations*. Paper 1227. <https://dc.etsu.edu/etd/1227>

This Thesis - Open Access is brought to you for free and open access by the Student Works at Digital Commons @ East Tennessee State University. It has been accepted for inclusion in Electronic Theses and Dissertations by an authorized administrator of Digital Commons @ East Tennessee State University. For more information, please contact digilib@etsu.edu.

Using Geographical Information Systems to Investigate Spatial Patterns in Fossils of
Tapirus polkenis from the Gray Fossil Site, Washington County, Tennessee

A thesis
presented to
the faculty of the Department of Geosciences
East Tennessee State University

In partial fulfillment
of the requirements for the degree
Master of Science in Geosciences

by
Winn Addison Ketchum
December 2011

Steven C. Wallace, Chair
Chunhua (Daniel) Zhang
Michael J. Whitelaw

Keywords: tapirs, geographic information systems, Gray Fossil Site, spatial patterns

ABSTRACT

Using Geographical Information Systems to Investigate Spatial Patterns in Fossils of *Tapirus polkensis* from the Gray Fossil Site, Washington County, Tennessee

by

Winn Addison Ketchum

Discovered in 2000, the Gray Fossil Site provides a snapshot of the flora and fauna that lived during late Miocene to early Pliocene time in eastern Tennessee. These fossils occur in sediments consisting of fine-grained clays and sands of lacustrine origin, which were deposited after multiple sinkholes formed in the underlying Knox Group basement carbonates. Three-dimensional nearest neighbor analysis has been applied to fossils of *Tapirus polkensis*, characterizing the spatial patterns exhibited. These analyses determined the importance of taphonomic and depositional processes that occurred during the sites formation. Six characteristics were analyzed, four at the bone level including carnivore utilization, weathering, abrasion, and arthritis, and two at the specimen level, articulation and age class. Weathering, arthritis, and articulation, show clustered patterns indicating that the site had active predators, it consisted of many microenvironments, and deposition occurred in a passive setting. Although the current state of excavation makes any spatial analyses and taphonomic interpretations difficult, spatial analysis in both dimensions can be accomplished.

ACKNOWLEDGEMENTS

I would like to thank the following people for their continued help and advisement during the completion of this project and degree: Dr. Steven Wallace for his advisement on paleontological and taphonomic issues as they pertained to my work; Drs. Ke (Catherine) Chen and Chunhua (Daniel) Zhang for their help in understanding key GIS principles and techniques; Dr. Mick Whitelaw for his support as a friend and in providing me with the data needed to create not only a highly accurate and detailed surface model for the Gray Fossil Site, but also the TDOT data used to create a lower boundary of the site; Dr. Jim Mead for his help in providing me with the best education and experience possible here at ETSU and as a mentor/friend; Crystal Nelson for making sure that all paperwork and forms were filed on time and in correct order; Brian Compton for acquiring the spatial data used in this study as well as fixing any problematic survey data; April Nye and Brett Woodward for access to collections and their informative knowledge of various taphonomic indicators and processes; Sandy Swift for her aid in taking photos of important *Tapirus polkensis* bones at the fossil site; William Huber, Lauren Scott, and others on the ArcGIS Resource forums for their experience and help in understanding key principles of the software and analysis used in this study; Dr. Donald Sanderson, may he rest in peace, for his exceptional ability to work with my inexperience of basic database and programming principles; Matt Gibson, Patrick Hawkins, and Aaron Abernathy for their knowledge of tapir behavior and ecology, plus other fellow graduate students here at ETSU for their knowledge of key biological and paleontological ideas. Also, of course my friends and family were critical in supporting my needs and allowing me to vent my frustrations when this project weighed too heavy upon my shoulders.

CONTENTS

	Page
ABSTRACT.....	2
ACKNOWLEDGEMENTS.....	3
LIST OF TABLES.....	7
LIST OF FIGURES.....	8
LIST OF ABBREVIATIONS.....	10
Chapter	
1. INTRODUCTION.....	11
2. BACKGROUND.....	14
The Gray Fossil Site.....	14
Geographical Information Systems.....	14
3D GIS.....	15
GIS and Paleontology-Archaeology.....	16
Spatial Databases.....	17
Nearest Neighbor Statistic.....	18
Taphonomy.....	19
Carnivore Utilization.....	21
Weathering.....	22
Abrasion.....	23
Arthritis.....	24
Articulation.....	25
Age Class.....	25

<i>Tapirus</i>	26
3. METHODOLOGY	28
Database Design.....	28
Bone Attributes	31
Specimen Attributes.....	36
Database Implementation.....	37
Data Entry	37
Creation of a Geodatabase	39
Displaying Point Features.....	39
Mean Center Calculation	40
Creating Each Attribute Layer	41
Nearest Neighbor Analysis	42
Importing Python Modules	42
Acquiring Parameters.....	43
Calculating Nearest Neighbor Distances	43
Calculating Nearest Neighbor Statistic and Outputs	44
Cartographic Output.....	45
4. RESULTS	47
Geodatabase	47
Nearest Neighbor Program and Qhull Calculations.....	50
Base Maps	52
Carnivore Utilization	56
Weathering	61

Abrasion	70
Arthritis	70
Articulation	77
Age Class	81
5. DISCUSSION	86
Methods	86
Classification Schemes	87
Nearest Neighbor Statistic	89
Issues with Extent of Current Excavation	91
Taphonomic Interpretations	92
Carnivore Utilization	92
Weathering	94
Abrasion	97
Arthritis	97
Articulation	98
Age Class	99
6. CONCLUSIONS	102
Taphonomic Interpretations	102
Future Work	103
Recommendations for the Gray Fossil Site	104
REFERENCES	106
APPENDIX: Python Script Used to Calculate Nearest Neighbor Statistic	119
VITA	121

LIST OF TABLES

Table	Page
1: Descriptions of each point's, bone's, and specimen's attributes in the SDBMS.....	30
2: Types of carnivore utilization.....	31
3: Weathering stages defined for tapirs at the Gray Fossil Site.....	32
4: Abrasion types and descriptions used to characterize tapir fossils.....	34
5: Descriptions of the various stages of arthritis.....	34
6: Random set of rows from the completed 'Points' Table.....	48
7: Random set of rows from the completed 'Bones' Table.....	49
8: Random set of rows from the completed 'Specimens' Table.....	50
9: Results of nearest neighbor analysis for original survey points, averaged bone locations, and averaged specimen locations.....	52
10: Nearest neighbor results for different types of carnivore utilization.....	56
11: Nearest neighbor results for different stages of weathering.....	62
12: Nearest neighbor statistics for the tapir bone arthritis levels.....	71
13: Nearest neighbor statistics for specimens from the three articulation states.....	77
14: Results of nearest neighbor tapir distribution by age class.....	81
15: 2D results for the NN statistic from the NN script used in this study and that of ESRI ArcGIS NN tool.....	91

LIST OF FIGURES

Figure	Page
1: Entity-relationship diagram of the SDBMS.....	29
2: Tapir bones showing sequence of weathering stages	33
3: Tapir bones showing sequence of arthritis levels	35
4: Qhull results for area of survey points.....	51
5: Qhull results for volume of survey points	51
6: Spatial distribution of the survey points from tapirs.....	53
7: Spatial distribution of the averaged point locations for each bone.....	54
8: Spatial distribution of the averaged point locations for each specimen	55
9: Bones of <i>Tapirus polkensis</i> that show sign of carnivore utilization	57
10: Spatial distribution of bones that exhibit puncturing marks	58
11: Spatial distribution of the bones that exhibit pitting marks	59
12: Spatial distribution of bones lacking evidence of carnivore utilization.....	60
13: Spatial distribution of bones with a weathering stage of 5	63
14: Spatial distribution of bones with a weathering stage of 4	64
15: Spatial distribution of bones with a weathering stage of 3	65
16: Spatial distribution of bones with a weathering stage of 2	66
17: Spatial distribution of bones with a weathering stage of 1	67
18: Spatial distribution of bones with a weathering stage of 0	68
19: Spatial distribution of bones with a weathering stage of -1	69
20: Spatial distribution of bones with extreme arthritis.....	72
21: Spatial distribution of bones with moderate arthritis.....	73

22: Spatial distribution of bones with minor arthritis	74
23: Spatial distribution of bones with very minor arthritis	75
24: Spatial distribution of bones with no arthritis.....	76
25: Spatial distribution of articulated specimens	78
26: Spatial distribution of semi-articulated specimens	79
27: Spatial distribution of isolated bone elements	80
28: Spatial distribution of adult specimens	82
29: Spatial distribution of sub-adult specimens	83
30: Spatial distribution of juvenile specimens	84
31: Spatial distribution of specimens that could not be classified by age.	85
32: Comparison of weathering stages found at the GFS and in Kenya	96
33: Comparison of age classes at the GFS with other mortality types	101

LIST OF ABBREVIATIONS

Institutional Abbreviations

ESRI, Environmental Systems Research Institute. **ETMNH**, East Tennessee State University and General Shale Brick Museum of Natural History, Gray, Tennessee. **ETSU**, East Tennessee State University. **GFS**, Gray Fossil Site. **NAIP**, National Agriculture Imagery Program. **TDOT**, Tennessee Department of Transportation.

Geographic and Computer Abbreviations

3D, three dimensions. **2D**, two dimensions. **CSV**, comma-separated values. **DBMS**, database management system. **ER**, entity-relationship. **FID**, feature identification. **GIS**, geographical information system. **GUI**, graphical user interface. **HARN**, High Accuracy Reference Network. **ID**, identification. **MS**, Microsoft. **NAD**, North American Datum. **NAVD**, North American Vertical Datum. **NN**, nearest neighbor. **POSIX**, portable operating system interface for unix. **R**, nearest neighbor ratio of observed to expected values. **RDBMS**, relational database management system. **SDBMS**, spatial database management system. **SQL**, structured query language. **TIN**, triangulated irregular network.

Paleontological and Morphological Abbreviations

D, deciduous upper tooth. **d**, deciduous lower tooth. **M**, upper molar. **m**, lower molar. **P**, upper premolar. **p**, lower premolar. **OA**, osteoarthritis.

CHAPTER 1

INTRODUCTION

Remains of the extinct tapir, *Tapirus polkensis*, discovered at the Gray Fossil Site (GFS) provide an excellent set of spatial data to help understand the formation and the taphonomic processes that acted upon this species and the other taxa found. Over 75 individual tapirs have been recovered (Hulbert et al. 2009) so far from the site and the majority of each specimen's bones were surveyed using very accurate and precise methods, making the tapir fossils an excellent set of spatial data for the purpose of this study. To determine which taphonomic processes were controls on the location and preservation of the tapir remains, a geographical information system (GIS) was developed. Four taphonomic indicators were observed and recorded for each tapir bone and two for each individual specimen. These include marks from carnivore utilization, weathering extent, type of abrasion, and degree of arthritis for each tapir bone element. In addition, age class and state of articulation for each tapir specimen were noted. By analyzing the spatial distribution of each taphonomic indicator and their respective levels, the importance of each process and its effect on the fossil assemblage were determined.

Developing a GIS to analyze the spatial distribution of bones at the GFS is important as it allows patterns to be identified, with such applications as Environmental Systems Research Institute (ESRI) ArcGIS, and quantified using spatial statistics. Computer systems allow this calculation to be carried out for vast amounts of data in cases where manual calculations are near impossible (Valentine and Peddicord 1967). As it is still early in the excavation process of the fossil site, creating a methodology now will allow time for this system to be developed, and any problems associated with it to be

worked out before the entire site is excavated. Spatial statistics and analysis of objects in 3-dimensions is still a relatively new field in GIS, and therefore few analysis techniques exist. This makes work done at the GFS very important for furthering GIS capabilities. Moreover, development of an extensive database, not only for tapirs but other taxa found at the GFS, will provide a means to better understand connections and correlations (data mining) between different processes, whether taphonomic or ecologic. Lastly, little is known about modern tapirs in the wild, so study of the population dynamics of *T. polkensis* will provide more insight into the ecology and behavior of this elusive genus.

Patterns detected using the methods developed here will allow the effects of taphonomic processes to be discerned from those that result from the habitat that the GFS represents. As Wallace (2004) illustrates, using “modern surveying techniques and GIS analysis are essential” to understanding the “precise spatial relationships of every fossil” in the taphonomic reconstruction of the GFS and the interpretation of its deposits. Many questions can be answered from the data collected in this study that will paint a picture of how the site was formed. These questions include: To what extent did predation occur and which predators or scavengers were dominant or present? Do the weathering stages represent a homogenous environment consistent over the entire site or were there multiple microenvironments? How long were carcasses exposed before being buried? What type of abrasive action occurred and are there any indications of transportation or water flow into or out of the lake? Was arthritis a major influence on other taphonomic processes such as predation? Were remains deposited during catastrophic event(s) or by attrition of a stable population? Did other taphonomic processes cause the disarticulation of specimens or was it merely due to decay of connective tissues? These and other

questions can be explored and answered through the use of GIS and nearest neighbor analysis.

CHAPTER 2

BACKGROUND

The Gray Fossil Site

The GFS, located in Gray, Tennessee was discovered by the Tennessee Department of Transportation (TDOT) during a Highway 75 rerouting project in 2000 (Parmalee et al. 2002). The deposit formed in multiple (~ 11) paleo-sinkholes in Knox Group carbonates (Whitelaw et al. 2009). Site occurs in lacustrine fill composed of alternating fine-grained clays and sands (Wallace and Wang 2004, Shunk et al. 2006) of late Miocene to early Pliocene age. It has a rich fossil assemblage that includes tapirs, rhinoceroses, short-faced bears, camels, various birds, alligator, turtles, salamanders, and fish (Wallace and Wang 2004). Presence of alligators, turtles, salamanders, and fish all support the paleo-lake interpretation as the environment of deposition (Wallace and Wang 2004, Schubert and Wallace 2006). The location of fossils excavated from the site were surveyed by a very accurate and precise method, with x ,y , and z-coordinates measured using total stations and referenced to the Tennessee State Plane HARN (High Accuracy Reference Network) system (Nave et al. 2005). Each bone was then given an alphanumeric field number and an East Tennessee State University and General Shale Brick Museum of Natural History (ETMNH) number for storage in the collections (Nave et al. 2005).

Geographical Information Systems

A geographical information system (GIS) is a computer based system designed specifically to store, process, analyze, and present geographically referenced data (Worboy and Duckham 2004). First developed in the early 1960s, GISs have been used

to study natural and man-made systems by evaluating both an object's location and its attributes (Schon et al. 2009). A fundamental component of every GIS is a relational database that allows an organized and efficient approach for storing and retrieving either vector (points, lines, polygons) or raster (cell-based) geospatial data (Worboy and Duckham 2004). Storage of spatial data began with the development of non-topological representations known as shapefiles (Schon et al. 2009). This method was followed by coverages, where similar features are related with topology (mathematical and spatial relationships between features); and moved to modern approaches such as geo-databases, where multiple feature classes or types of data are stored and related in one location (Ellul and Haklay 2006; Schon et al. 2009). What makes a GIS powerful for studying spatial phenomena is its ability to recognize complex patterns inherent in the data that may otherwise go unnoticed with more conventional methods (Nigro et al. 2003).

3D GIS

Current advances in GIS allow the study of objects in true 3D, whereas in the past GIS was only designed to handle analysis of 2D features (Koller et al. 1995). Consequently, data from natural and man-made phenomena that might otherwise be lost if represented in 2D are retained using 3D GIS (Choi and Park 2006). With the addition of the z-value or elevation field, 2D objects can be adapted for 3D representation (Schon et al. 2009). Such 3D objects, where volume is an important characteristic, are built with a new feature class called multipatches (boundary-representations), developed by ESRI (Gold 2008; Katsianis et al. 2008). Spatial analysis and 3D functionality, however, are major challenges in developing 3D GIS as complex algorithms and complex computations are required (Katsianis et al. 2008; Lee 2008). Visualization of 3D data is

accomplished using ESRI ArcScene, a program capable of texture mapping, flyby viewing, 3D symbol utilization, and animation of vector and raster datasets (Zlatanova et al. 2002).

GIS and Paleontology-Archaeology

Little work has been undertaken in which GIS has been used to study paleontological or archaeological sites, with an even smaller number of studies implemented using 3D GIS (Kvamme 1995; Conroy 2006). Nigro et al. (2003) developed a method for the Swartkrans archaeological site in South Africa, in which excavated artifacts and remains were mapped in 3D. This overcame a major problem in GIS software, where at the time it could only represent objects in 2.5 dimensions with only 1 elevation value for each (latitude, longitude) point. Using modern 3D GIS software, Jennings and Hasiotis (2006) were able to implement ESRI ArcScene to map sauropod remains in the Upper Jurassic Morrison Formation in north-central Wyoming to differentiate between two different *Allosaurus* feeding sites. Katsianis et al. (2008) also used the ESRI ArcGIS software package to map artifacts from an archaeological site in Greece and were able to complete various spatial analyses, including nearest neighbor distances, which they used in other software packages to calculate the actual nearest neighbor statistic. Chew and Oheim (2009) implemented GIS to study the influence of two taphonomic biases, species richness and relative body size, in a vertebrate fossil assemblage in the Willwood Formation, central Bighorn Basin, Wyoming. They concluded that GIS was instrumental in determining species richness and that relative body size was dependent on the size of sampled area.

Spatial Databases

As stated previously, the key to organizing the vast amount of data collected in many studies involving GIS is an organizational system such as a database. A standard database management system (DBMS) is comprised of “software that controls the storage, organization, and retrieval of data” ensuring consistency and a reduction of redundancies that occur in file systems (Schon et al. 2009). Present versions of some DBMSs are known as relational database management systems (RDBMSs) because they allow relationships to be developed between various types of data (or entities) stored in the database (Cyran et al. 2010). As a majority of current data collected has some sort of spatial component (Schon et al. 2009), spatial database management system (SDBMS) began to be used, and as the name implies, allow storage of objects depicted in space, space itself, as well as conventional data (Guting 1994). As a software module, a SDBMS can work as both an object-relational and/or an objected-oriented database management system, with the major systems using an object-relational DBMS, such as Oracle Spatial in Oracle’s 11g release (Murray et al. 2010) and ESRI’s ArcGeodatabase (Schon et al. 2009). Standard SDBMSs support spatial data models, abstract data types (Gandhi et al. 2008), spatial data types, a query language for retrieval of stored data, and various algorithms to manipulate the stored data (Guting 1994). Current SDBMSs, such as those used in ArcGIS, can either be set up on personal computers, as personal or file geo-databases, or for use with enterprise databases like ESRI’s ArcSDE (Schon et al. 2009).

Nearest Neighbor Statistic

Spatial statistics provide tools to model and describe spatial patterns that aid in the assessment of trends and distributions that occur (Scott and Janikas 2010). The nearest neighbor (NN) statistic, as derived by Clark and Evans (1954), is used to quantify the degree and direction of distribution of individuals in a population away from that of a randomly distributed population. Also known as the R statistic, the NN statistic is calculated using the following equation ($R = r_{obs}/r_{exp}$), where the observed average nearest neighbor distance (r_{obs}) is divided by the expected average nearest neighbor distance (r_{exp}) (Wong and Lee 2005). Although the original equation was derived for plant populations in two-dimensional space, the equation can be adapted for objects in three-dimensional space (Clark and Evans 1954). The expected average nearest neighbor distance for 2D points is calculated using equation 1 and for 3D points with equation 2 (Clark and Evans 1979); where N is the number of individual points, V is the volume of the study site, and A is the area of the study site. The expected distance is equal to the average nearest neighbor distance for a randomly distributed set of points (Clark and Evans 1979). The value of R will determine if the observed population distribution is clustered, random, or dispersed, with $R < 1$ indicating a clustered pattern, $R \sim 1$ a random pattern, and $R > 1$ a dispersed pattern (Silk 1979). The null hypothesis for point patterns analyzed using this statistic is that the observed point pattern is significantly similar to the random point pattern. Rejecting the null hypothesis is only valid if the p-value (α) is less than 0.05, a value used in most statistical tests (Barber 1988). In order to calculate the p-value, the Z-value must first be calculated using the equation: $Z\text{-value} = (r_{obs} - r_{exp})/SE$ (Wong and Lee 2005), where the standard error (SE) is calculated using the following

equations developed by Clark and Evans (1979): equation 3 for 2D features and equation 4 for 3D features.

$$r_{\text{exp}} = 1.0 / (2 * ((N / A) ^ 0.5)) \quad (1)$$

$$r_{\text{exp}} = 0.55396 / ((N / V) ^ (1/3)) \quad (2)$$

$$\text{SE (2D)} = 0.261362 / ((N / A) ^ 0.5) \quad (3)$$

$$\text{SE (3D)} = (0.201335 * V ^ (1/3)) / N ^ (5/6) \quad (4)$$

In paleontology and archaeology the NN statistic is becoming more common among whole-site analyses. For example, a correlation between Pueblo home locations and arable land for sites in eastern New Mexico was established using NN analysis and found that over time home locations became more clustered around arable land (Washburn 1974). Bishop (2010) used spatial distribution and the NN statistic to understand self-organization and maturity of dune fields in the Ar Rub' al Khali sand sea and the dune field's response to changes in wind direction, sediment supply, and transportation capacity. Clapham et al. (2003) used the NN statistic to compare spatial patterning of epibenthic slope communities from the Neoproterozoic to similar modern communities and found that the ancient species had similar distribution patterns to those observed today.

Taphonomy

“Taphonomy” was first coined by Efremov (1940) and is derived from the Greek words taphos (burial) and nomos (laws) and is the study of the postmortem modification of fossils. In short, taphonomy refers to any process that occurs between the time an

organism dies until the time its remains are buried or embedded within the lithosphere (Lyman 1994). Three primary sub-disciplines within taphonomy are: necrolysis, the study of the death and decomposition of an individual; biostratinomy, the study of processes occurring after death and prior to burial; and fossil diagenesis studies or study of those processes that occur after remains are buried (Dodd and Stanton 1981; Brett and Baird 1986; Wilson 1988). Biostratinomy is dominated by mechanical processes, whereas fossil diagenesis is dominated by chemical processes (Brett and Baird 1986). Remains of postmortem organisms can also be classified as autochthonous, remains preserved and buried at the site of death; or allochthonous, remains that are preserved away from the site of death and outside the organism's natural habitat (Kidwell et al. 1986). The term parautochthonous may also be used to define remains that are buried away from the site of death but within the organism's habitat (Behrensmeyer and Hook 1992).

Understanding the taphonomic processes that impact fossil assemblages allows a better understanding of the environmental setting in which the bones were deposited (Brett and Baird 1986; Badgley et al. 1995; Behrensmeyer et al. 2000). The depositional environment, in turn, determines the quality of preservation, number of specimens recovered, and taxonomic resolution; thus creating sampling biases that must be identified before the paleoecology can be accurately interpreted (Badgley et al. 1995; Behrensmeyer et al. 2000; Chew and Oheim 2009). Consequently, an important reason to conduct taphonomic studies is to identify the patterns of origin and magnitude exhibited by the taphonomic biases in a given fossil assemblage (Behrensmeyer et al. 2000). In order to fully comprehend how taphonomic processes affect what is preserved

in a fossil site and how to identify them as causes of bias, a great deal of experimental work is still needed (Denys 2002). Moreover, it is also important to have an extensive knowledge of the behavior and habits of those species found and preserved in the fossil assemblage (Lawrence 1968). However, some general trends can still be observed at the the GFS, indicating which taphonomic processes were important.

Carnivore Utilization

One main element of taphonomy is to identify the cause of an individual's death, such as whether it was a victim of carnivorous taxa. Carnivore utilization is indicated by any mark or fracture that preserves use of an animal or bone element by known carnivore species during either predation or scavenging (Haynes 1982). Large carnivores, when utilizing prey material, tend to leave predictable, patterned gnaw/tooth damage that can assist in discerning the carnivore species that caused it (Haynes 1983). Bone damage is caused when sufficient pressure is applied to deform or break the surface and often produces grooves and tooth impressions (Haynes 1983). Valuable diagnostic characteristics of these tooth marks and grooves include location with respect to anatomical landmarks and fractures, orientation of mark relative to the element's long axis, and number of marks occurring (Olsen and Shipman 1988; Blumenschine et al. 1996).

Haynes (1983) points out that although various predators and scavengers may not be preserved in a specific fossil assemblage, evidence that they utilized the area can be ascertained from gnaw marks on the prey animal's bones. Known predators and scavengers from the GFS include a saber-toothed cat (cf. *Machairodus* sp.), a canid, the mustelid (*Arctomeles dimolodontus*), the red panda (*Pristinailurus bristoli*), alligators

(*Alligator* sp.), and perhaps the tremarctine bear (*Plionarctos* sp.) (DeSantis and Wallace 2008). Modern large cats produce rough and irregular marks on the epiphyses of long bones that are caused by biting down with cheek teeth; canids gradually wear away epiphyses leaving numerous marks; and bears generally round the ends and occasionally leave tooth impressions and parallel furrows (Haynes 1983). On the diaphysis, canids leave numerous parallel scratches that are oriented transverse to the long axis and are much more numerous than those left by felids, while bears tend to crush the bone shaft (Haynes 1983). Crocodylian tooth marks differ from major mammalian carnivores, as they create bisected and hooked marks on the bone shaft and a lack of gnawing damage (Njau and Blumenschine 2006).

Weathering

As defined by Behrensmeyer (1978), weathering (another important taphonomic factor) is “the process by which the original microscopic organic and inorganic components of bone are separated from each other and destroyed by physical and chemical agents operating on the bone *in situ*, either on the surface or within the soil.” Soil pH and light intensity have been shown to determine the rate at which weathering acts on a bone (Tappen 1994), and if these conditions are consistent, can be used to estimate the length of time a bone was exposed before burial (Behrensmeyer 1978). However, this assumes that weathering stops once a bone is buried or is minimally weathered (Lyman 1994). Lyman and Fox (1989), based on research by Brain (1967), Miller (1975), and Cook (1986), suggest that the most important factors in determining the rate of weathering are temperature, moisture content, variations of these between seasons, as well as sediment type.

Other studies on weathering rates have been performed to better understand how habitats can affect variation in weathering rates. For example, Behrensmeyer (1978) conducted a study in the Amboseli Basin of southern Kenya where, after 15 years in a savanna habitat, 38% of various large herbivore carcasses were between stage 3 and 5, 55% were of stage 1 or 2, and 7% were fresh, stage 0 (stage descriptions shown in Table 3). Tappen (1994) observed that elephant bones left in the rain forest of Zaire showed much slower rates of weathering than those in the African savanna. Andrews and Cook (1985) also observed delayed weathering on a cow carcass in England, which after 7 years had yet to form cracks (weathering stage 1-2). Delayed and slower rates of weathering are suggested to result from a lack of intense UV light that is typically abundant in savanna habitats (Tappen 1994). Study of weathering damage on fossil bones from the GFS will allow a better understanding of why certain bones are found in various conditions of decay across the site and possibly help determine rates of sedimentation.

Abrasion

Abrasion, a third possible contributor to the taphonomic record at the GFS, occurs on bones when particles such as silt, sand, or gravel move against the bone surface creating scratches and/or a polishing effect (Fiorillo 1989; Fernandez-Jalvo and Andrews 2003). Such interactions can be caused by fluvial (Behrensmeyer 1982), eolian (Shipman and Rose 1983; Lyman 1994), or trampling action (Olsen and Shipman 1988). Thompson et al. (2011) note that the extent of wear is also a result of the bone's condition prior to abrasive exposure, whether fresh, dry, weathered, or fossilized. Bone abrasion due to fluvial action often indicates transportation with modification occurring with

transportation distance as little as a kilometer (Aslan and Behrensmeyer 1996); however, carcasses may be transported for longer distances with no wear due to floatation (Coard 1999), while others may become highly abraded while remaining fixed in one location along the stream channel (Behrensmeyer 1982).

Arthritis

Another possible taphonomic influence at the GFS is osteoarthritis (OA), a degenerative joint disease often related to age, caused by mechanical “wear and tear” or inflammation of the joints that destroys cartilage at articulating surfaces (Rothschild and Rothschild 1994; Wu and Kalunian 2005). Osteological changes to articulating surfaces may include bulbous growth, spike or spur formation, and synovial joints where lipping of bone occurs (Greer et al. 1977; Rothschild and Rothschild 1994). Greer et al. (1977) point out that OA is widespread in wild mammal populations, although the cause is unknown. Peterson (1988) speculates that arthritis found in moose from Isle Royale National Park, USA is due to malnutrition of individuals during early years in life, which causes the cartilage to be underdeveloped and more susceptible to damage later on. Arthritis is also caused by fractures that do not heal properly and dislocations at articulation sites, both causing bones to rub against each other (Bock and Atkins 1970). OA and other arthritis-like bone conditions may not directly influence the development of the GFS, although its occurrence may hinder an animal’s ability to move properly causing that animal to be more susceptible to predation. Bone density loss associated with OA may cause a bone to be more susceptible to weathering and abrasion.

Articulation

A major indicator of how individuals may be affected by taphonomic processes is articulation. Articulation is defined by Sorg and Haglund (2002) as when an individual's bones are united by joints that allow motion between them, while disarticulation is when the bones become disconnected at the joints. Postmortem disarticulation of an animal begins when the skull and limb bones detach from the rest of the carcass. Then the ribs fall off, followed by further disarticulation of the limbs, scattering of major elements, and lastly, separation of the vertebral column into individual vertebrae (Toots 1965). Based on this sequence of disarticulation, the state of an individual found in a fossil assemblage may indicate how long it took for it to become buried (Hill and Behrensmeyer 1984). Extent of disarticulation is also an indicator of how a specimen has been affected by other taphonomic processes (Hill 1979; Hill and Behrensmeyer 1984). Disarticulation causes bone ends to be more susceptible to abrasion and weathering, increases transport potential and scattering, and also allows greater access of a carcass to scavengers (Hill 1979; Hill and Behrensmeyer 1984).

Age Class

Classification of specimen ages, another important taphonomic indicator within a fossil assemblage, allows the origin and cause of death to be better understood (Haynes 1985; Lyman 1987). Two main mortality patterns can be determined from the frequencies of age classes: attritional, where the assemblage depicts a natural environment and a stable species population; and a catastrophic or mass-death sequence (Haynes 1985). Attritional fossil assemblages can be identified by an overabundance of young and old individuals, whereas a catastrophic event results in the number of

individuals declining as age increases (Lyman 1987). However, in order to understand what type of mortality event(s) occurred, one must first be able to determine the age of each individual accurately and consistently. The three main ways to determine the age of an individual tapir are (i) based on tooth eruption patterns using an age classification scheme developed by Hulbert et al. (2009), (ii) a count of the number of annuli rings after a tooth is dissolved (Maffei 2003), and (iii) state of fusion at the epiphyses of post-cranial bones when teeth are not available (Grossman 1938). These age classification methods can be used to determine the underlying cause, normal attrition or catastrophic events, to be determined for the GFS fossil assemblage.

Tapirus

To understand what taphonomic processes affected the distribution of tapir remains excavated at the GFS, the ecology and behavior of tapirs must first be characterized. Tapirs are “odd-toed” ungulates within the Order Perissodactyla (Owen 1848), which also includes modern and ancestral horses, rhinoceroses, and the extinct chalicotheres and brontotherioids (Froehlich 1999). All modern tapirs are classified within the family Tapiridae, defined by Gray (1821) as having well developed grooves within the narial opening that are believed to hold cartilaginous nasal diverticulae found in the fleshy proboscis. All modern tapirs are grouped within the single genus *Tapirus* (Colbert and Schoch 1998; Lizcano et al. 2002), which also include several extinct taxa such as *T. polkensis* found at the GFS (Hulbert et al. 2009). Tapirs evolved from *Hyracotherium*, an early Eocene horse (Radinsky 1966), and the genus *Tapirus* evolved from *Homogalax*, an early tapiroid of middle to late Miocene age (Colbert and Schoch 1998). Extant species include: *T. indicus*, *T. bairdii*, *T. terrestris*, and *T. pinchaque*, and

are found in southeast Asia, the lowlands of Central and South America, and the Andes highlands of Colombia, Ecuador, and Peru, respectively (Williams and Petrides 1980; Salas 1996; Lizcano and Cavalier 2000; Tobler 2002). All extant tapirs, and it is believed *T. polkensis* as well, are selective browsers that typically forage solitarily in either secondary or primary forests (Williams and Petrides 1980; Salas 1996; Lizcano and Cavalier 2000; Downer 2001; Foerester and Vaughan 2002; Tobler 2002; Noss et al. 2003; DeSantis and Wallace 2008; Tobler 2008; Hulbert et al. 2009). However, the presence of salt licks and watering holes may occur at overlaps in habitat, causing multiple tapir individuals to occupy one area simultaneously (Tobler 2008). Correlating these types of behavior for tapirs with the population at the GFS will allow a better understanding of the habitat setting.

CHAPTER 3

METHODOLOGY

Five basic procedures were used for this study: 1) designing a SDBMS and collection of the various attributes for each bone and specimen of *T. polkensis*, 2) implementation of the database design by the creation of a geodatabase in ESRI ArcGIS, with data attributes for each bone and specimen feature included, 3) separation of the bones and specimens into different attribute classes and creation of separate point sets, 4) creation of a statistical analysis script using python coding language that is able to calculate the nearest neighbor statistic for each point set, and 5) cartographic production of a 2D map of each point set and 3D animation, along with nearest neighbor calculation.

Database Design

Analysis of GFS patterns of tapir bone distributions required that each bone was given a series of attributes along with its recorded spatial data. In order to store the vast bone data set and specimens, their respective locations, and all attribute information, a relational database was needed. An entity-relationship diagram (ER) (Figure 1) was used to organize the relational database, which defined the relationships between the points, bones, and specimens. Attributes for each entity are described in Table 1, with the survey data described in the 'Points' Table, attributes for each bone in the 'Bones' Table, and those for each specimen in the 'Specimens' Table.

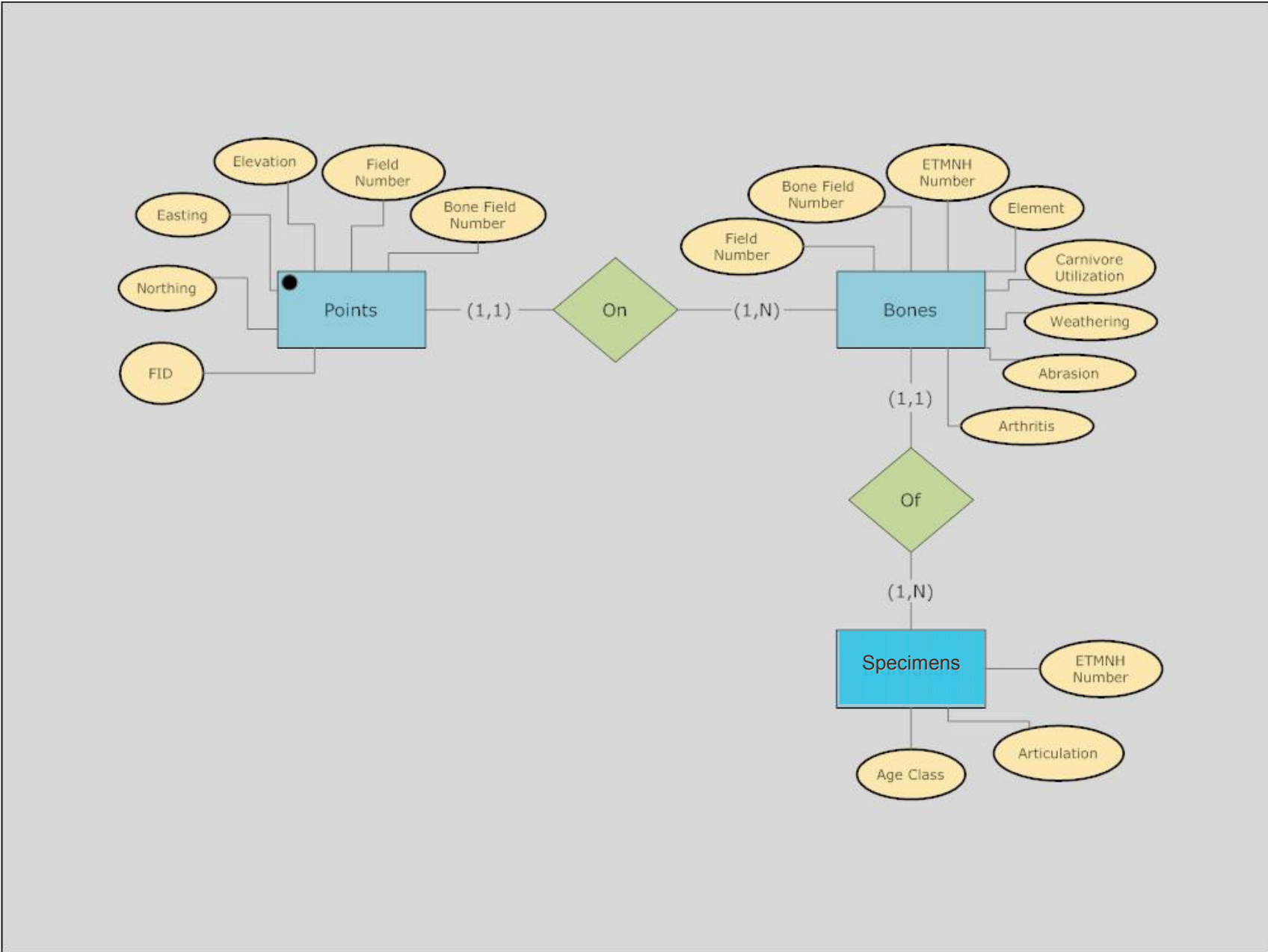


Figure 1: Entity-relationship diagram showing the organization of the spatial database management system

Each entity is represented by a rectangle in Figure 1, with the three entities including points, bones, and specimens. Relationships between entities are represented by connecting them with a particular preposition, as shown in Figure 1: 1) a surveyed point is “on” a bone and 2) a bone is “of” a specimen. Numbers in parentheses on either side of the verb indicate whether the relationship is one-to-one or one-to-many. The number of bones that a particular point lies upon must be at least one and no greater than one while bones on the other hand must be represented by at least one point, but can theoretically be represented by an infinite number of points. Bones, however, must be of a single specimen, while a specimen may be composed of at least one or more bones, with the maximum number equal to the expected number of bones normal for a fully articulated specimen. Each instance of an entity is given a value for every attribute, represented by an oval in the ER diagram.

Table 1: Descriptions of each point’s, bone’s, and specimen’s attributes in the SDBMS

Attribute	Description
Points Table	
FID	Unique identifier for each point
Northing	Y-coordinate in meters
Easting	X-coordinate in meters
Elevation	Z-coordinate in meters
Field Number	Alphanumeric number assigned to point when surveyed
Bone Field Number	Alphanumeric number of bone point is associated with
Bones Table	
Field Number	Alphanumeric numbers representing associated points
Bone Field Number	Alphanumeric number as unique identifier for bone
ETMNH Number	Specimen number assigned by ETMNH
Element	Type of bone; humerus, radius, etc.
Carnivore Utilization	Type of mark left by carnivore if any
Weathering	Degree of weathering observed
Abrasion	Type of abrasion shown
Arthritis	Level of arthritis
Specimens Table	
ETMNH Number	Specimen number assigned by ETMNH
Age Class	Age class of specimen
Articulation	Articulation type for specimen

Bone Attributes

Four attributes were classified for each bone in the database. These include type of carnivore utilization, if any; degree of weathering; type of abrasion, if any; and level of arthritis. Five types of carnivore utilization (Table 2) were used to classify each bone that exhibited predatory markings, with the type of marking entered into the database for the bone and a value of 'none' entered if no markings were found. Weathering stages (Table 3) were defined for all bone elements and teeth recovered, ranging from -1 for isolated teeth and 5 for the highest state of weathering that occurred, with examples shown in Figure 2. Three main types of abrasion caused by fluvial, eolian, and trampling processes were recognized, with the damage patterns caused by each described in Table 4. The final attribute characterized for each bone was whether arthritis or arthritis-like pathologies, which may cause the same amount of pain and resistance to articulation as traditional arthritis, were present and to what level (described in Table 5 with examples of each level in Figure 3). For the purpose of this study, the term arthritis denotes both traditional types of arthritis as well as those features that might be associated with other pathologies.

Table 2: Types of carnivore utilization after Binford (1981)

Type	Description
None	No evidence of carnivore utilization.
Crenulated-Edges	Material is removed from the ends of long bones and thin bones.
Furrowing	Removal of inner bone tissue.
Pitting	Formation of non-collapsed concave structures on bone surface.
Puncturing	Formation of collapsed concave structures on bone surface.
Scoring	Short, parallel grooves created on bone surface perpendicular to the bone's long axis.

Table 3: Weathering stages defined for tapirs at the Gray Fossil Site, adapted from Behrensmeyer (1978)

Stage	Description
-1	Isolated tooth with no associated bone material resulting in unknown weathering state.
0	Bone surface showing little or no discoloration and not pitted or hummocky in texture.
1	Little to extensive discoloration with loss of glossy bone surface. Cracking of bone surface parallel to fiber structure on long bones and mosaic on articular surfaces. Little to no pitted or hummocky surface.
2	Extensive discoloration of bone surface with extensive pitting and minor loss of bone material.
3	Extensive flaking and splintering of bone with definite loss of bone material. Minor exposure of tooth root showing.
4	Extensive loss of bone material with moderate amounts of tooth root exposed. Integrity and structure of bone element is upheld.
5	Integrity and structure of bone element lost with only fragments remaining, and loss of element shape.

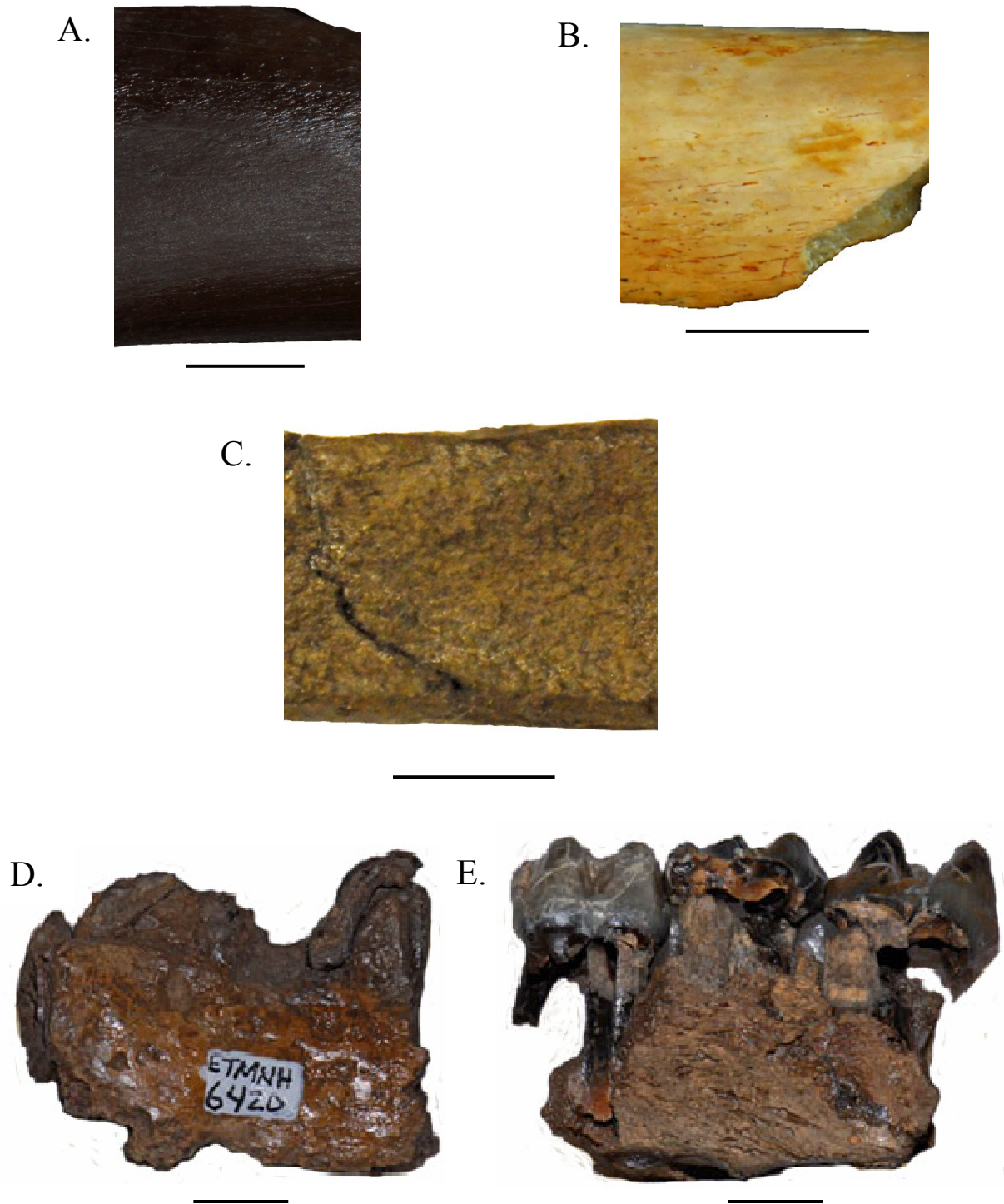


Figure 2: Tapir bones that show the weathering stages found at the Gray Fossil Site: A. fibula at a 0 stage, ETMNH 3700; B. bone fragment at stage 1-2, ETMNH 3811; C. radius at stage 3, ETMNH 6934; D. jaw fragment at stage 4, ETMNH 6420; E. left maxilla fragment at stage 5, ETMNH 3702. Scale bar is 1 centimeter.

Table 4: Abrasion types and descriptions used to characterize tapir fossils from the Gray Fossil Site, adapted from Shipman and Rose (1983); Olsen and Shipman (1988); Fernandez-Jalvo and Andrews (2003)

Type	Description
None	No sign of abrasion.
Fluvial	Polishing and rounding of bone by abrasive particles and transportation, covering most of bone surface.
Eolian	Similar polishing as fluvial abrasion, but only occurring on exposed areas.
Trampling	Produces small, shallow scratches with no orientation pattern.

Table 5: Descriptions of the various stages of arthritis present in bones of *Tapirus polkensis* at the Gray Fossil Site

Level	Description
None	No indication of arthritis on the bone. All articulating edges are rounded and smooth.
Very Minor	Most edges of articulation surfaces are smooth and rounded. Some articulating edges are sharpened with minor lipping occurring.
Minor	Most edges of articulating bones have become sharpened with minor lipping. Growth of extra bone material occurring along epiphysis-diaphysis suture, but not around articulating surfaces.
Moderate	Most edges of articulating bones have become sharpened with minor lipping. Growth of extra bone material occurring around articulating surfaces
Extreme	Growth of bone material occurs around and on articulating surfaces.

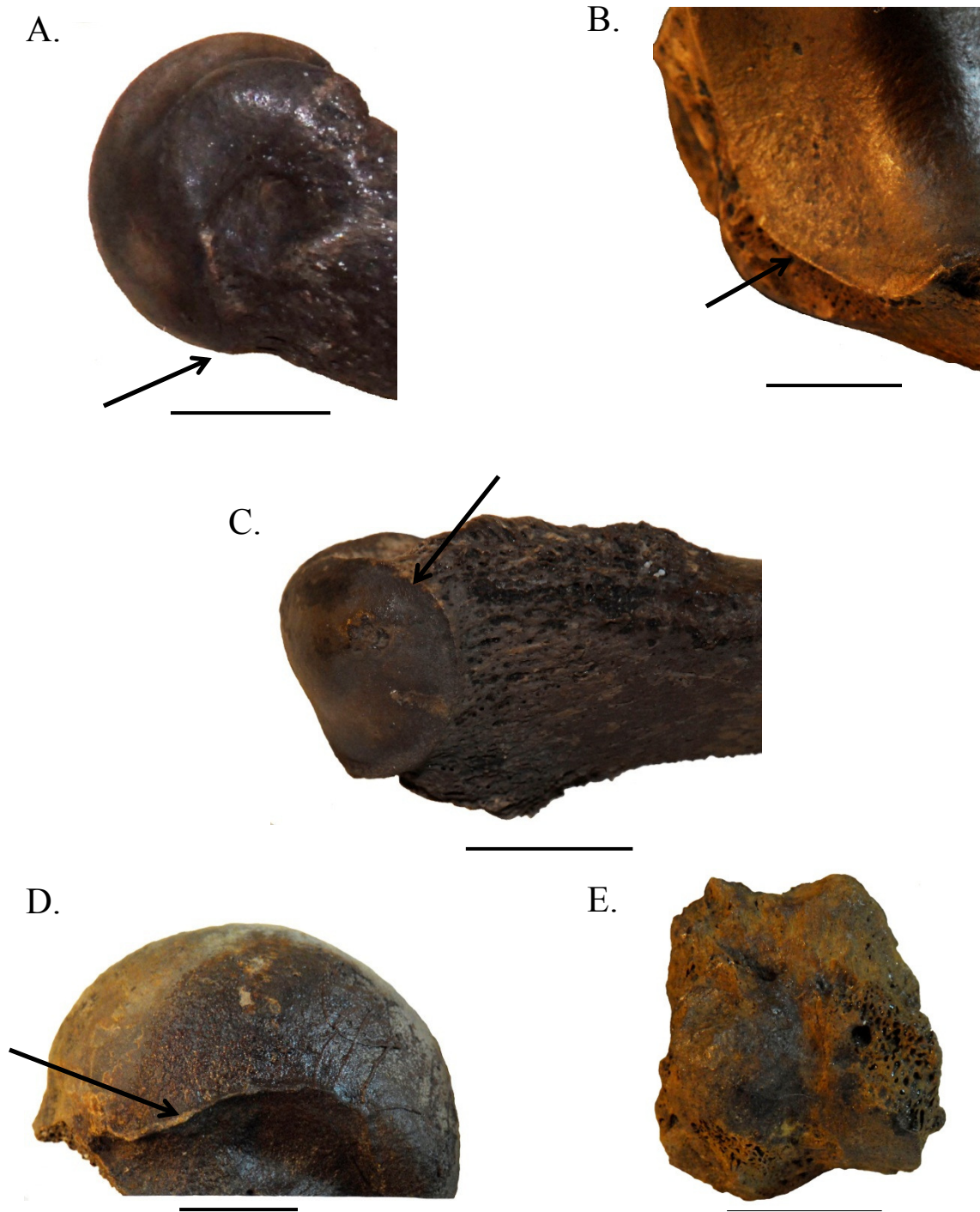


Figure 3: Examples of arthritis levels in *Tapirus polkensis* specimens at the Gray Fossil Site: A. distal end of metatarsal with no arthritis, ETMNH 478; B. proximal epiphysis of tibia showing very minor arthritis, ETMNH 4964; C. distal end of metacarpal with minor arthritis, ETMNH 3573; D. proximal epiphysis of a femur showing moderate arthritis, ETMNH 599; E. phalanx with extreme arthritis, ETMNH 4887. Arrows note lack of lipping on A and slight lipping on B with heavy lipping on C and D. Scale bar is 1 centimeter.

Specimen Attributes

Once all of the bones for each tapir specimen were assigned attributes, the specimen was assigned an age class. Approximate age of a specimen can be determined by observation of tooth eruption and wear, and/or by evaluation of the fusion of the proximal and distal epiphyses to the diaphysis of a bone (Klein and Cruz-Uribe 1984). Criteria for age classification of a specimen was based on tooth eruption and wear, adapted from Hulbert et al. (2009), with three age classes (juvenile, sub-adult, and adult). Juvenile age was defined as a specimen within the range of having only DP1-3 and dp2-3 fully erupted, to having DP1-M1 and dp2-m1 fully erupted with the adult premolars and second molars fully formed in crypts. Sub-adult age was defined as having all adult premolars, M1-2, and m1-2 fully erupted with wear, while M3 and m3 might be erupting or erupted with little to no wear. Adult age was defined as having all adult premolars and molars, with M3 and m3 exhibiting moderate wear, and possible exposure of dentine.

If teeth were not present or were not still in the tooth socket of the skull and/or lower jaw, fusion of the distal and proximal epiphyses to the diaphysis of various bone elements was used to determine age. The use of this criterion assumes that the rate of epiphysis fusion matches the rate of tooth eruption. A juvenile age attribute was assigned if both proximal and distal epiphyses were not fused to the bone shaft at the epiphysis-diaphysis suture. If either the proximal or distal epiphysis was fused but not both, then the individual was assigned a sub-adult age. If both distal and proximal epiphyses were fused, the specimen was considered an adult. Null values were given to a specimen where neither tooth eruption nor epiphyseal fusion could be used to classify a specimen.

If a mixture of age classes was found for a specimen with multiple bones, the age class with the majority of bones was used.

After determination of the specimen's age class, the articulation state of that specimen was evaluated. Each specimen was assigned an articulation state that included (i) an isolated bone element, (ii) a semi-articulated skeleton, or (iii) an articulated skeleton. A specimen was considered isolated if it was composed of one or two bones that were not in correct anatomical position or articulated. Semi-articulated specimens were comprised of multiple bones that were associated with each other and consisted of either post-cranial or cranial material, but not both. A specimen was also considered semi-articulated even if both post-cranial and cranial material were present if either was composed of isolated material not associated with other bones from that skeletal region. Specimens were designated as articulated if they contained both post-cranial and cranial material, with both regions had multiple associated bones.

Database Implementation

Data Entry

In order to implement the database design for this study, the primary tables: 'Points', 'Bones', and 'Specimens' were created using Microsoft (MS) Excel. Survey data for the points taken at the GFS were contained within a series of text files which, for this project, were merged into one file and opened in MS Excel. For each GFS bone a search was done to locate the field number of the bone within the survey data. If the point data were located it was copied to the point data spreadsheet, which was later used to create the 'Points' Table. If point data were not found (i.e. no spatial data exists for

that particular bone), that bone specimen was purged from the database and not classified.

Once the spatial data for a bone was copied to the point data spreadsheet, a new bone field number was created. As described in the database design, this was represented by an alphanumeric value that included the date the specimen was excavated, followed by a dash and then the specimen number. Bones that contained multiple points, for example 051206-001A1 to 051206-001A3, were given a unique bone identifier that was common for all the points associated with that bone (in this case 051206-001A). In some cases, one set of points was used for multiple bone fragments of the same bone, with points 051206-001B1-3 given to one part and 051206-001B4-6 to the other. To account for this in the bone field number value, the first set was referred to as Ba and the second set as Bb. For bones or specimens that simply had a date-dash-specimen number identifier, this number was copied to the unique bone identifier field. It is important to note that a unique FID number for each point was carried over to the point data spreadsheet from the original survey data spreadsheet.

After the point data were retrieved and entered, the field number and bone field number were entered into the 'Bones' Table spreadsheet. Here the field number was represented as the range of points associated with the bone, allowing a user to understand which points relate to it. For example, if a bone has a bone identifier of 051206-001A, then the field number for this bone would be 051206-001A1-3, allowing a user to see that the bone was represented by three points. The ETMNH number and element description were taken from either the information card that accompanies each bone or the GFS collections database and were then entered into the spreadsheet. Each attribute was then

collected and entered into the 'Bones' Table spreadsheet. After all bones for each specimen were analyzed, the ETMNH number was entered into the 'Specimens' Table spreadsheet, along with its associated attributes.

Creation of a Geodatabase

Using ESRI ArcCatalog (a data management program within the ArcGIS suite) a file geodatabase was created and named "GFS_Tapirs.gdb". Next, the tables were imported from the MS Excel spreadsheets using the import wizard in ArcCatalog and into separate tables, with the input rows parameter as the spreadsheet and the output table as the name given to each table. Tables containing point data, bone data, and specimen data were imported and named 'Points' Table, 'Bones' Table, and 'Specimens' Table, respectively. Although the ETMNH number in both the 'Bones' and 'Specimens' Tables is considered a numeric value in MS Excel, once these tables were imported into ESRI ArcCatalog the number was changed to a string value to allow the two tables to be joined properly.

Displaying Point Features

To represent the bones as actual objects in space, a new feature class was created in ESRI ArcMap using the Display XY Data function from the 'Points' Table x, y, and z data set. For each point, the x-coordinate was selected as the easting value, the y-coordinate as the northing value, and the z-coordinate as the elevation value, with the output feature class saved into the GFS Tapirs geodatabase as Points. The projection type used for these features was Tennessee State Plane using the 1983 HARN North American Datum (NAD) in meters and the 1988 North American Vertical Datum (NAVD). The points feature was joined to the 'Bones' Table based on matching values

in the 'bone field number' field. This feature was then joined to the 'Specimens' Table based on matching ETMNH numbers between the 'Specimens' Table and the 'Bones' Table, with this product being exported as a new feature to preserve the joins and allow additional processing to be completed. Due to excavation methods used at the GFS, all bones and specimens were represented by multiple points and additional steps had to be completed in order to reduce each bone or specimen feature to one point.

Mean Center Calculation

The mean center tool in ArcToolbox was used to calculate the mean center for each bone or specimen by averaging the x, y, and z coordinates of every point within each point set. By using the bone field number as the case field for each bone and the ETMNH number for each specimen, this function created one x, y, z coordinate for each bone and specimen. The z-value, representing elevation, was not calculated with the default settings of this function but, instead, was calculated by setting the dimension field to the z-value. Once the mean center was calculated for each bone and specimen, another tool was used to add the x and y data to the resulting feature class, as the mean center function when displaying the x and y data rounds to the nearest integer. The mean center function does not round during the actual calculation, just when displaying the results, and adding the x-y data to the attribute table allowed the true x-y coordinates to be displayed. Another aspect of the mean center result is that the ordering of the x, y, z coordinates could not be processed correctly using the nearest neighbor script. Therefore, the new feature classes were exported as a .dbf file, and the fields were rearranged with MS Excel into the order of easting, northing, elevation, and bone field number. Using the

display xy function a second time permitted the correctly arranged mean center data to be displayed as points, allowing further data processing and analysis.

Creating Each Attribute Layer

Upon creation of the mean center features for both single bones and specimens in ESRI ArcMap, each was exported to the “GFS_Tapirs” geodatabase as new feature classes called ‘Bones’ and ‘Specimens’. ‘Bones’ and ‘Specimens’ Tables were then added to ArcMap, where the ‘Bones’ Table was joined to the ‘Bones’ Feature by matching bone field number values, and the ‘Specimens’ Table was joined to the ‘Specimens’ Feature by matching ETMNH numbers. A function in ArcMap called “Select by Attributes” was used to separate the attributes into different feature classes. The Select by Attributes tool uses the structured query language (SQL) to select all objects that fit a certain selection query parameter(s). Using this, the various taphonomic levels were separated into the following feature classes: carnivore utilization was separated into bones that show no carnivore markings, those that show pitting, those that show punctures, etc.; the weathering attribute was separated into weathering stages -1 to 5; abrasion was separated by abrasion type; and arthritis into five stages from none to extreme. Attributes for each specimen (age class and articulation) were then separated into the four age classes and the three states of articulation. When exported into the geodatabase, each new attribute feature class was placed into a corresponding feature dataset that includes all stages of each attribute, with separate feature datasets for each attribute.

Nearest Neighbor Analysis

After creation of a new feature class for each attribute value in the geodatabase, the nearest neighbor statistic was calculated in both the 2- and 3-dimensions for each attribute feature class. As discussed previously, the nearest neighbor statistic quantifies the spatial pattern for a set of objects. The process by which the nearest neighbor statistic was calculated is described by outlining the program designed and built using the python coding language. The basic outline for this process is as follows: A) specific modules (pre-built python code) are imported to allow the use of various needed functions; B) specific parameters are entered that are: the input feature class, the near feature class, the output feature class, and the values for the volume and area of the study site; C) nearest neighbor distances are calculated and D) the R statistic is calculated, with z-values and p-values for 2- and 3-dimensions, along with each calculated value placed into a comma-separated value (csv) file that can be opened in MS Excel.

Importing Python Modules

The nearest neighbor statistic program (Appendix) begins by importing modules and packages of python script utilized in calculating the statistic. In order for python to correctly compute the division of values using the “/” operator, the feature class division must be imported from the future module (Hetland 2005). The locale module is imported to allow “programmers to deal with certain cultural issues in an application, without requiring the programmer to know all the specifics of each country where the software is executed”, by providing access to the POSIX database and functions (van Rossum 1997). Arcpy, a module produced by ESRI to allow access to tools and scripts commonly used in ArcGIS software, is then imported (Knight 2011). Other modules imported into the

script include: “SSUtilities”, a basic assemblage of pre- and post-processing functions (van Rossum 1997); csv, a module used to format data into comma separated values (Choirat and Seri 2009); and Stats, a collection of basic statistical functions for python (Oliphant 2007).

Acquiring Parameters

Once all the required modules are obtained, the parameters that are input feature, near feature, and output feature, as well as the volume and area for the study site are retrieved. The input feature is a set of points that comprise each attribute feature class analyzed, the near feature is the same set of points as the input feature, and the output feature is the csv file where all the calculated values will be stored. Area input is the size of the study area (m^2), and is used to calculate the nearest neighbor statistic in 2-dimensions. Volume input (m^3) is used in the 3-dimensional nearest neighbor statistic calculations. Two text files containing all of the survey points acquired for tapirs at the GFS were used to generate a minimum convex hull for both 2- and 3-dimensions with a program known as qhull. This program, after creating the convex hulls, calculates the size of the convex hulls and outputs this as area (m^2) and volume (m^3) (Barber et al. 1996).

Calculating Nearest Neighbor Distances

Upon retrieving all the necessary parameters, the NN program measures the distances between each point and its closest neighboring point by implementing a tool in ESRI ArcMap known as “Near3D” from the arcpy module. The input and near feature classes are entered into the Near3D tool’s parameters and the other parameters are set to

their default values. Near distances in both 2- and 3-dimensions are then determined by the Near3D tool and appended to the attribute table of the input feature class.

Once the Near3D tool has successfully run, the measured distances are determined and stored in the input feature classes attribute table. Once completed, a variable designated “cnt” is created with the SSUtilities module and counts the number of points in the input feature class. A search cursor is then implemented from the arcpy module that retrieves the 2- and 3-dimensional nearest neighbor distances from the input feature class and stores them in a variable called “rows”. Here a row search is iterated, searching each row in the input feature class and totaling the 2D and 3D near distances into two separate variables. After all the variables are determined and set, the various components that make up the nearest neighbor statistic are processed and calculated.

Calculating Nearest Neighbor Statistic and Outputs

The first aspect of the nearest neighbor statistic that must be calculated is the average observed nearest neighbor distance (r_{obs}) for both dimensions. This is calculated by taking the sum of the nearest neighbor distances and dividing it by the number of points in the input feature class. Next, the expected average nearest distance is calculated using equation 1 for 2-dimensions and equation 2 for 3-dimensions, again where r_{exp} is the expected average nearest neighbor distance, N is the number of points analyzed, A is the area of the study site, and V is the volume of the study site. Upon completing the calculations for observed and expected average nearest distances, the program calculates the standard error (SE) for the points in both dimensions using equation 3 for the 2nd dimension and equation 4 for the 3rd dimension. Calculating the actual nearest neighbor statistic involves producing the ratio r_{obs}/r_{exp} in 2- and 3-dimensions. Results from the

standard error calculations are then used to produce the z-value, or standard deviation, by subtracting the expected average nearest neighbor distance from the observed and dividing the result by the standard error. The last calculation is performed by using the stats module, which uses a z-probability function to determine the p-value for both dimensions. Once all the calculations are completed for a set of points, the values are formatted using the locale module. A MS Excel csv file is created as the output file for the nearest neighbor statistical program, and it includes the observed average nearest neighbor distance, the expected average nearest neighbor distance, the nearest neighbor ratio, the z-value, and the p-value all written to an output file.

Cartographic Output

Using ESRI ArcMap, maps were produced that document the location of each classification level for all attributes analyzed, all survey points of tapir bones, mean centers of each bone, and the mean centers of each specimen. Survey data collected from each excavation pit, as latitude and longitude (northing and easting), were used to create 2D polygons representing areas where fossils were recovered from pits. With the aid of aerial imagery from the U.S. Department of Agriculture's 2007 National Agriculture Imagery Program (NAIP), the corners of the ETMNH building were digitized to create a polygon for this dominant site feature. Whitelaw et al. (2009) developed a grid of highly accurate latitude, longitude, and elevation points while conducting gravity research at the site. These points were used to create a surface model in the TIN (Triangulated Irregular Network) format with ESRI 3D Analyst tools. The ETMNH building and excavation pits used the TIN surface model for elevation reference, with the building extruded 9 meters above the TIN surface and the pits extruded 2 meters below the surface. ESRI ArcMap

was used to create maps and figures for the 2D analysis of this project, and ESRI ArcScene was implemented to create 3D animations for 3D analysis.

CHAPTER 4

RESULTS

As noted in the methods section, the first step in this study was to create a database to store and organize the attribute data for each entity analyzed. A representative sample of rows from the database is presented in section 1. Section 2 describes the python script used to calculate the nearest neighbor statistic and results from the program qhull. Section 3 includes base maps of the site, showing the locations of the original survey points, averaged bone points, and averaged specimen points. Sections 4-7 provide the spatial distribution of the attributes for the bone points, including carnivore utilization, weathering, abrasion, and arthritis. Sections 8 and 9 depict the tapir specimen positions differentiated by age class and articulation state. All sections, with the exception of 1 and 2, include maps created ESRI's ArcGIS software which show spatial distribution of the point sets in 2-dimensions and the results of the nearest neighbor calculations. Animations for visualization of the site and each attribute in 3D were created. They are not included in this document as they are too large to be embedded in this text.

Geodatabase

Creation of a database to characterize location, state of each bone, and condition of each tapir specimen required the creation of three entity tables. The first entity table, the 'Points' Table, includes each survey point's latitude, longitude, elevation, field number, and the identifier number of the bone it is associated with. The structure of this table is shown by a random selection of points in Table 6. Table 7 shows the 'Bones' Table that includes the survey points associated with each bone, the bone identifier

number, ETMNH number, type of element, carnivore utilization type if any, degree of weathering, abrasion type, and level of arthritis. Lastly, Table 8 depicts a randomly selected set of rows from the ‘Specimens’ Table including the ETMNH number, age class, and state of articulation when uncovered. During the period 2001-2009, 6292 points related to tapir remains were surveyed, 3145 tapir bones were recovered, and 1836 tapir specimens were documented in the GFS collections. Although 1836 ETMNH specimens are documented, the bones from this data set likely only represent approximately 75 actual tapir individuals (Hulbert et al. 2009).

Table 6: Random set of rows from the completed ‘Points’ Table

FID	Northing	Easting	Elevation	Field Number	Bone Field Number
719	233350.4583	914094.0257	501.529119	121801-010G	121801-010G
603	233359.3696	914147.5289	501.876282	111901-005	111901-005
498	233361.1875	914131.0354	503.418959	102401-004	102401-004
3698	233358.6603	914126.7475	502.285285	082004-002A3	082004-002A
2308	233377.2674	914109.2042	499.993548	081503-005	081503-005
1529	233416.9266	914195.7218	499.27674	073102-005	073102-005
3037	233357.2047	914126.822	502.758767	072904-002	072904-002
2701	233393.297	914130.4196	500.345118	071304-008	071304-008
1352	233417.9744	914201.2221	499.78066	070502-002	070502-002
6439	233352.6527	914135.4288	503.024226	052105-003	052105-003
5903	233399.2818	914097.1038	497.567627	051805-001L1	051805-001L
1132	233353.4288	914136.4402	502.485474	050802-010	050802-010
5817	233404.4931	914094.6675	497.426339	041805-001NN4	041805-001CNN
5653	233403.9399	914093.4638	497.480536	041805-001N1	041805-001N
1008	233361.1664	914126.1856	503.143329	041802-004	041802-004
938	233350.2856	914094.5991	501.962816	041202-007	041202-007
803	233350.6669	914135.3603	503.856699	032902-009B	032902-009
4769	233402.7868	914093.0225	497.358317	022305-004	022305-004
2547	233369.2157	914095.8309	498.918546	022004-002	022004-002
4720	233406.7861	914100.0652	497.473694	021805-005B3	021805-005B

Table 7: Random set of rows from the completed 'Bones' Table

Field Number	Bone Field Number	ETNMH Number	Element	Carnivore Utilization	Weathering	Abrasion	Arthritis
012308-001A1	012308-001A	6603	vertebra	none	1	none	none
022004-004	022004-004	3455	ulna proximal end	none	1	none	none
060506-003C1-3	060506-003C	5531	thoracic vertebra	none	3	none	none
101306-001BP1-4	101306-001BP	3719	skull and mandible	none	1	none	none
040302-009	040302-009	172	sesamoid	none	0	none	moderate
073107-003A1	073107-003A	3805	rt maxilla, petrosal	none	0	none	none
060106-012A1-3	060106-012A	6401	rt femur	none	2	none	none
052206-005D1-D2	052206-005D	3680	rib fragment	none	1	none	none
031502-018	031502-018	52	phalanx	none	1	none	v. minor
050605-001A1-B3	050605-001AB	5044	partial humerus	none	0	none	none
070506-002A1-A3	070506-002A	3696	none	none	2	none	none
091207-004A1-3	091207-004A	6441	metacarpal	none	2	none	minor
082107-001A1-A3	082107-001A	3806	maxilla, rt DP1-3, rt dp2	none	0	none	none
FJ070505-001	FJ070505-001	4018	lt p3	none	-1	none	none
113004-002	113004-002	714	jaw fragment	none	3	none	none
030802-003	030802-003	62	humerus proximal end	none	1	none	none
121806-008A1	121806-008A	5762	femur distal end	none	1	none	none
060506-014AY1	060506-014AY	3573	distal end metapodial	none	1	none	v. minor
062906-007A1-2	062906-007A	5610	caudal vertebra	none	1	none	none
071304-004	071304-004	5818	bone fragment	none	3	none	none

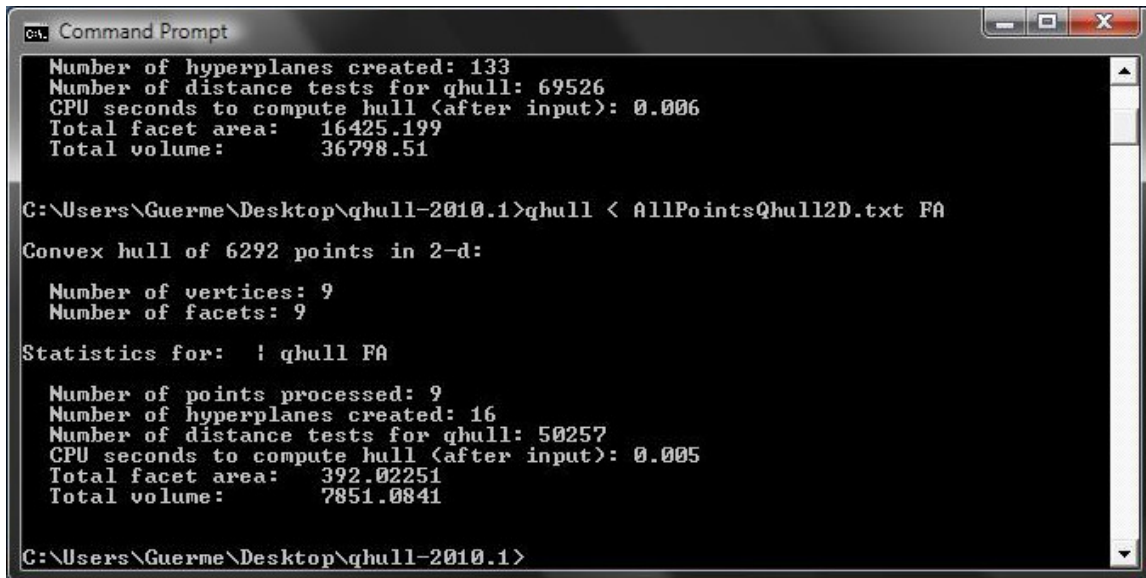
Table 8: Random set of rows from the completed ‘Specimens’ Table

ETMNH Number	Age Class	Articulation
693	Juvenile	Isolated
11	Adult	Isolated
7742	Sub-adult	Semi-articulated
137	NULL	Isolated
3679	Juvenile	Isolated
4067	NULL	Isolated
10602	Juvenile	Isolated
55	Sub-adult	Isolated
3683	Juvenile	Semi-articulated
8264	Adult	Semi-articulated
567	Sub-adult	Isolated
3696	Juvenile	Semi-articulated
6845	Adult	Isolated
192	Juvenile	Isolated
6634	Adult	Semi-articulated
3806	Juvenile	Isolated
4163	Juvenile	Isolated
3426	Sub-adult	Semi-articulated
299	NULL	Isolated
6838	Sub-adult	Isolated

Nearest Neighbor Program and Qhull Calculations

In order to calculate the nearest neighbor statistic for any group of points measured at the GFS, a program was written in python coding language (Appendix). Although programs in python can be integrated into ArcGIS, the nearest neighbor program is currently still in a basic state, and can only be accessed externally using the python 2.6 graphical user interface (GUI) by locating each parameter by a specific file pathname. Input area and volume values used for this statistic were calculated with the qhull program using all the survey points associated with tapir remains, thus providing a maximum extent in both 2- and 3-dimensions for any subsequent point set analyzed in this project. Figure 4 shows the qhull output of the area calculation for all surveyed points associated with tapirs to be 7851 m² and Figure 5 shows the volume calculated

output, as 36799 m³, for the same points. Although the value in Figure 4 is listed as total volume, it really represents total area as the points used in the calculation solely consisted of latitude and longitude coordinates, and the output for some reason refers to it as volume.

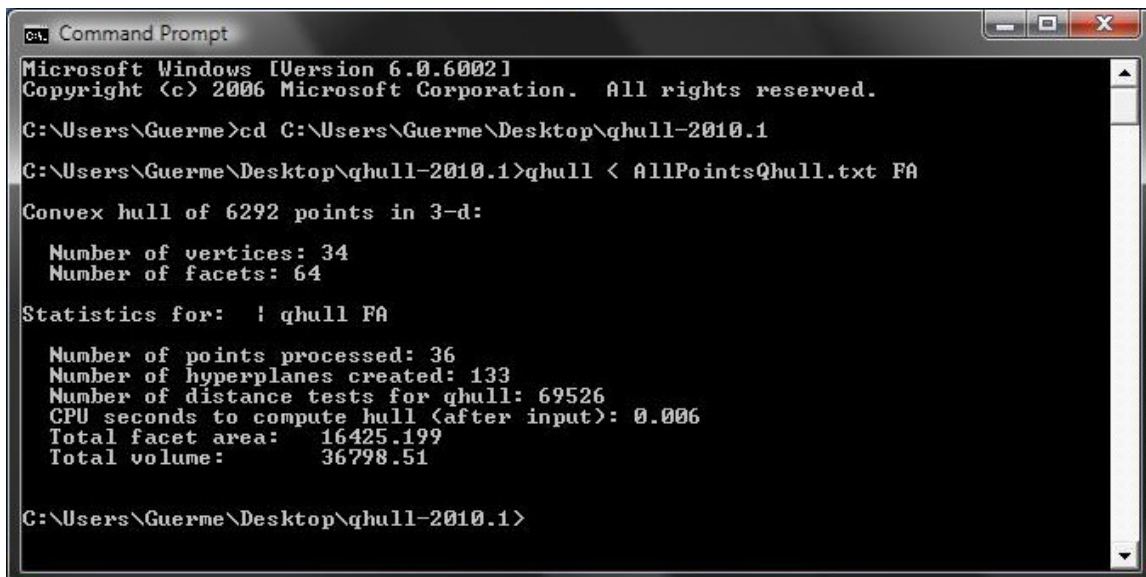


```
ca. Command Prompt
Number of hyperplanes created: 133
Number of distance tests for qhull: 69526
CPU seconds to compute hull (after input): 0.006
Total facet area: 16425.199
Total volume: 36798.51

C:\Users\Guorme\Desktop\qhull-2010.1>qhull < AllPointsQhull2D.txt FA
Convex hull of 6292 points in 2-d:
    Number of vertices: 9
    Number of facets: 9
Statistics for: | qhull FA
    Number of points processed: 9
    Number of hyperplanes created: 16
    Number of distance tests for qhull: 50257
    CPU seconds to compute hull (after input): 0.005
    Total facet area: 392.02251
    Total volume: 7851.0841

C:\Users\Guorme\Desktop\qhull-2010.1>
```

Figure 4: Qhull result showing the calculated area for the survey points



```
ca. Command Prompt
Microsoft Windows [Version 6.0.6002]
Copyright (c) 2006 Microsoft Corporation. All rights reserved.

C:\Users\Guorme>cd C:\Users\Guorme\Desktop\qhull-2010.1
C:\Users\Guorme\Desktop\qhull-2010.1>qhull < AllPointsQhull.txt FA
Convex hull of 6292 points in 3-d:
    Number of vertices: 34
    Number of facets: 64
Statistics for: | qhull FA
    Number of points processed: 36
    Number of hyperplanes created: 133
    Number of distance tests for qhull: 69526
    CPU seconds to compute hull (after input): 0.006
    Total facet area: 16425.199
    Total volume: 36798.51

C:\Users\Guorme\Desktop\qhull-2010.1>
```

Figure 5: Qhull result showing the calculated volume for the survey points

Base Maps

Following the successful completion of the nearest neighbor program and area-volume calculations, the original survey points were mapped using ArcGIS software (Figure 6) with a superimposed surface model of the GFS for visual reference. The survey point map clearly shows that the tapir fossils are spatially clustered, with a nearest neighbor ratio of 0.23 (2D) and 0.14 (3D). Both clustered values are statistically significant with z-values well below -1.96 and p-values of zero (Table 9). It is also important to note that in 3D the points were less dispersed than in 2D, most likely due to a lack of vertical range at the site compared to the horizontal range. As the bone points at the site are averaged values of the survey points, they display a similar spatial distribution (Figure 7), with slightly less clustering and nearest neighbor ratio values of 0.35 (2D) and 0.24 (3D). Again note the statistical significance of the bone distribution shown in Table 9 by the z and p-values. Figure 8 illustrates the tapir specimen locations and depicts a clustered spatial pattern, similar to the surveyed and bone point sets, with statistically significant R values of 0.42 (2D) and 0.31 (3D). The spoil pile (Figure 6) is an area where bones are moved to after excavation but before they are surveyed. This situation is problematic and further reviewed in the discussion.

Table 9: Results of nearest neighbor analysis for original survey points, averaged bone locations, and averaged specimen locations

Point File	Dimension	r_{obs}	r_{exp}	R	Z-value	p-value
All Survey Points	2nd	0.129421	0.558522	0.231720	-116.585	0.000000
	3rd	0.139564	0.998065	0.139835	-187.731	0.000000
All Bones	2nd	0.275637	0.789995	0.348910	-69.8521	0.000000
	3rd	0.301277	1.257617	0.239562	-117.337	0.000000
All Specimens	2nd	0.430126	1.033947	0.416003	-47.8712	0.000000
	3rd	0.469692	1.504750	0.312140	-81.0953	0.000000

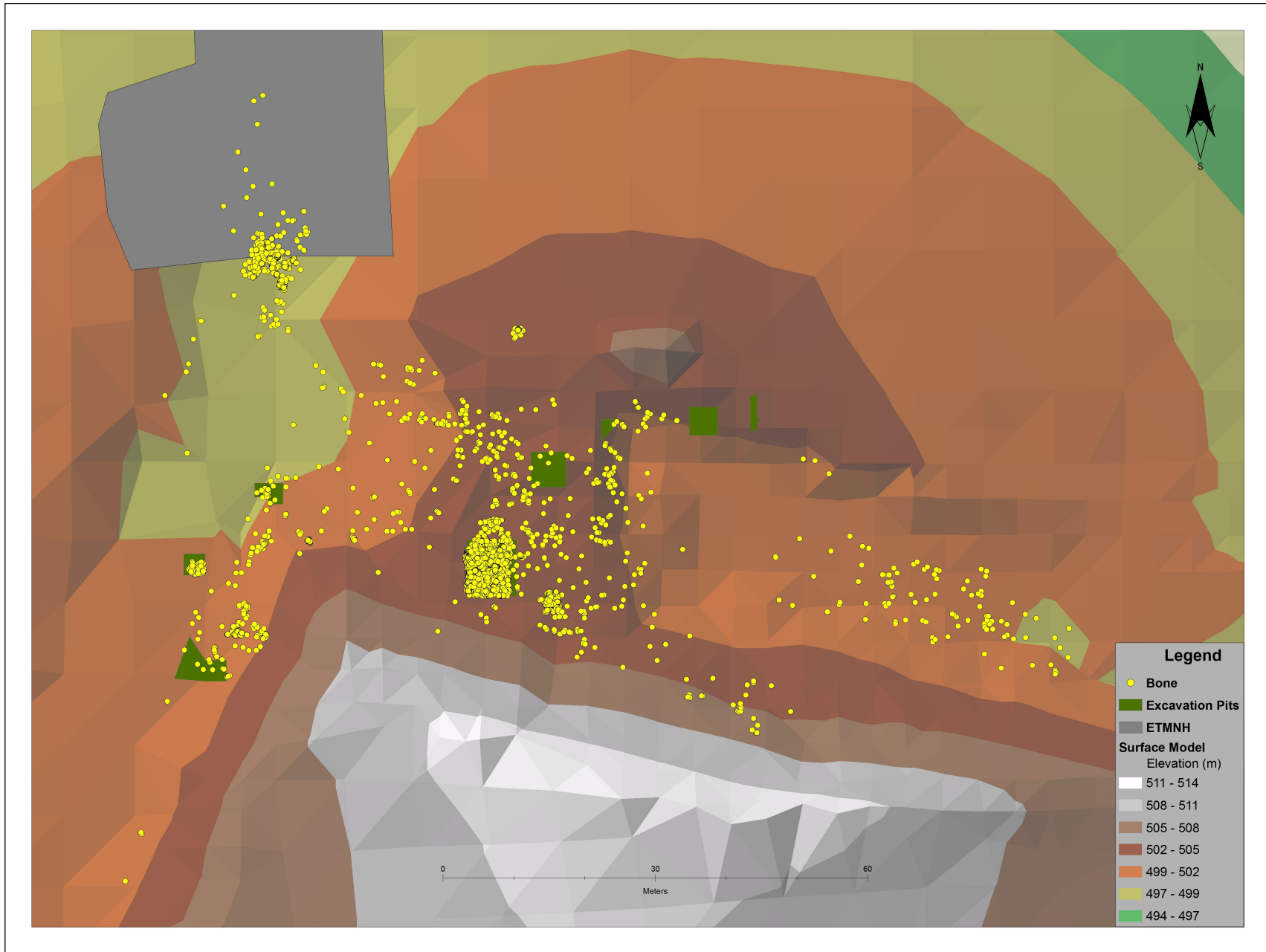


Figure 6: Spatial distribution of survey points for *Tapirus polkensis* between 2001 and 2009, as well as the spoil pile

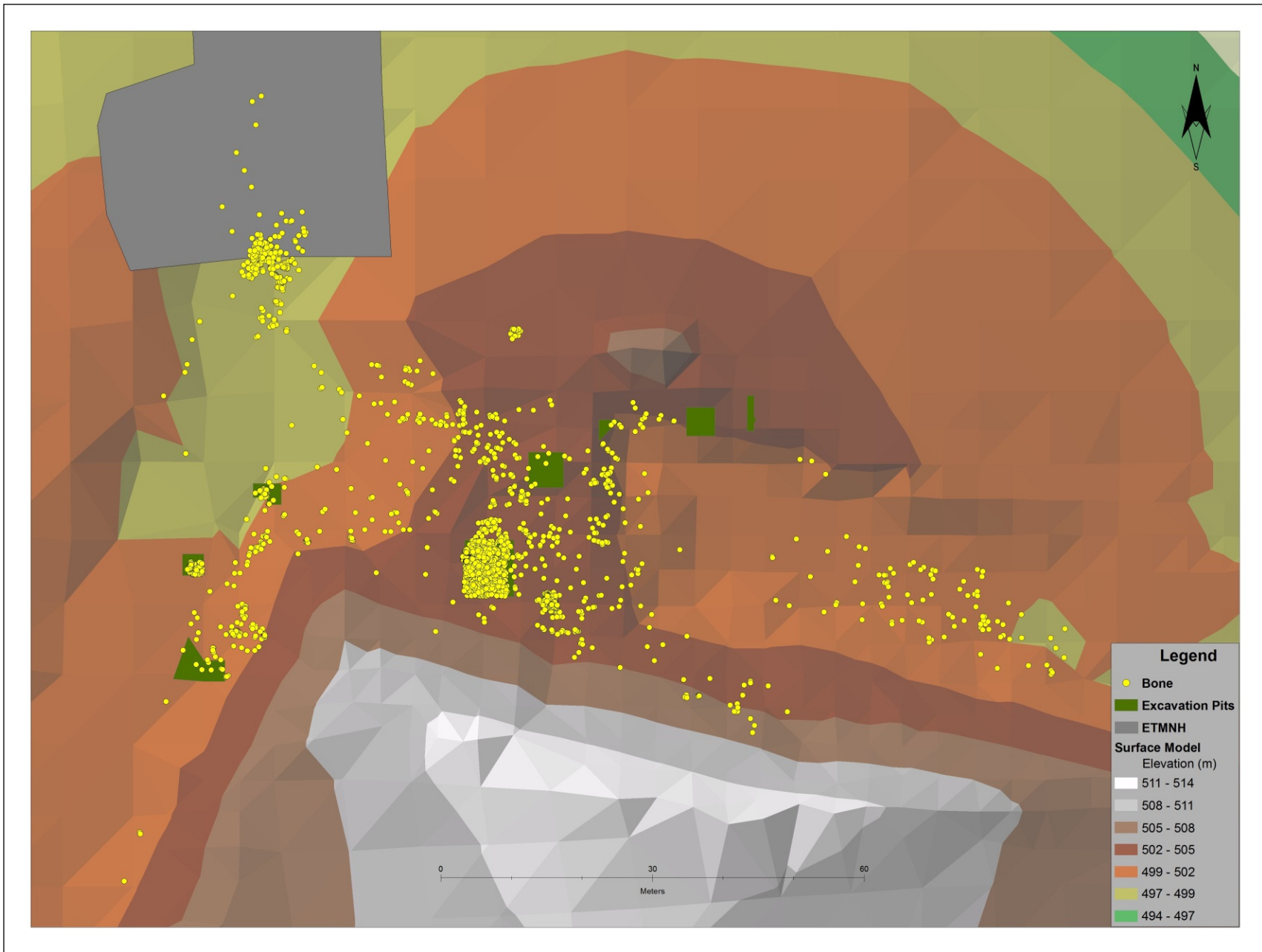


Figure 7: Spatial distribution of averaged point locations for each bone of *Tapirus polkensis* at the Gray Fossil Site

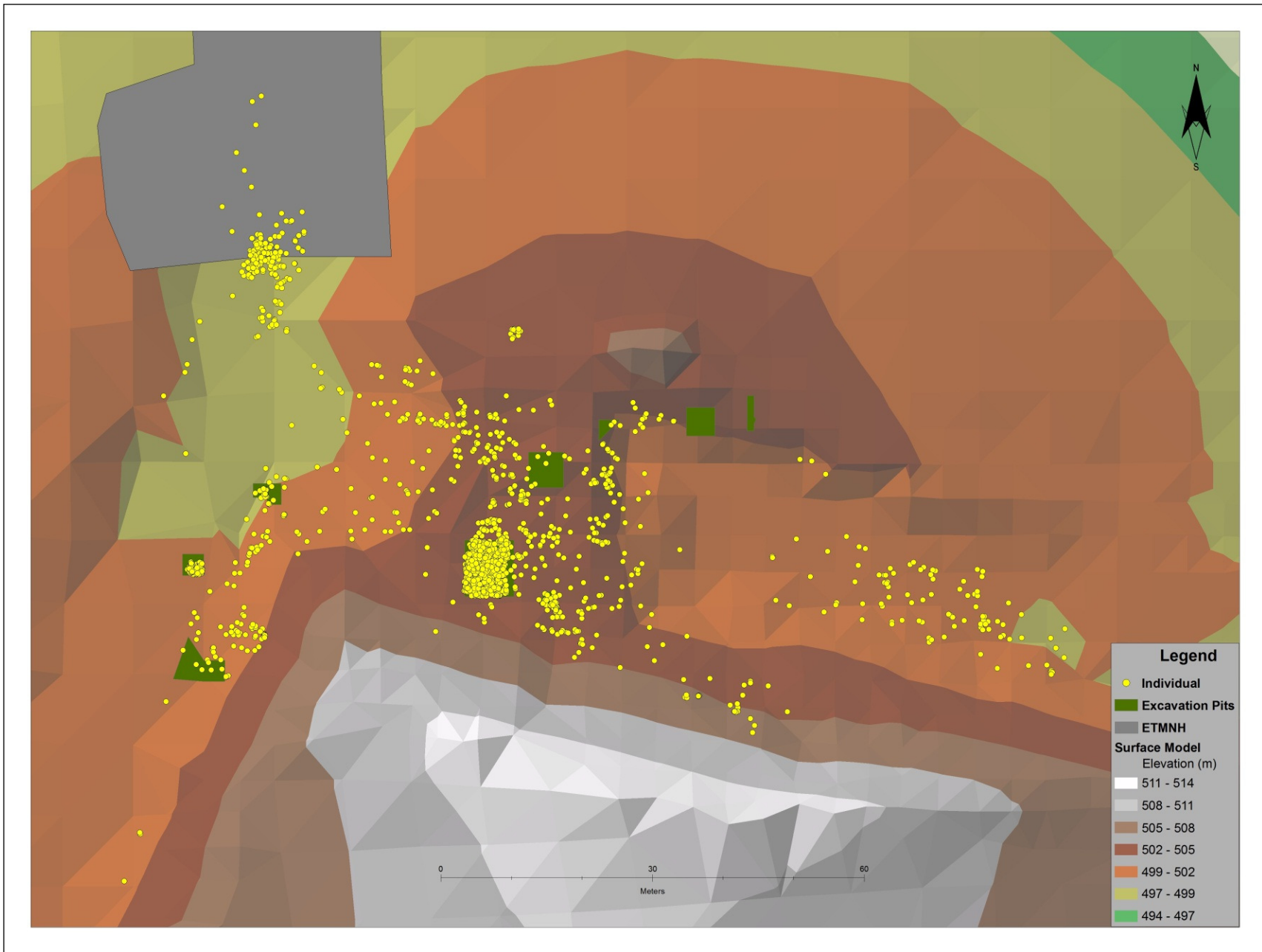


Figure 8: Spatial distribution of averaged point locations for each specimen of *Tapirus polkensis* at the Gray Fossil Site

Carnivore Utilization

Several GFS tapir bones (Figure 9) were found to exhibit signs of carnivore utilization although only two have associated survey data and were excavated between 2001 and 2009. An atlas that has a fairly large puncture depression was found in July of 2006. A second bone, recovered in October of 2006, is a rib fragment with lots of small pit markings all over its surface. As Figures 10 and 11 show, both bones were found in the rhino pit with nearest neighbor ratios of -0.02 (2D) and -0.05 (3D) (Table 10). These values indicate that both points appear clustered with the 2D value nearly significant with a z-value of -1.956 and a p-value of 0.05, and in 3D statistically significant given z- and p-values of -2.90 and 0.0037. However, whether these points are actually clustered or not will be further investigated in the discussion (p. 91). No other tapir bones show signs of carnivore utilization (Figure 12) and Table 10 corroborates the observed clustering pattern with R values very similar to those of the bones in both 2D and 3D, with z- and p-values that are statistically significant.

Table 10: Nearest neighbor results for different types of carnivore utilization

Type	Dimension	r_{obs}	r_{exp}	R	Z-value	p-value
Puncture	2nd	-1.000000	44.30317	-0.022572	-1.95624	0.050437
	3rd	-1.000000	18.42561	-0.054272	-2.90076	0.003723
Pitting	2nd	-1.000000	44.30317	-0.022572	-1.95624	0.050437
	3rd	-1.000000	18.42561	-0.054272	-2.90076	0.003723
None	2nd	0.275703	0.790247	0.348882	-69.8328	0.000000
	3rd	0.301334	1.257883	0.239556	-117.300	0.000000

A.



B.



Figure 9: Bones of *Tapirus polkensis* that show sign of carnivore utilization and have spatial data at the Gray Fossil Site: A. a rib with extensive pitting, ETMNH 3808; B. an atlas with puncture mark, ETMNH 3659. Scale bar is 1 centimeter.

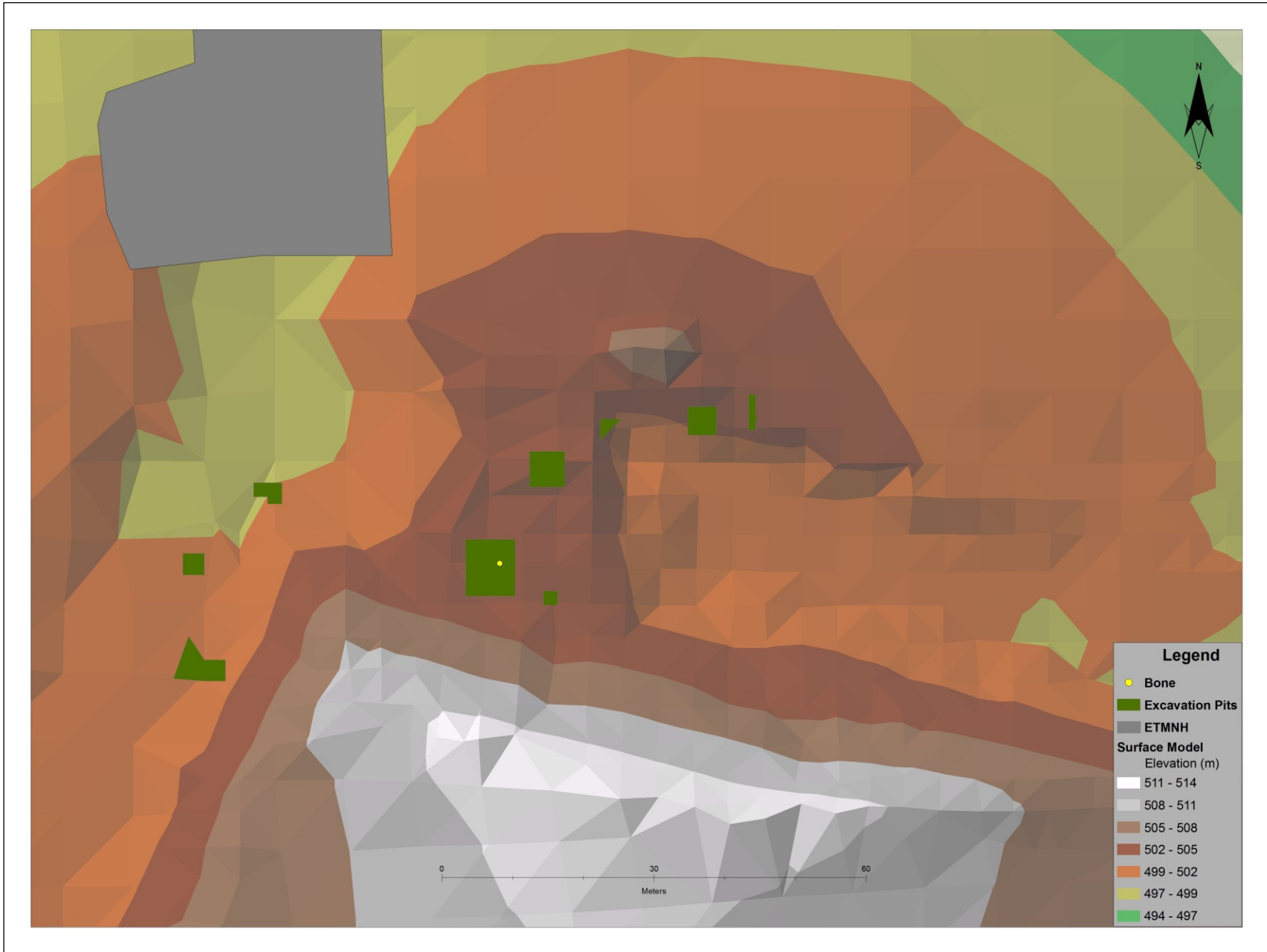


Figure 10: Spatial distribution of *Tapirus polkensis* bones at the Gray Fossil Site with puncturing marks

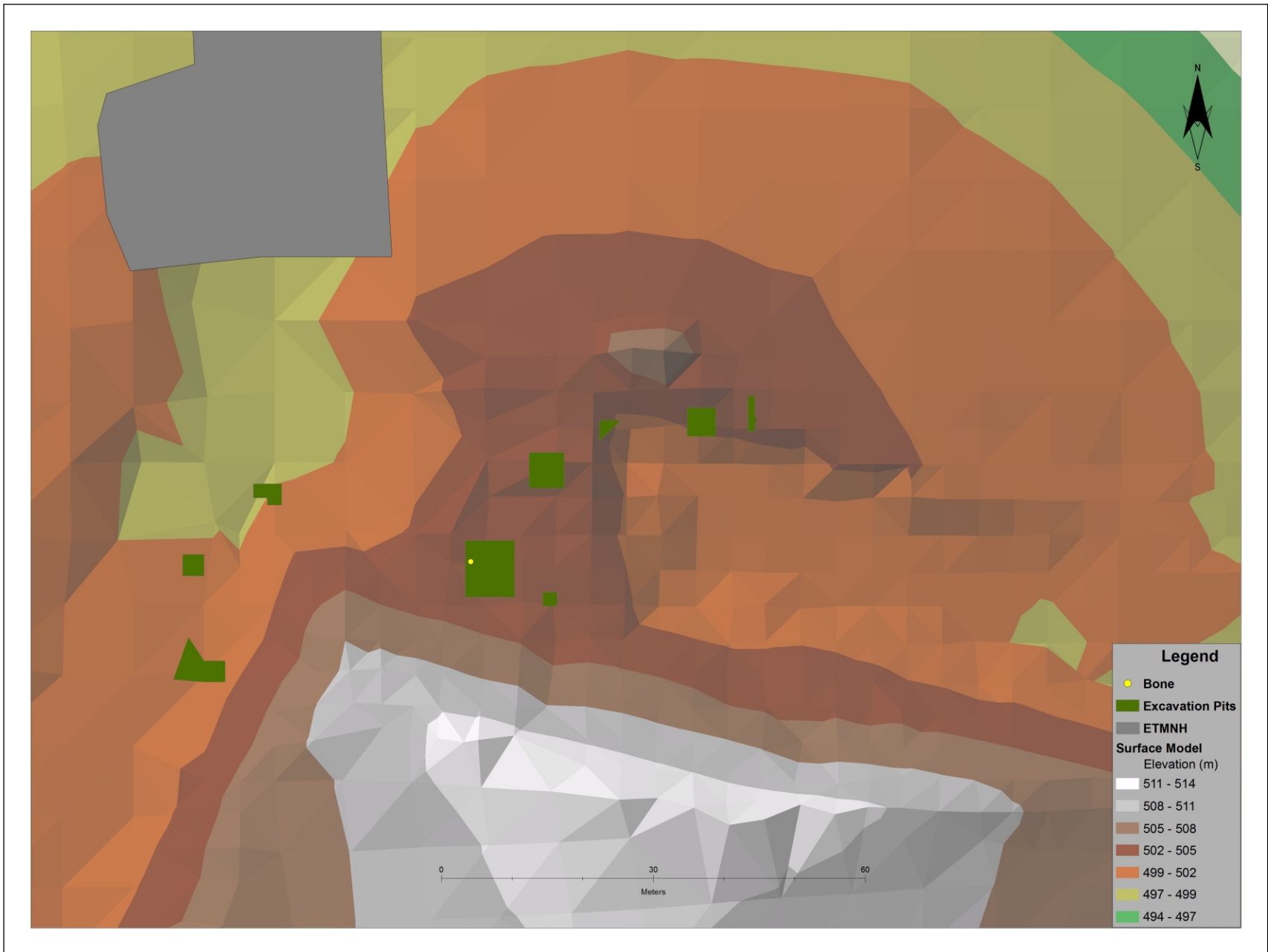


Figure 11: Spatial distribution of *Tapirus polkensis* bones at the Gray Fossil Site with pitting marks

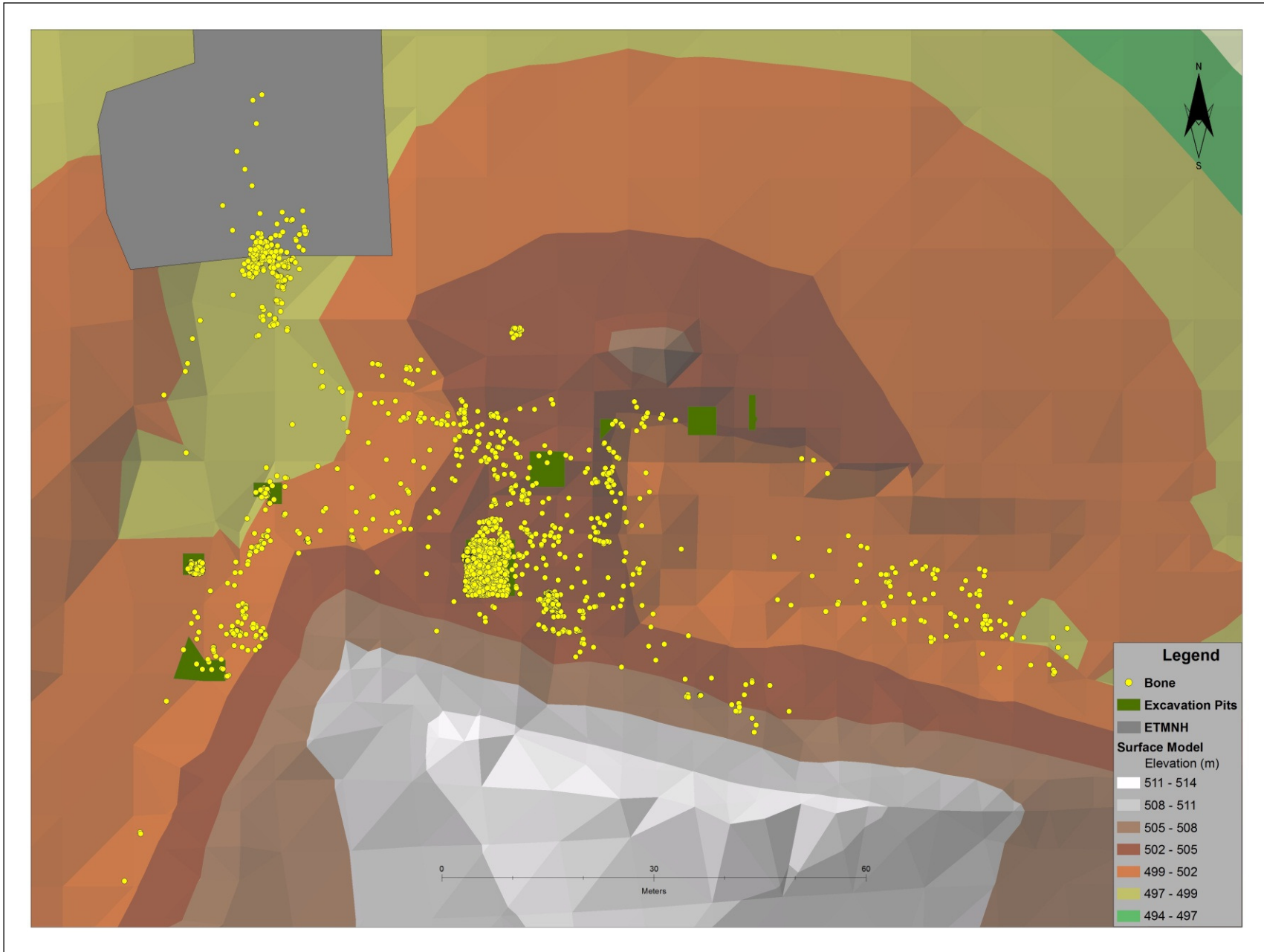


Figure 12: Spatial distribution of *Tapirus polkensis* bones at the Gray Fossil Site lacking evidence of carnivore utilization

Weathering

Seven stages of weathering were identified for tapir bones at the GFS, and of the 3145 bones excavated between 2001 and 2009, 4 were classified as stage 5, 3 as stage 4, 37 as stage 3, 455 as stage 2, 926 as stage 1, and 1596 with no weathering or stage zero. In addition 124 were identified as isolated teeth and classified as stage -1. Figure 13 illustrates that the most strongly weathered bones (stage 5) were found in the rhino pit, the cat pit, and 10 meters southeast of the rhino pit. The spatial pattern of these stages indicates clustering in 2D and dispersal in 3D, although the p- and z-values in Table 11 indicate that neither can be considered statistically significant. Stage 4 bones were recovered from the rhino pit and below the ETMNH building and depict a mild clustering pattern in 2D (as shown in Figure 14) and a dispersed pattern in 3D (Table 11), with only the 3D pattern having statistical significance. Stage 3 weathered bones were recovered throughout the site (Figure 15) and represent a clustered distribution in 2D and a near random distribution in 3D. However, as Table 11 illustrates, the 3D pattern is not statistically significant while the 2D pattern is. Figure 16 indicates that stage 2 weathered bones had a distribution similar to those of the original bone set, with significant clustering in both dimensions (Table 11). Stage 1 weathered bones (Figure 17), no weathering or stage 0 bones (Figure 18), and isolated teeth or stage -1 elements (Figure 19) were recovered from all across the site, and are all statistically clustered in both 2D and 3D (Table 11).

Table 11: Nearest neighbor results for different degrees of weathering

Degree	Dimension	Γ_{obs}	Γ_{exp}	R	Z-value	p-value
5	2nd	13.93882	22.151586	0.629247	-1.4185	0.156032
	3rd	14.05418	11.607405	1.210794	1.1600	0.246059
4	2nd	22.07406	25.578448	0.862994	-0.4540	0.649851
	3rd	22.43040	12.775603	1.755722	3.6015	0.000316
3	2nd	4.83717	7.186923	0.673051	-3.8557	0.000115
	3rd	4.95548	5.480590	0.904187	-1.6251	0.104145
2	2nd	0.64887	2.054510	0.315824	-28.2242	0.000000
	3rd	0.70559	2.378323	0.296673	-41.7295	0.000000
1	2nd	0.58752	1.441182	0.407663	-34.8347	0.000000
	3rd	0.62593	1.877635	0.333358	-56.3855	0.000000
0	2nd	0.31122	1.102083	0.282393	-55.1868	0.000000
	3rd	0.34196	1.570151	0.217787	-86.5177	0.000000
-1	2nd	1.86414	3.946840	0.472313	-11.3316	0.000000
	3rd	1.93635	3.675347	0.526847	-14.6132	0.000000

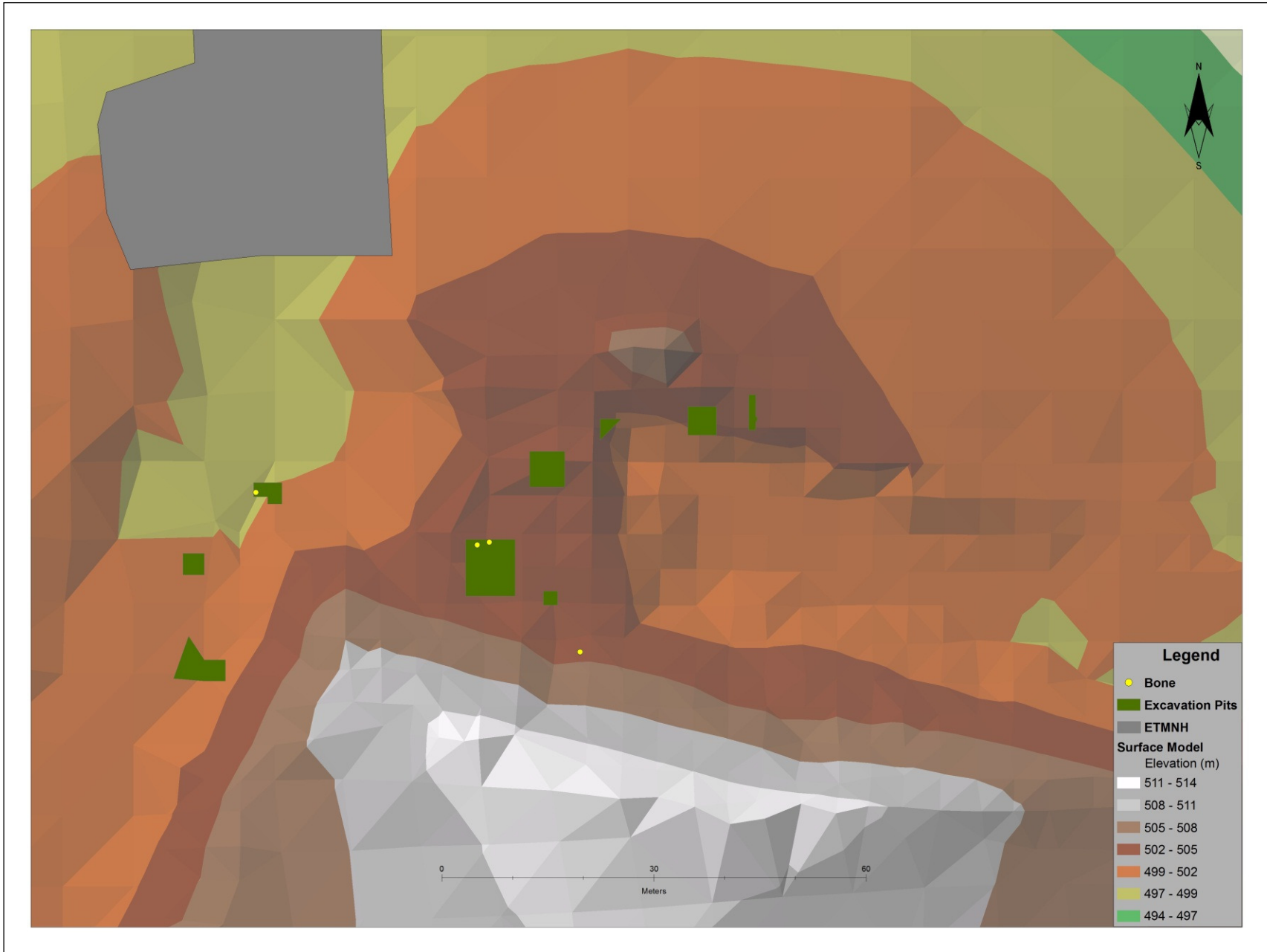


Figure 13: Spatial distribution of *Tapirus polkensis* bones at the Gray Fossil Site with weathering stage 5

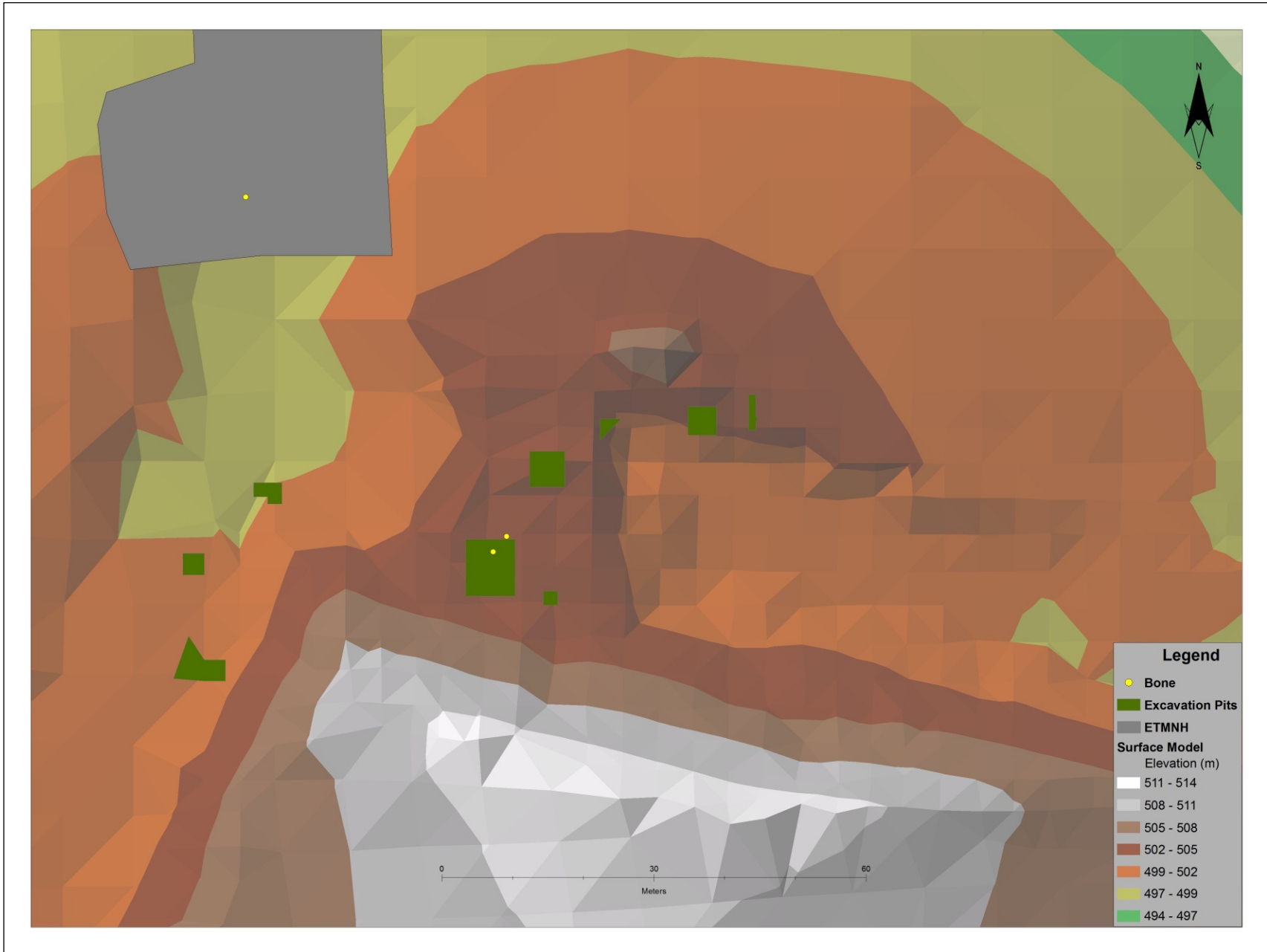


Figure 14: Spatial distribution of *Tapirus polkensis* bones at the Gray Fossil Site with weathering stage 4



Figure 15: Spatial distribution of *Tapirus polkensis* bones at the Gray Fossil Site with weathering stage 3

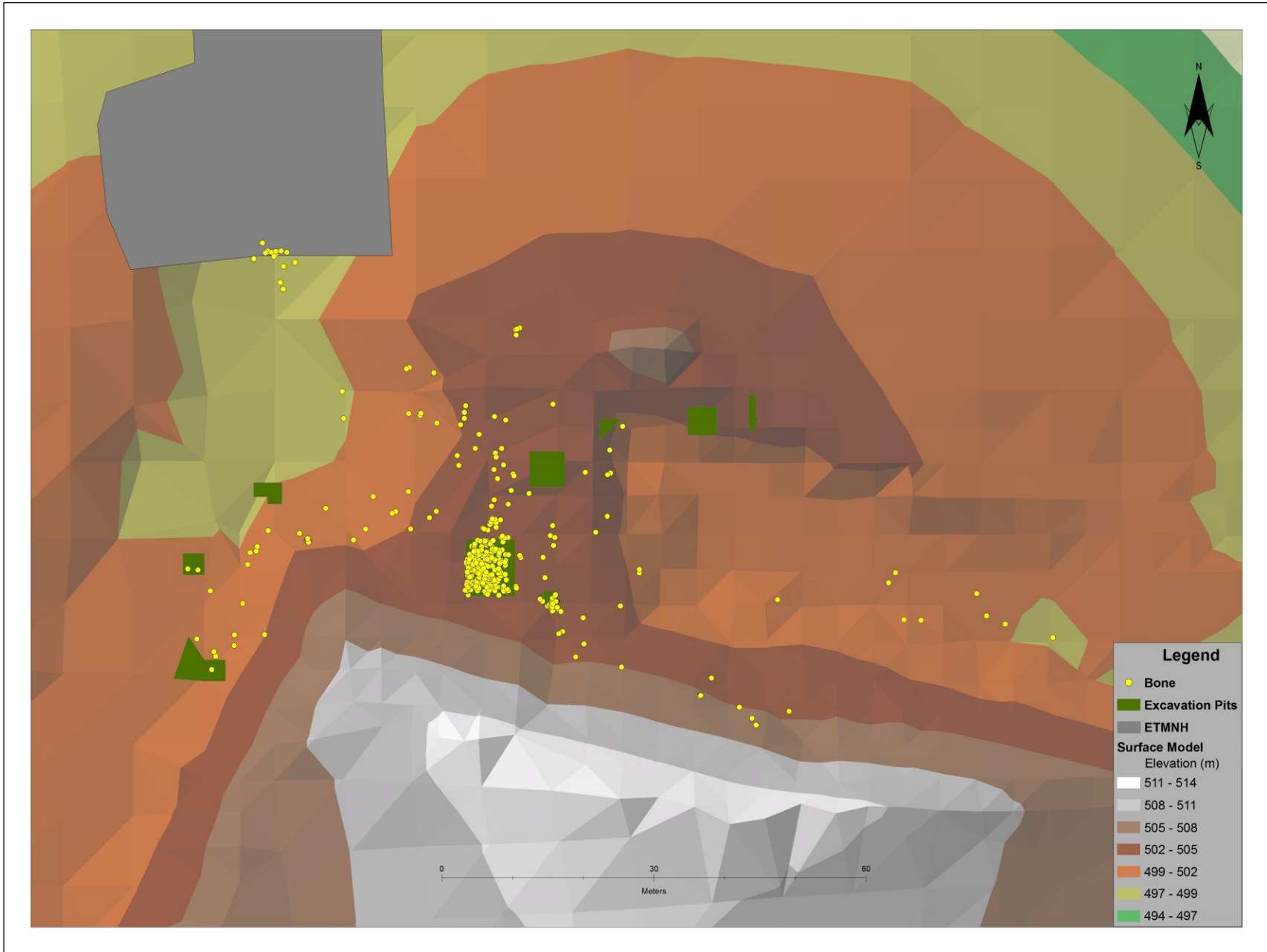


Figure 16: Spatial distribution of *Tapirus polkensis* bones at the Gray Fossil Site with weathering stage 2

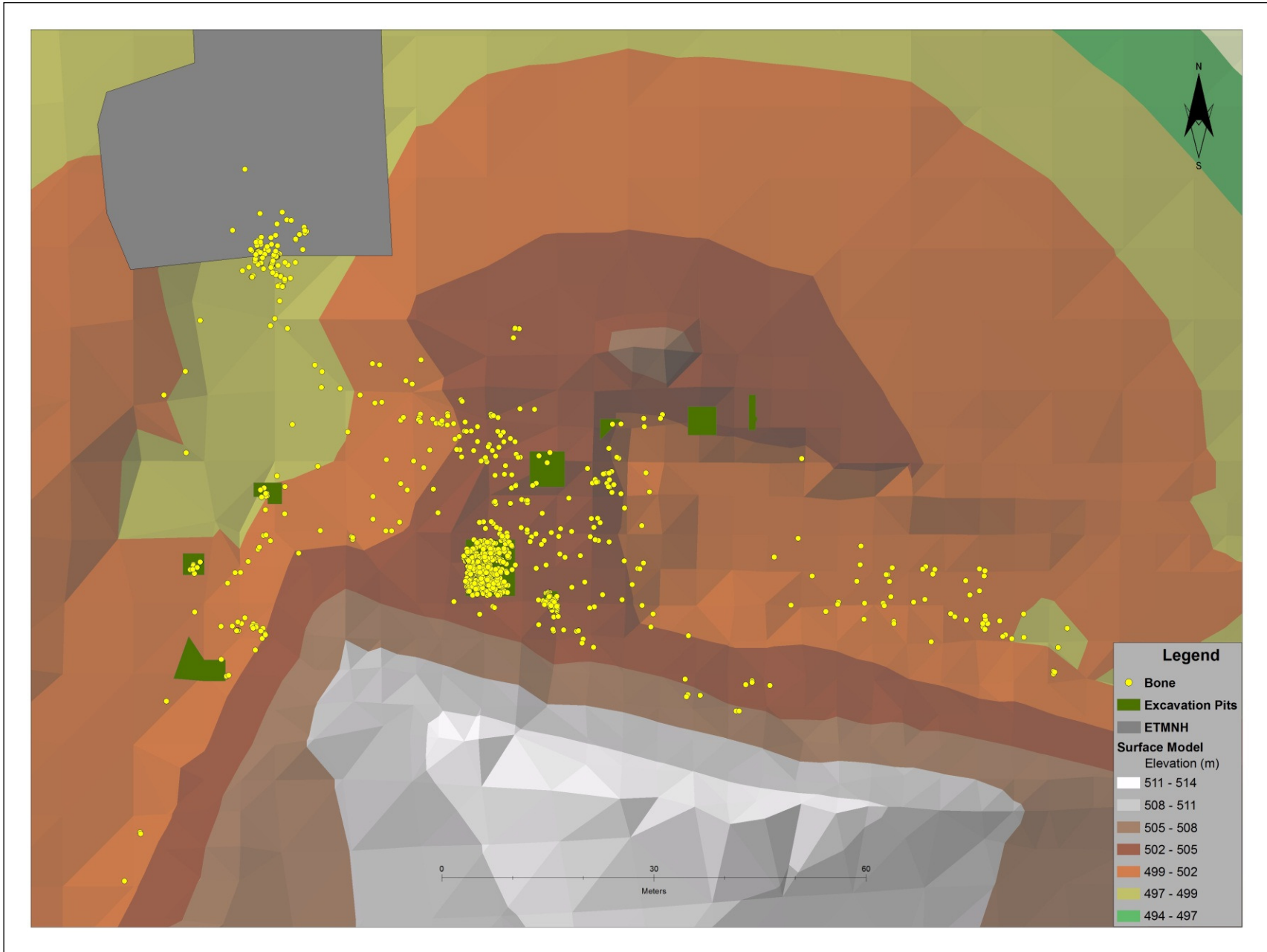


Figure 17: Spatial distribution of *Tapirus polkensis* bones at the Gray Fossil Site with weathering stage 1

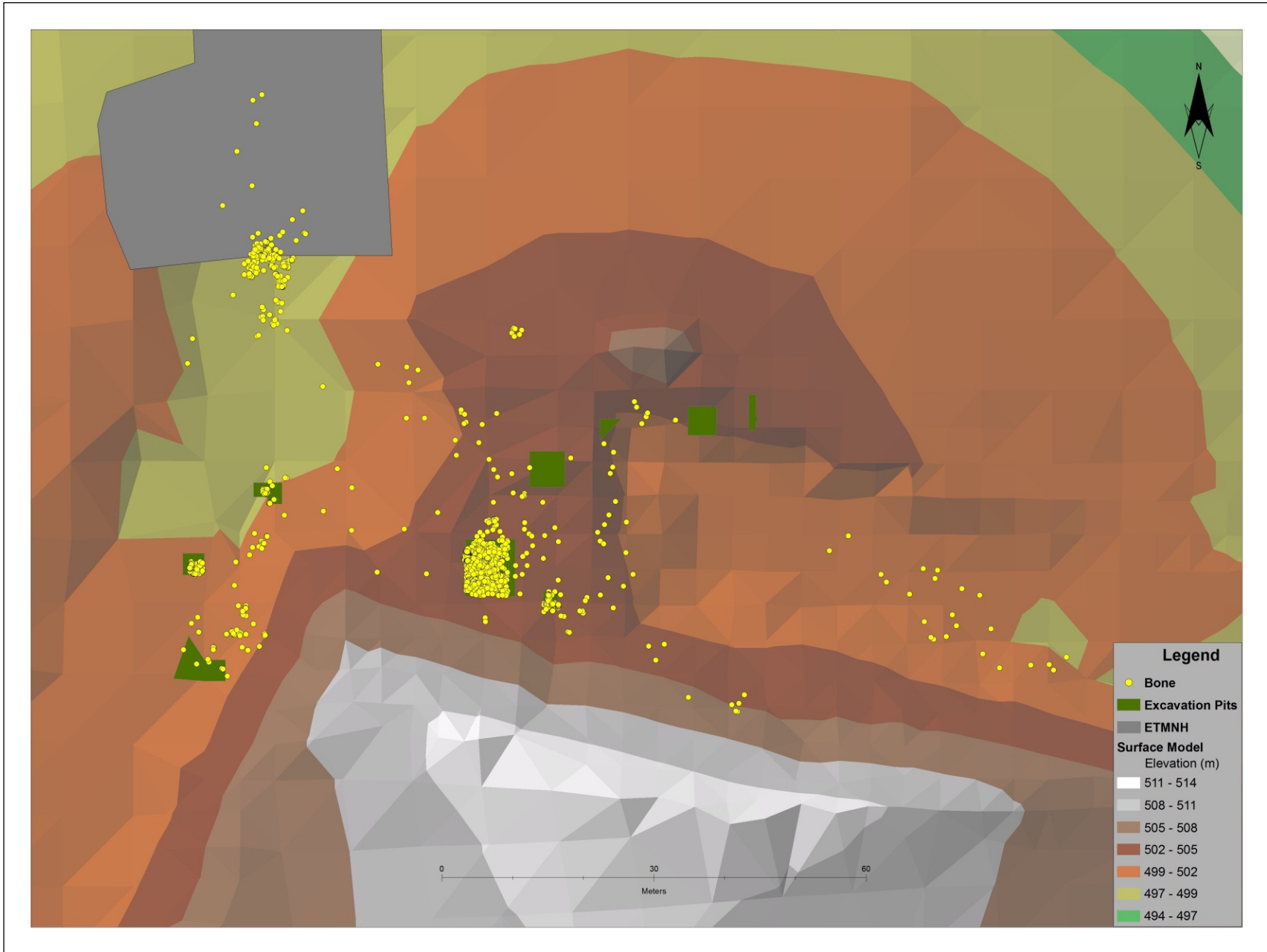


Figure 18: Spatial distribution of *Tapirus polkensis* bones at the Gray Fossil Site with weathering stage 0

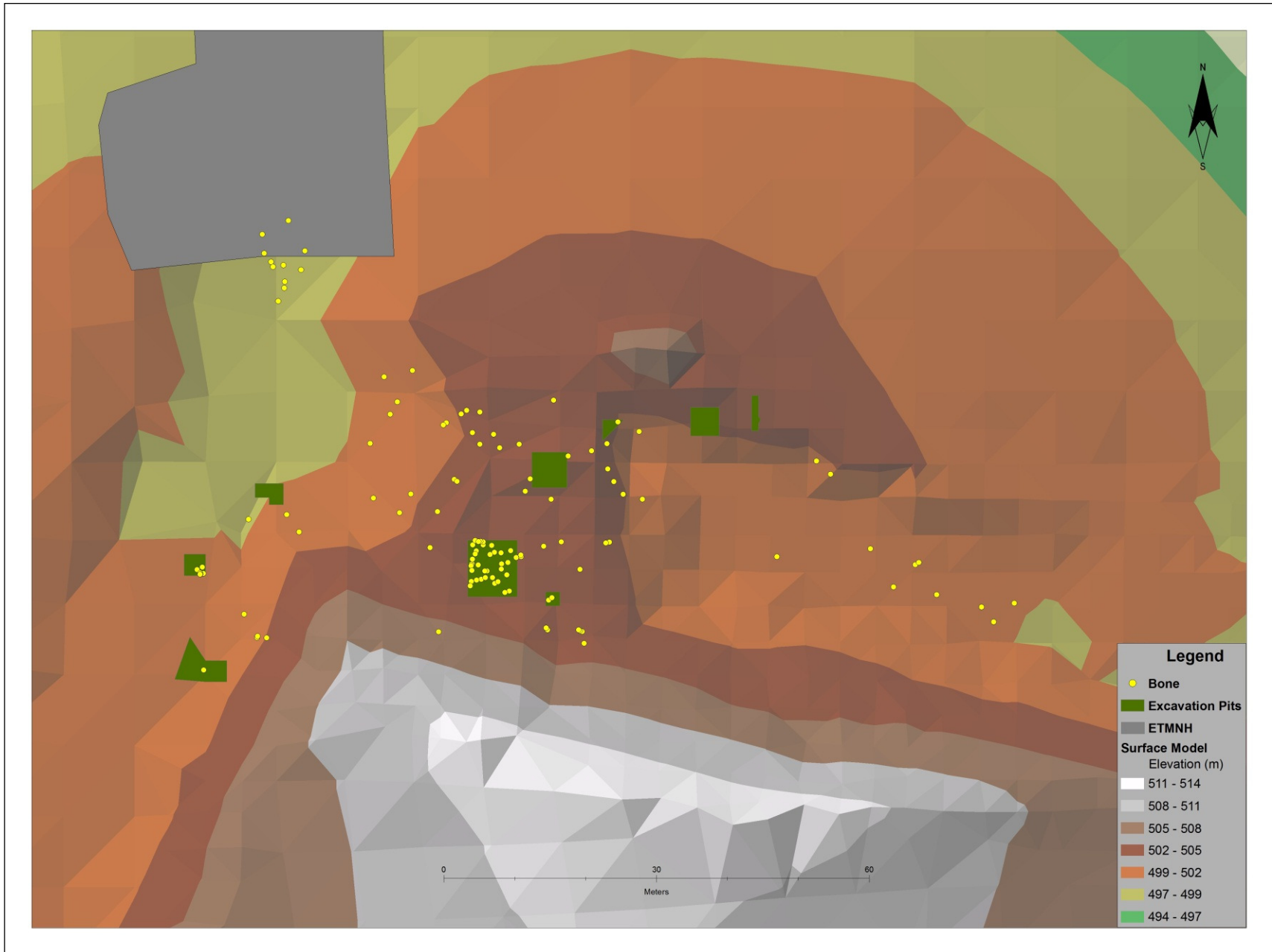


Figure 19: Spatial distribution of *Tapirus polkensis* bones at the Gray Fossil Site with weathering stage -1

Abrasion

No bones of *T. polkensis* observed in this study showed evidence of abrasion caused by eolian, fluvial, or trampling processes. Because of this, no maps were produced and the nearest neighbor program was not used.

Arthritis

Five levels of arthritis were found to occur in *T. polkensis* bones recovered from the site. This includes 2656 bones that showed no evidence of arthritis, 321 with very minor arthritis, 144 with minor arthritis, 22 with moderate arthritis, and 2 with extreme arthritis. Both bones with extreme arthritis were recovered in the vicinity of the rhino pit (Figure 20). They have a spatial pattern observed to be clustered (Table 12), although is not statistically significant in either dimension because a population of 2 observed points is insufficient at this level. Bones exhibiting moderate arthritis were found in three main areas including, around and within the rhino pit, the cat pit, and underneath the museum (Figure 21). Table 12 indicates that there are statistically significant clustering patterns in both 2D and 3D for these bones. Bones exhibiting the other 3 levels of arthritis are distributed throughout the site in a very similar pattern to that of the original 'Bones' Feature. Table 12 shows that these three levels form statistically clustered patterns, and this is supported by Figure 22 (map of minor arthritis), Figure 23 (map of very minor arthritis), and Figure 24 (map of no arthritis).

Table 12: Nearest neighbor statistics for the tapir bone arthritis levels

Type	Dimension	r_{obs}	r_{exp}	R	Z-value	p-value
Extreme	2nd	10.110453	31.327073	0.322739	-1.83231000	0.066905
	3rd	10.113101	14.624414	0.691522	-1.20032400	0.230013
Moderate	2nd	1.5036610	9.2378500	0.162772	-7.68131100	0.000000
	3rd	1.5249120	6.4790680	0.235360	-10.0897450	0.000000
Minor	2nd	0.9776730	3.6540640	0.267558	-16.9886770	0.000000
	3rd	1.0021650	3.4912640	0.287049	-23.7835860	0.000000
Very Minor	2nd	0.7007920	2.4425130	0.286914	-24.7438490	0.000000
	3rd	0.7320140	2.6690490	0.274260	-36.2191200	0.000000
None	2nd	0.3091510	0.8570710	0.360707	-63.2187130	0.000000
	3rd	0.3365490	1.3278320	0.253457	-106.177383	0.000000

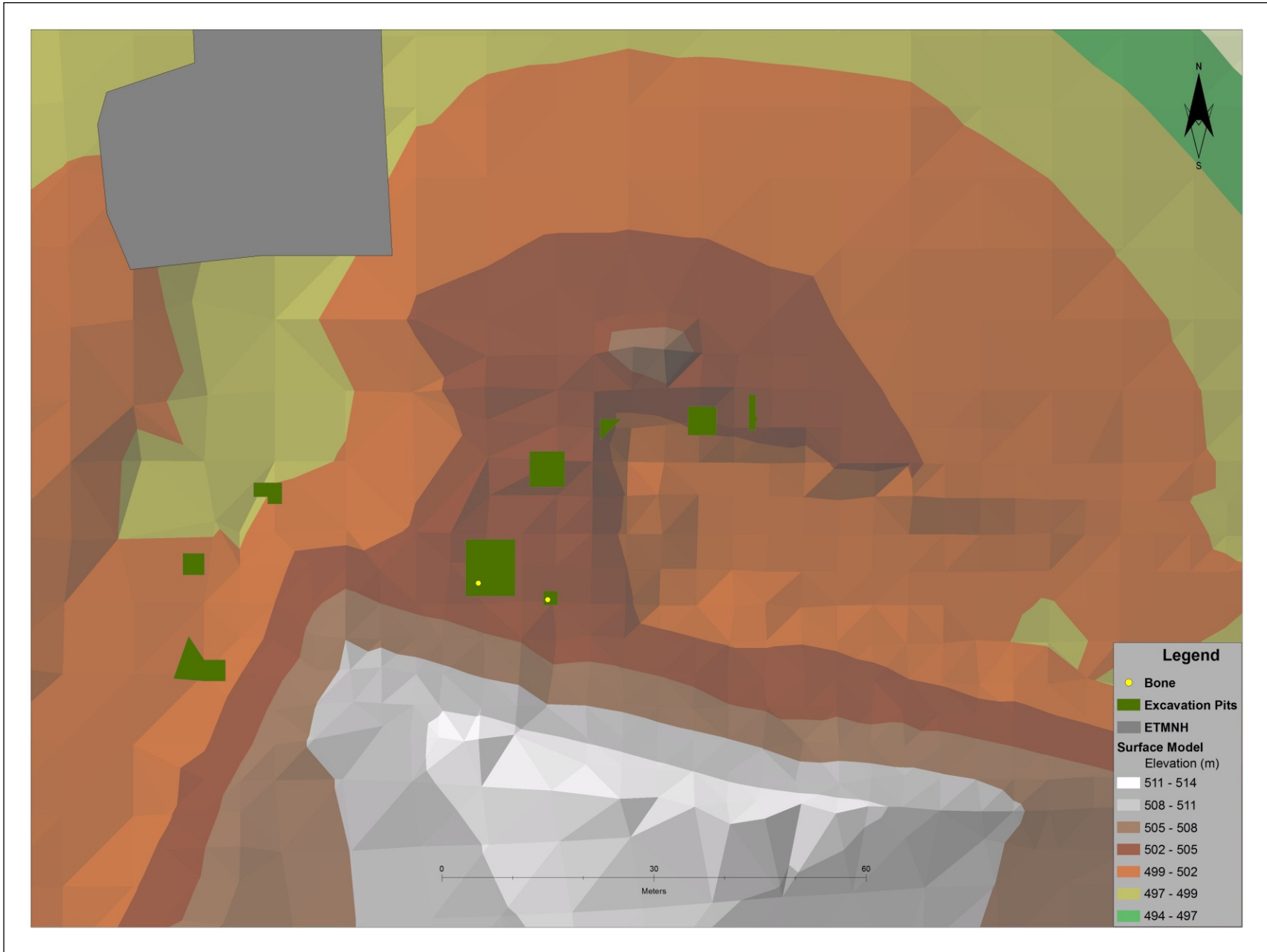


Figure 20: Spatial distribution of *Tapirus polkensis* bones at the Gray Fossil Site with extreme arthritis

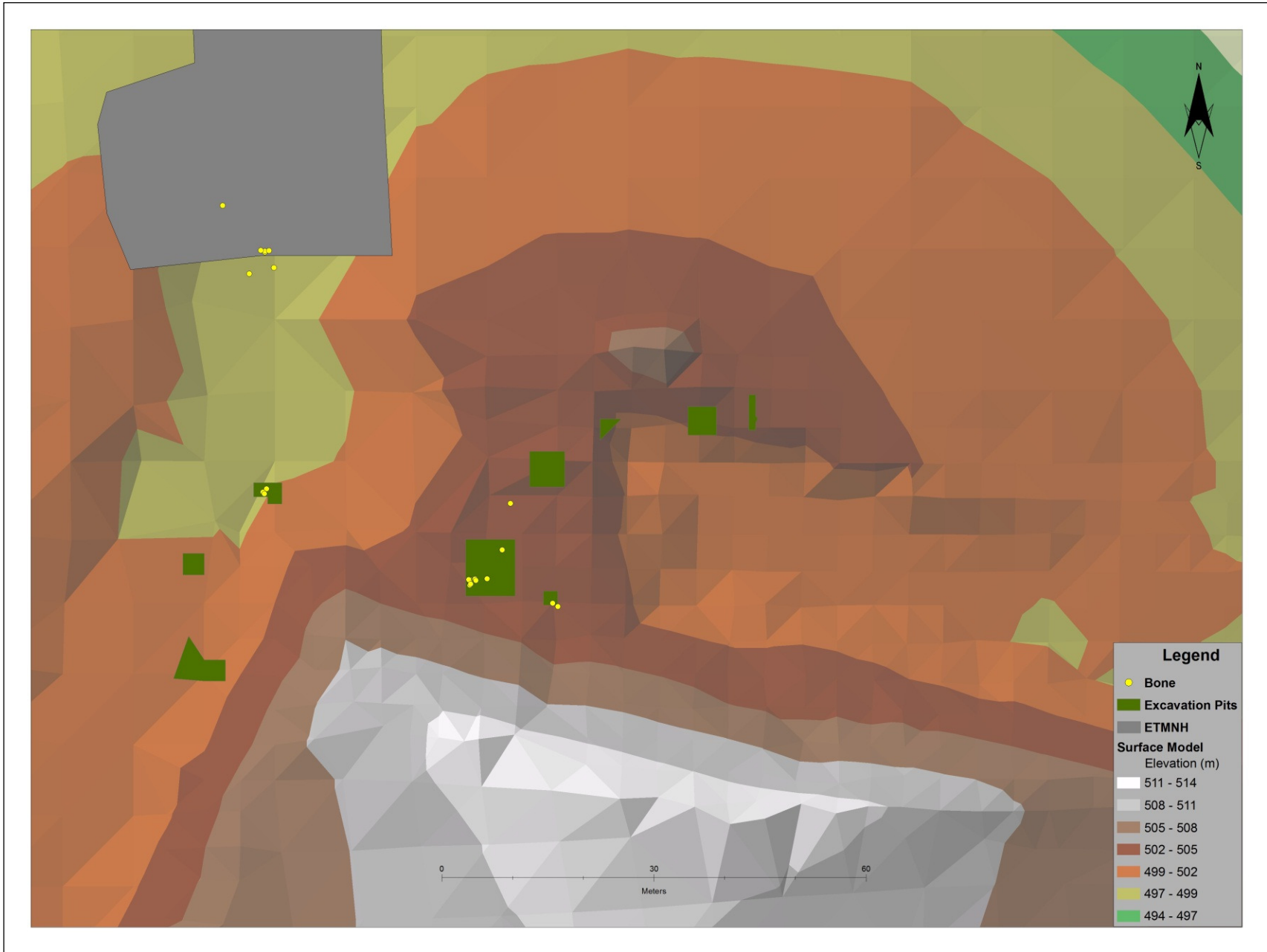


Figure 21: Spatial distribution of *Tapirus polkensis* bones at the Gray Fossil Site with moderate arthritis

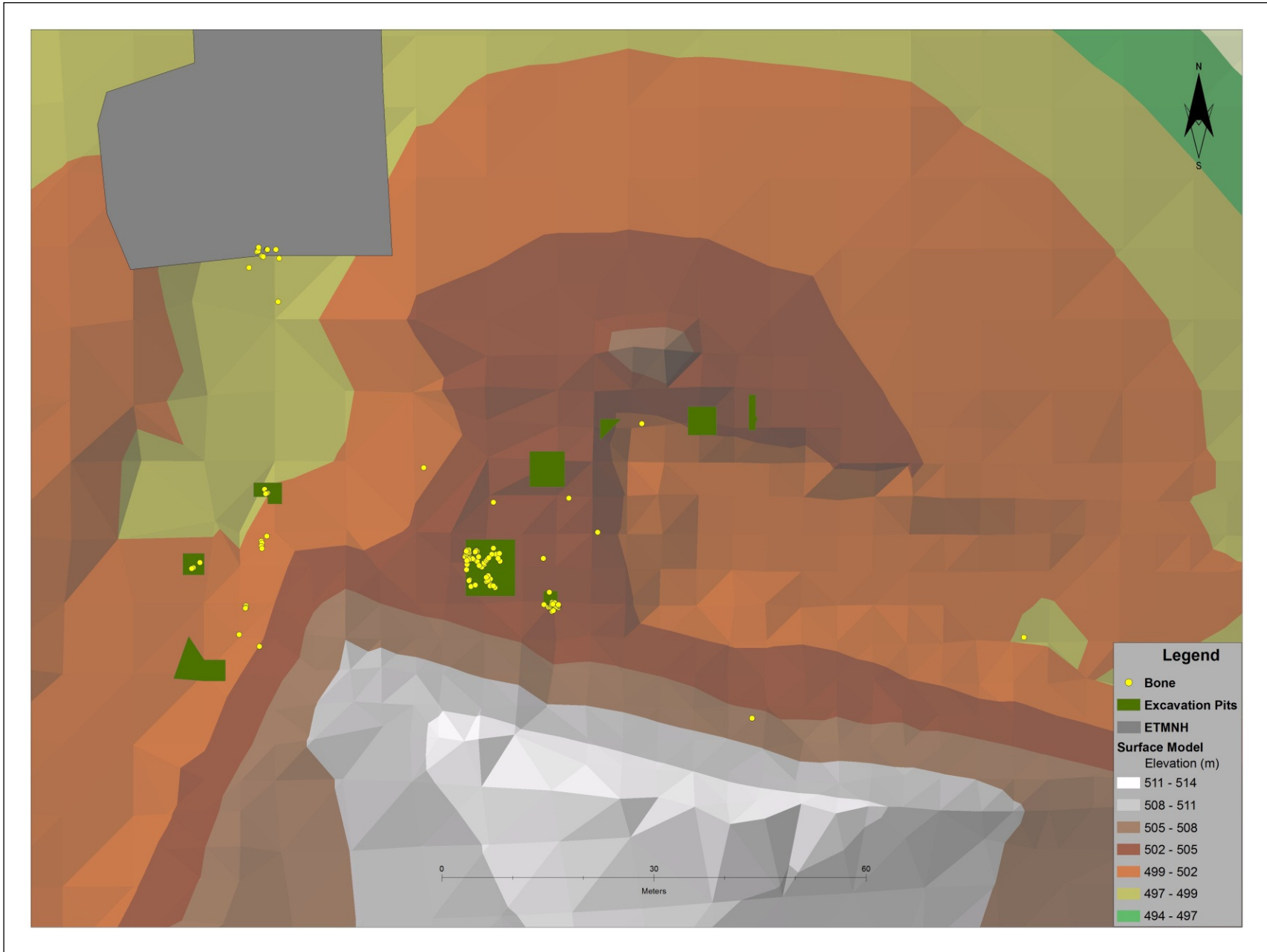


Figure 22: Spatial distribution of *Tapirus polkensis* bones at the Gray Fossil Site with minor arthritis

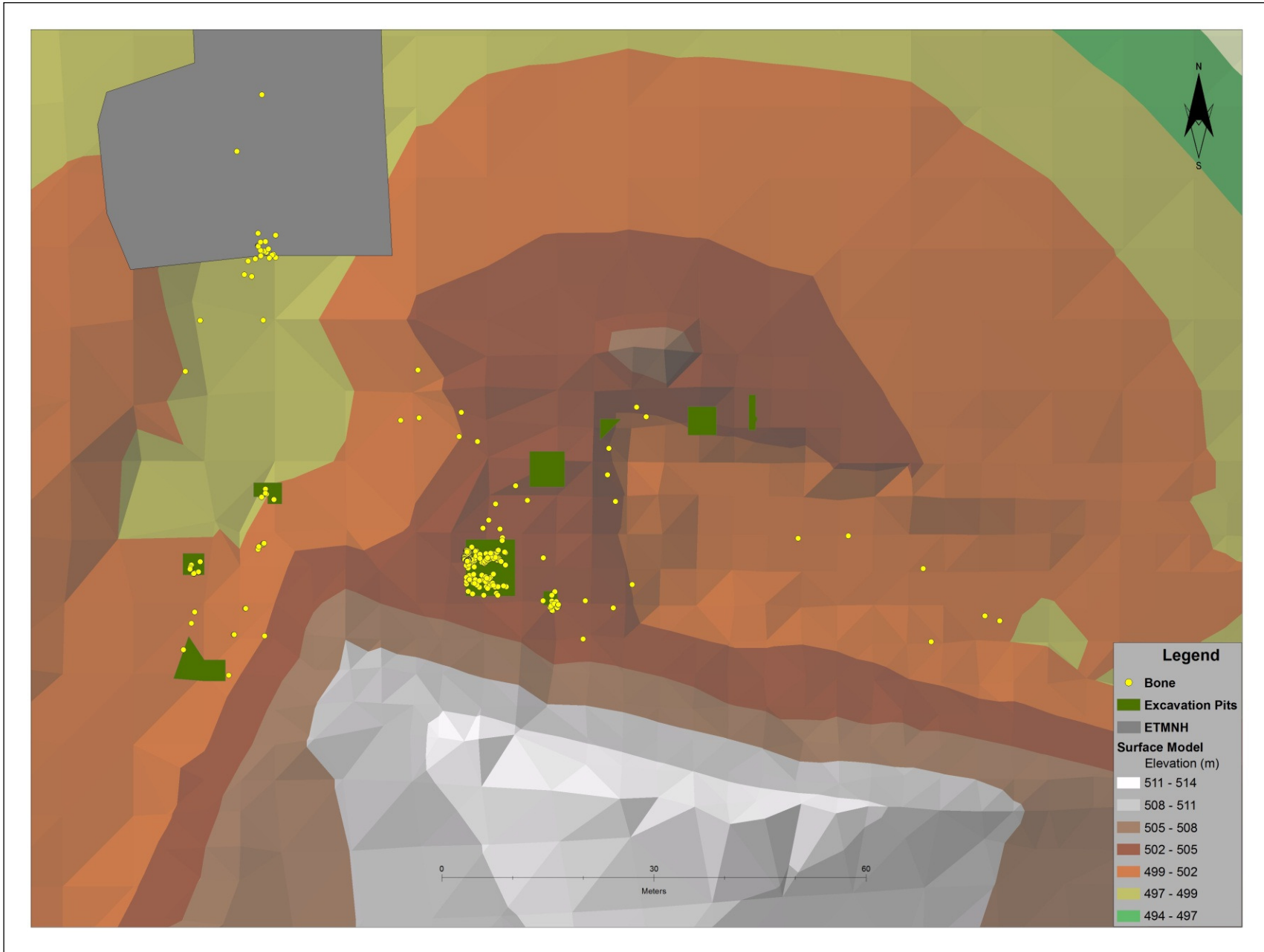


Figure 23: Spatial distribution of *Tapirus polkensis* bones at the Gray Fossil Site with very minor arthritis

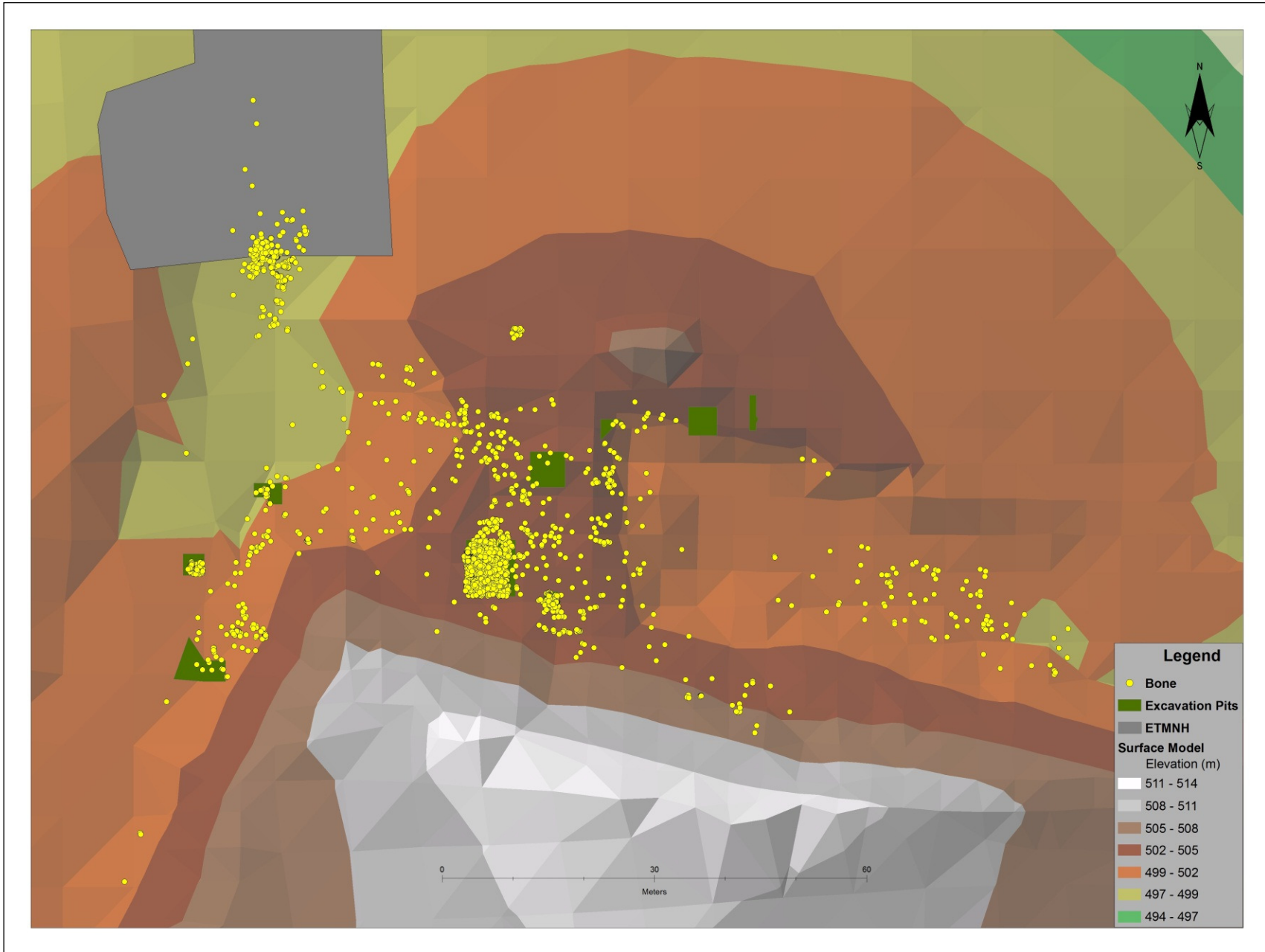


Figure 24: Spatial distribution of *Tapirus polkensis* bones at the Gray Fossil Site with no arthritis

Articulation

After observing all the bones of each *T. polkensis* specimen that had associated spatial data, 27 were classified as articulated, 72 as semi-articulated, and 1737 as isolated bone elements. Figure 25 illustrates that the fully articulated specimens were recovered primarily from the rhino pit and underneath the ETMNH building, with single articulated specimens recovered in the southwest and southeast areas of the site. These specimens are clustered in 2D but less so in 3D (Table 13). Semi-articulated specimens were found scattered throughout the site with a notable exception being the eastern area where no semi-articulated specimens have been reported (Figure 26). Table 13 indicates that this pattern is statistically clustered in both dimensions. Isolated bone elements occur throughout the site (Figure 27) and cluster in a statistically significant pattern in both dimensions.

Table 13: Nearest neighbor statistics for specimens from the three articulation states

Type	Dimension	r_{obs}	r_{exp}	R	Z-value	p-value
Articulated	2nd	4.450919	8.526149	0.522032	-4.751260	0.000002
	3rd	4.521033	6.141869	0.736101	-3.772940	0.000161
Semi-articulated	2nd	1.743365	5.221179	0.333903	-10.81264	0.000000
	3rd	1.826190	4.429054	0.412321	-13.72037	0.000000
Isolated	2nd	0.437995	1.063004	0.412035	-46.87905	0.000000
	3rd	0.476541	1.532811	0.310894	-79.02149	0.000000

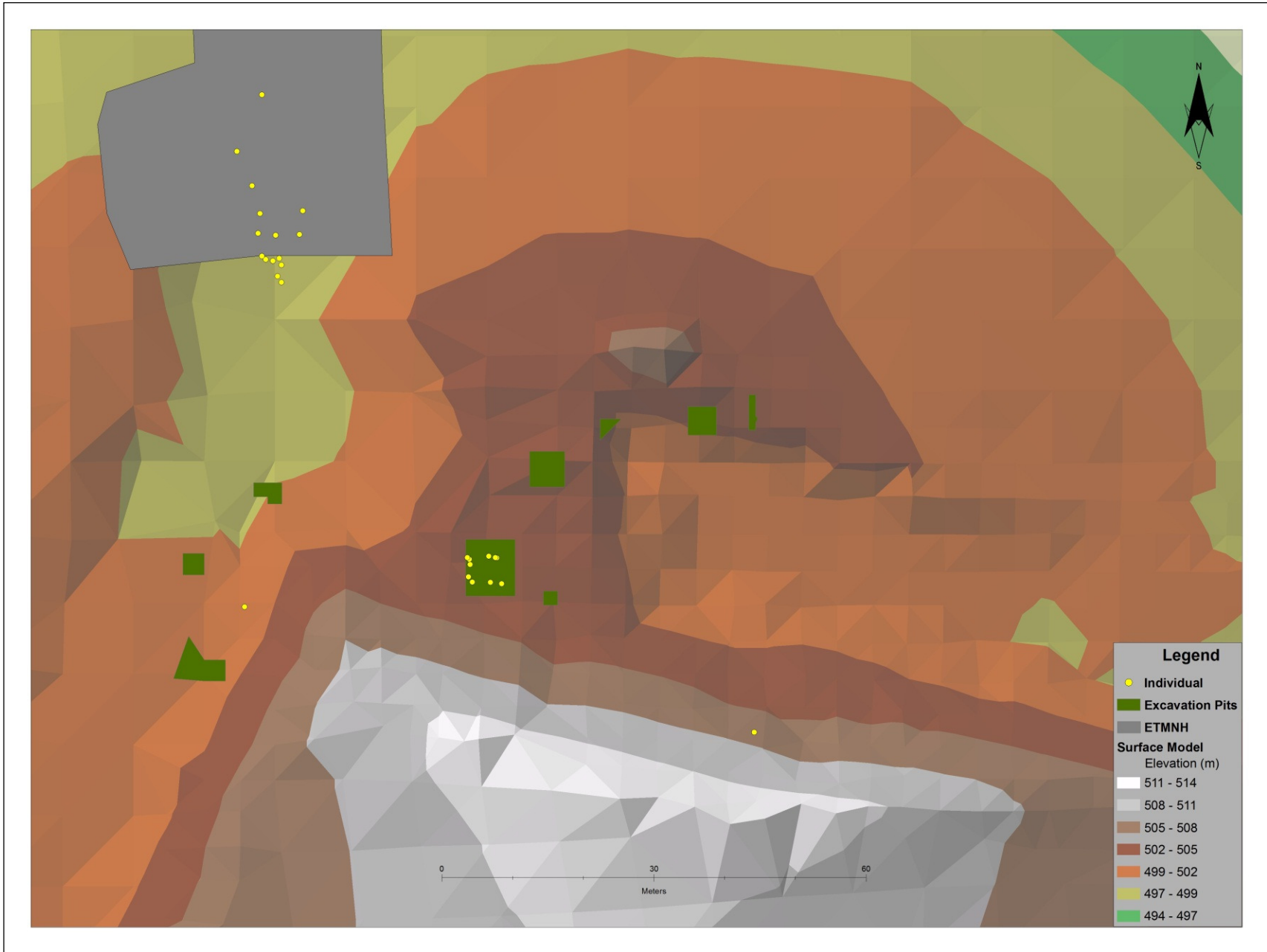


Figure 25: Spatial distribution of articulated *Tapirus polkensis* specimens at the Gray Fossil Site

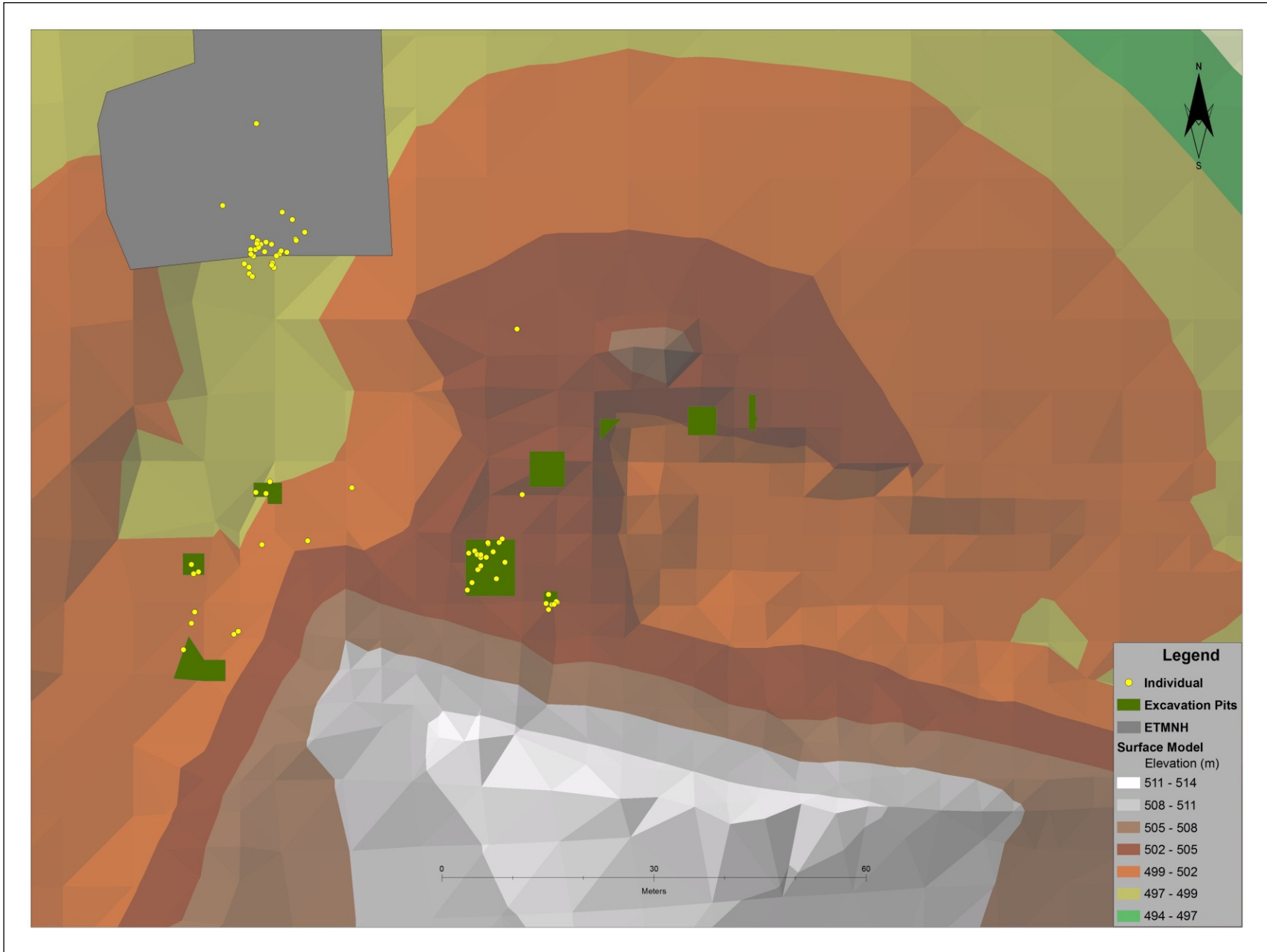


Figure 26: Spatial distribution of semi-articulated *Tapirus polkensis* specimens at the Gray Fossil Site

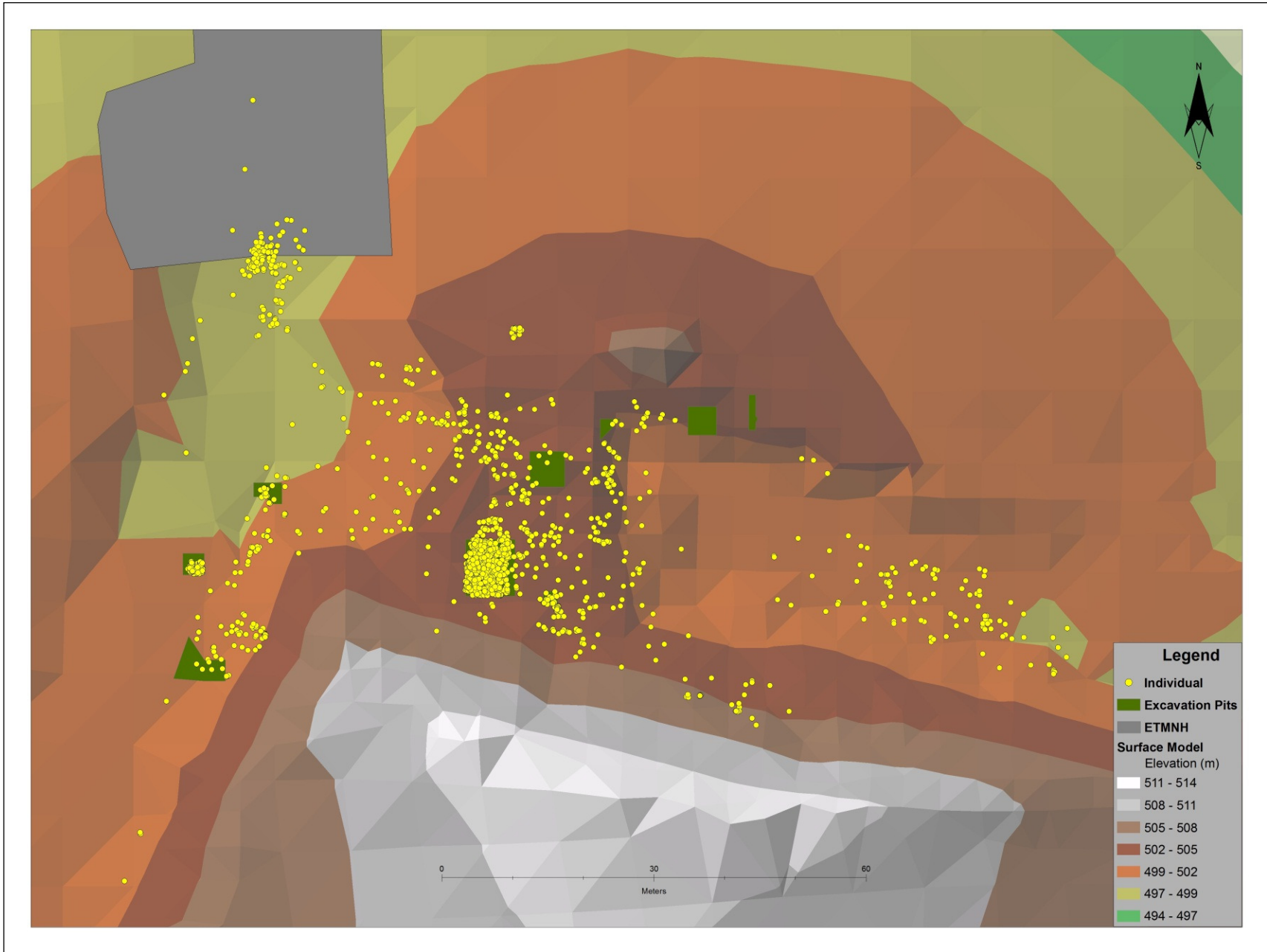


Figure 27: Spatial distribution of isolated *Tapirus polkensis* bone elements at the Gray Fossil Site

Age Class

Condensing the age classification developed by Hulbert et al. (2009) resulted in the use of four age classes in this study. These include adult, sub-adult, juvenile, and null (those specimens that could not be properly classified). Of the recovered specimens classified by age, 266 were identified as adult, 211 as sub-adult, 351 as juvenile, and 1008 could not be classified. Figures 28-31 show the 2D distribution patterns found at the GFS for adult, sub-adult, juvenile age classes, and those not determined, respectively. Table 14 indicates that these 2D patterns, and those documented in 3D, are statistically clustered, with R-values between 0.35 and 0.45.

Table 14: Results of nearest neighbor distribution by tapir age class at the Gray Fossil Site

Type	Dimension	r_{obs}	r_{exp}	R	Z-value	p-value
Adult	2nd	1.126502	2.716402	0.414704	-18.261828	0.000000
	3rd	1.191600	2.865022	0.415913	-26.210636	0.000000
Sub-adult	2nd	1.267541	3.049956	0.415593	-16.239900	0.000000
	3rd	1.354069	3.095002	0.437502	-22.481300	0.000000
Juvenile	2nd	0.945661	2.364728	0.399903	-21.508100	0.000000
	3rd	0.998857	2.612078	0.382399	-31.836100	0.000000
Null	2nd	0.605979	1.394036	0.434694	-34.369400	0.000000
	3rd	0.647614	1.836460	0.352643	-56.606200	0.000000

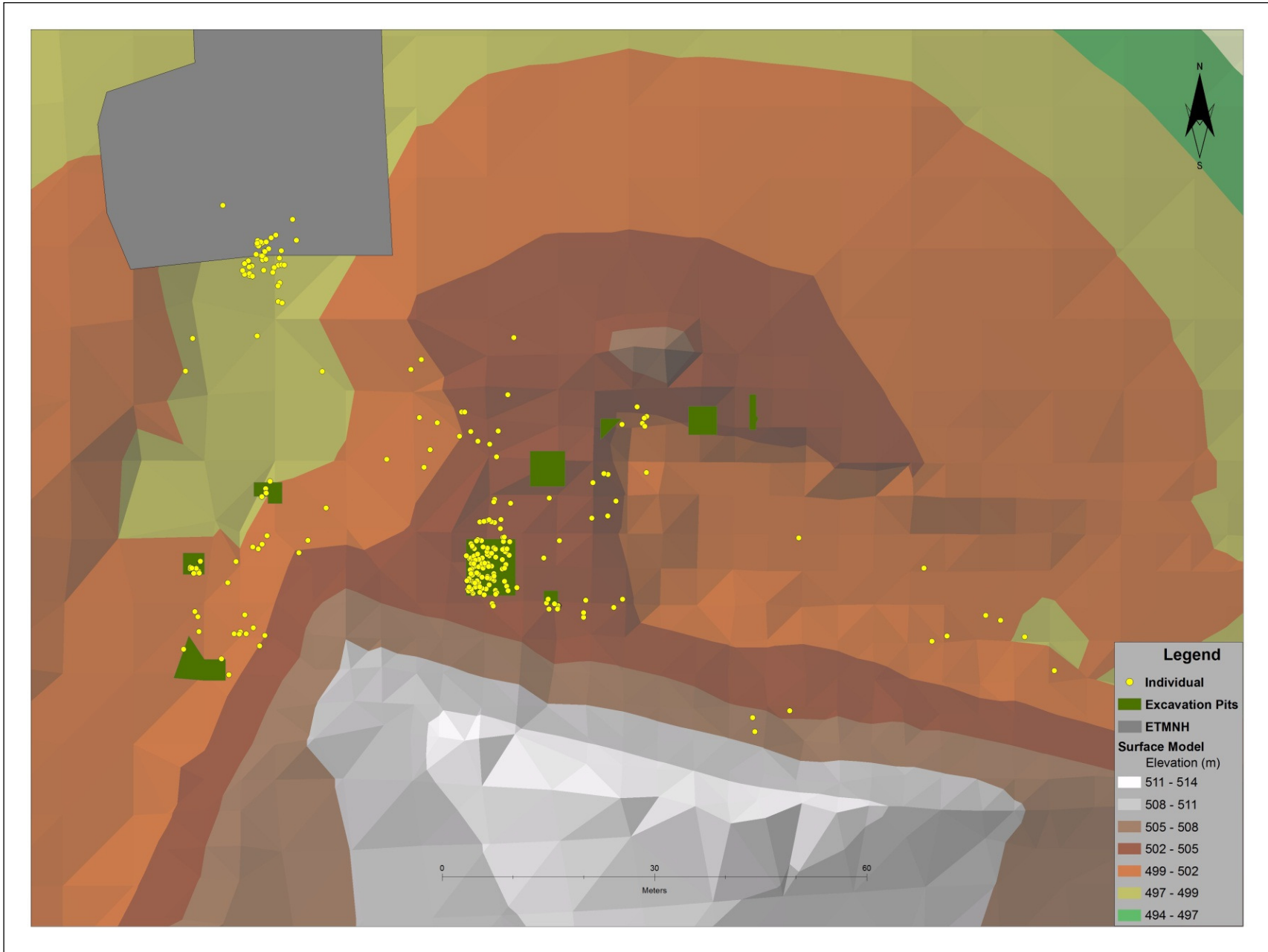


Figure 28: Spatial distribution of adult *Tapirus polkensis* specimens at the Gray Fossil Site

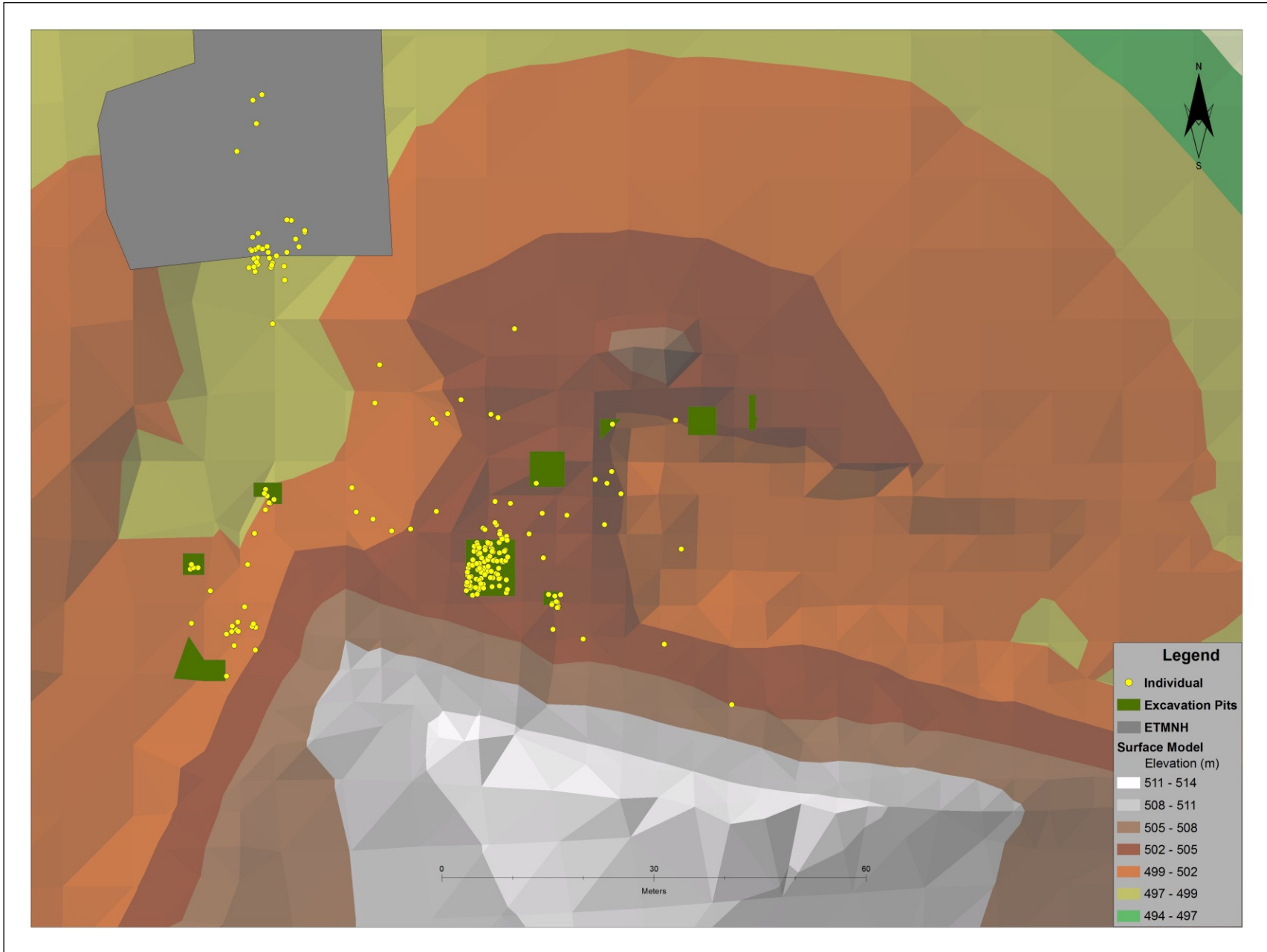


Figure 29: Spatial distribution of sub-adult *Tapirus polkensis* specimens at the Gray Fossil Site

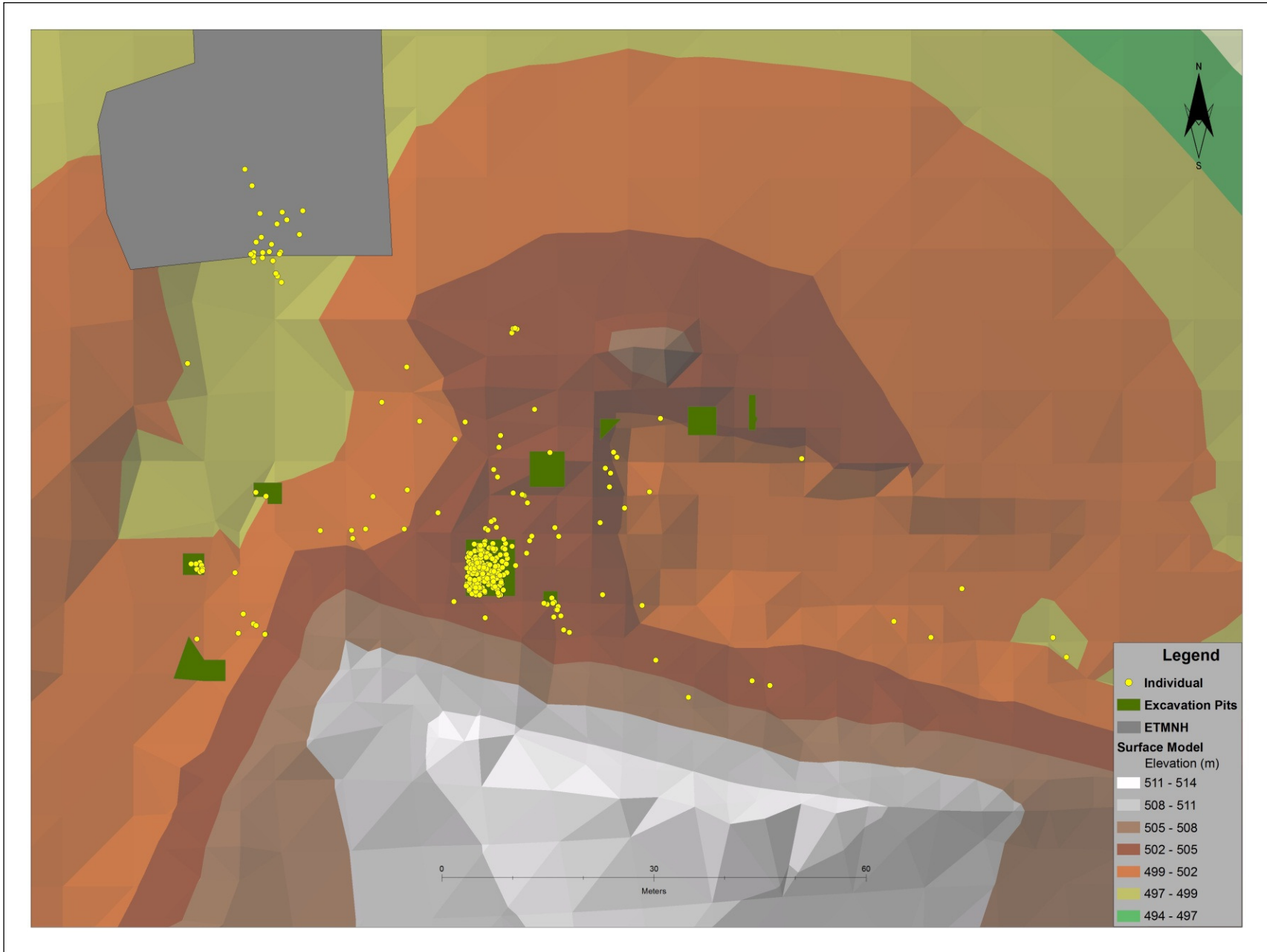


Figure 30: Spatial distribution of juvenile *Tapirus polkensis* specimens at the Gray Fossil Site

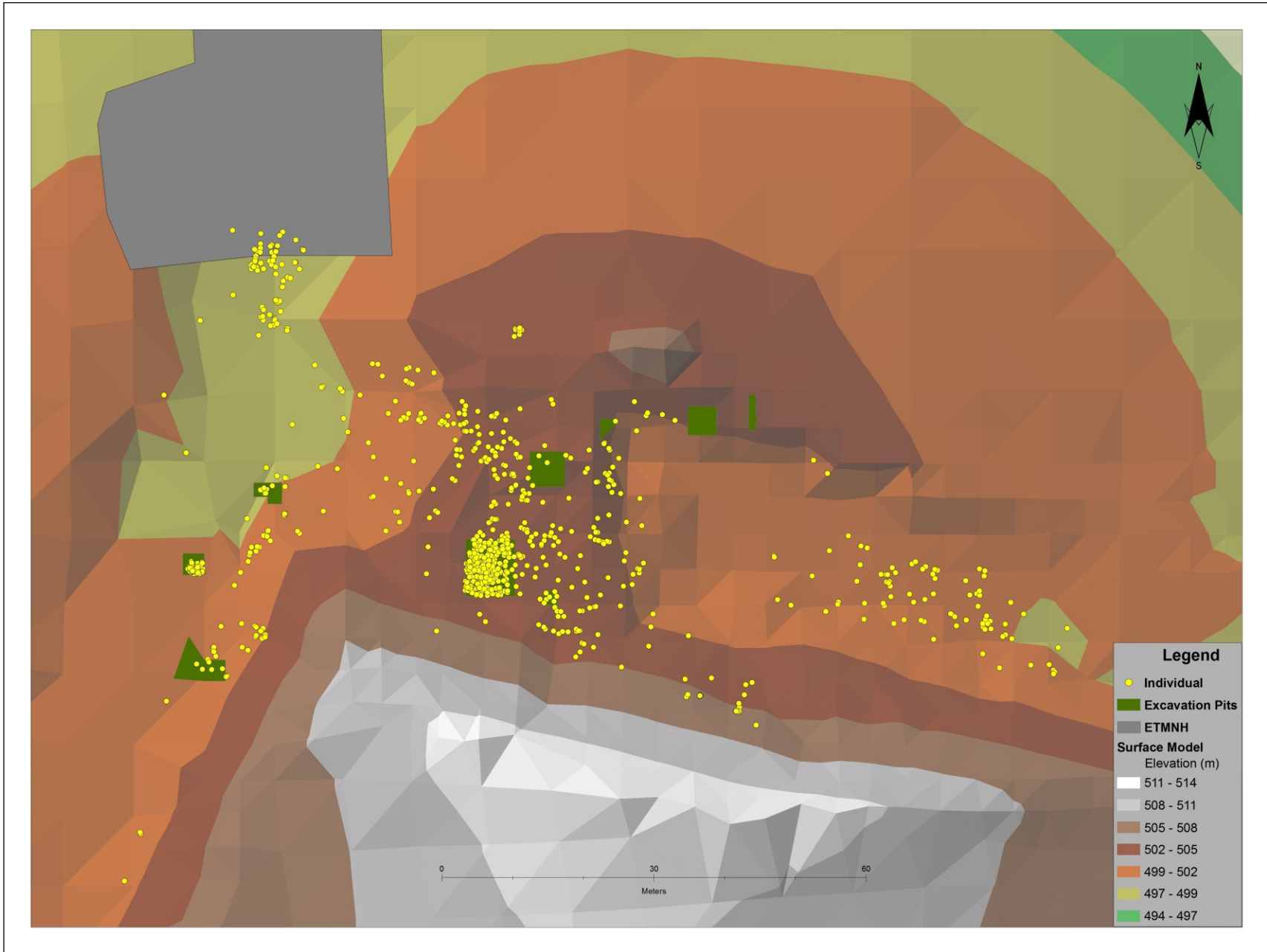


Figure 31: Spatial distribution of *Tapirus polkensis* specimens at the Gray Fossil Site that could not be classified by age

CHAPTER 5

DISCUSSION

Methods

ESRI ArcGIS software was used for this study for the following reasons: 1) the software allows all the major project components to be completed with one software package, 2) it has 3D analysis and visualization capabilities, 3) use of python code allows creation of new tools, 4) the software was accessible via ETSU's license, and 5) it is a leading software package in the GIS industry. In order to store the necessary data for this project into a format that ESRI ArcGIS could understand, a file geodatabase was created. This type of geodatabase was optimal for this project as there is no cap on the amount of data that can be stored. As the excavators at the GFS are continually recovering tapir remains, the ability for the database to expand and include all recovered taxa, as well as tapirs becomes very important. File geodatabases are also important because they allow the integration of both vector and raster data types (Childs 2009), enabling the survey data to be stored with the surface model. The surface model and the footprints of the ETMNH building and excavation pits were digitized in ArcGIS to provide a visual reference with which to identify spatial patterns. Specifically, the ETMNH building and pits were extruded from the surface model in order to provide the visual reference when viewing the data in ESRI ArcScene.

During this study, a system used in the collections became important when identifying which field numbers had spatial data associated and which did not. If a field number consisted solely of a date, then that bone was not represented by point data, whereas if the field number contained a date followed by a dash and a number (often 001

or similar), that bone likely also had spatial data associated with it. However, this was found to not always be the case. In addition, over the years some spatial data had been lost. Data from late 2002 to mid-2003 had been accidentally erased. Although redundant, the field number attribute was retained in the 'Bones' Table to allow quick identification of associated spatial data.

Averaging the survey data so that each bone and each individual specimen were represented by one point feature was done for three reasons. First, nearest neighbor analysis, using the program developed for this project, can only handle one input feature at a time. Bones, when excavated, were given anywhere from one to as many as a dozen points, depending on size. The ideal option for representing these features would be to create polygons or polylines for those with multiple survey points, while others would be represented by single points. However, this would cause bones from the same attribute class to be represented by different feature types and thus could not be analyzed. Second, leaving each bone represented by the original survey data, and in many cases by multiple points, would cause a bias towards clustering, as some points' nearest neighbors would be part of the same bone. Third, there would be the difficulty of trying to visually discern spatial patterns in such a high density data set, a problem clearly illustrated by examination of the excavated pit maps. For these reasons it was important to utilize one point for each feature mapped and analyzed at the GFS.

Classification Schemes

Based on the literature, there are two basic classification schemes that could be used for carnivore utilization: mark type (furrowing, scratches, etc.) or creator (cat, bear, etc.). As time was the important factor for classification of each bone, the mark type was

used. Weathering stages used were adapted from Behrensmeyer's (1978) work as it appears to be the only well documented sequence of weathering stages for large mammals. Because her observations were taken from carcasses exposed in multiple environments (swamps, savanna, lake beds, etc.) that are similar to those seen at the GFS, her general classification was adopted. The only major difference in weathering stage is an orange tinge found on some weathered bones which is assumed to be particular to the paleo-environment at the GFS. Isolated teeth were not classified in terms of weathering and were placed in their own category, as it was not possible to determine whether a particular tooth became isolated due to weathering of the jaw or skull, or simply fell out prior to death of the individual. The classification scheme for abrasion follows previous work outlined in chapter 2. Conclusions of those authors were matched with observations of bones recovered from the GFS but little evidence of abrasion was observed. Arthritis or arthritis-like pathologies were classified by extent of growth on articulating surfaces as this proved to be a simple way of evaluating the difficulty and pain an individual might have experienced while moving the joint. Origin of the observed arthritic growth was not evaluated. However, now that bones expressing high or moderate levels of arthritis have been identified, it will be easy for a researcher to find these elements in the GFS collections.

Following the classification schemes used for *T. polkensis* bone elements recovered from the GFS, are the two methods for classifying each specimen. The Hulbert et al. (2009) scheme, based on tooth eruption, was simplified into 3 categories in order to directly correlate them with the 3 levels of epiphyseal fusion of Grossman (1938). An inherent assumption in doing this is that both the distal and proximal epiphyses of each

bone, whether vertebrae or long bones, fuse at the same time or rate, and that they correlate with the timing of tooth eruption. Assignment of skeletal articulation state was based on the association of material with a specific ETMNH specimen number, assuming that elements from various parts of the body were found in correct anatomical position during excavation. However, the only way to confirm this would be to map every bone from that specimen separately. With this in mind, use of the terms “articulated”, “semi-articulated”, and “isolated” to classify each specimen allows their degree of disarticulation or scattering to be easily categorized.

Nearest Neighbor Statistic

The nearest neighbor program as designed quantifies spatial patterns found in both the 2nd and 3rd dimensions and determines whether these patterns are statistically significant. Unlike other spatial statistic tools, the nearest neighbor program does not aide in visualization of the patterns found but requires the point pattern to be determined by the researcher. Written for stand alone use in the Python GUI and being designed to perform only what is necessary to complete the NN statistic, the script has not been adapted for use within ESRI ArcGIS. As the author of this script has been the only one to use it in practice, error handling has not been implemented and thus no specific error messages will show, and the program will simply stop running if an error occurs. Calculation of area and volume for various point sets performed within the program also have not been implemented as the complexities of computational geometry (required for the minimum convex hull to be determined) have been deemed too great for current purposes and are reserved for such external programs as qhull.

By omitting error handling from the script, a phenomenon was discovered when the nearest neighbor statistic was calculated for point sets containing a single point. As Table 10 shows, the R statistic is a negative value for both of the point sets containing bones with signs of carnivore utilization. Cause of this was discovered when researching how the Near3D tool functions and it was found that when the near tool does not find a neighbor for a particular point, it gives a value of -1 as the distance. As both the puncture and pitting sets contain only one point each, and thus no neighbor, both were given near values of -1 in the 2nd and 3rd dimension. Due to there not being any error handling for the nearest neighbor script, calculations using the -1 value were performed and resulted in negative R-values. Although this outcome could be prevented by requiring a minimum number of points to run the analysis, the incorrect results were included in this study to illustrate this issue. Another issue detected was how the boundary or edge of the study area may affect the results of nearest neighbor analysis, and that points lying outside the study area might influence results. However, as the GFS ultimately has a discrete boundary (the paleo-lake shoreline) there will not be any outside points and therefore this can be ignored.

Due to a lack of GIS software capable of performing the nearest neighbor statistical analysis in the 3rd dimension, the results from this study were not able to be compared to other studies. However, as ESRI ArcGIS is capable of calculating this statistic in the 2nd dimension, the bones point set was analyzed using both ArcGIS and the script written for this project. As Table 15 shows, the resulting R statistic is close to the same for both programs with similar Z- and p-values. It is also important to note that results from the nearest neighbor calculation for each GFS point set analyzed can be

directly compared without using further statistics (such as the t-test), as using the same volume and area values for each point set produces a direct correlation to spatial distribution. As demonstrated, the nearest neighbor program allows a simple yet robust method for quantifying the bone and specimen spatial distribution patterns at the GFS. However, more work must be completed for this program to be used by others. The script should be adapted to be used within other GIS software packages, such as ESRI ArcGIS, and to notify the user with error messages when specific parameters are not met.

Table 15: 2D results for the NN statistic from the NN script used in this study and that of the ESRI ArcGIS NN tool

NN Program	Dimension	r_{obs}	r_{exp}	R	Z-value	p-value
Built in this study	2nd	0.129421	0.558522	0.231720	-116.585	0.000000
	3rd	0.139564	0.998065	0.139835	-187.731	0.000000
ESRI ArcGIS	2nd	0.119896	0.558522	0.214666	-119.173	0.000000

Issues with Extent of Current Excavation

A major issue that results from carrying out a spatial analysis early in the GFS site excavation process is the strong bias towards a clustered pattern of the recovered bones because they were recovered from a small number of pits and not from an evenly distributed dig pattern across the whole site. This situation causes the majority of point sets analyzed to have R values of between 0.2 and 0.4 with z-values indicating that the clustered distribution is statistically significant and limits interpretation of finer scale distribution patterns. Therefore, interpretation of the taphonomic processes in the following sections were made by considering general patterns across the site and the occurrence of bones with unique attribute classes within each pit. Once the entire site has been excavated, any significant distribution patterns will be the result of natural processes and not a sampling bias.

Another problem that must be taken into account when interpreting the pattern of tapir bone distribution is that the points in the eastern part of the site represent bones that were recovered from a spoil pile and not *in situ* (indicated by Figure 7). It is unknown why these points are still included in the main database of surveyed recovered bones without any indication that they were not recovered *in situ*. However this issue was not brought to the attention of the author until after all analyses were completed. It is possible that these data may be useful in the future, but at this time there appears to be no practical use for these data. No important attribute classes were discovered in the spoil pile bones, so their inclusion in the data set does not affect my interpretations.

It is important to note that there were no evident patterns associated with differences in elevation at which bones were discovered. This is most likely due to the site only having been excavated to a depth of 1-2 meters. Consequently, the 3D aspect of this analysis more of a novelty at this time, but because the site is at least 39 m thick, 3D patterns will likely become more important as the site continues to be exhumed. However, another aspect of the site that must be taken into account is that bones from different depths and elevations were deposited at different times. This means that any studies applying 3D analyses must incorporate stratigraphic controls that acted upon the fossil assemblage.

Taphonomic Interpretations

Carnivore Utilization

Regardless of what carnivore taxa were active at the GFS, carnivore utilization does not appear to be a dominant taphonomic control on bone preservation, as only 2 of the 3145 tapir bones studied show signs of utilization. A few other tapir bones have been

recovered that exhibit carnivore utilization, but these do not have associated spatial data and therefore were not included in this study. Even with the addition of these other carnivore utilized bones, there is still a lack of material and this may be due to four possible reasons:

- 1) There was simply a lack of predation or scavenging occurring during the deposition of the site and individual tapirs died from other causes. Gibson (2011) shows that the recovered tapir material represents a stable population consistent with the paleo-lake as their natural habitat.
- 2) Bones that received damage from crocodylians may have been quickly destroyed post-digestion, as crocodylian stomach acid has a very low pH and makes consumed bones susceptible to rapid weathering and decay (Blumenshine et al. 1996; Fernandez-Jalvo et al. 2002).
- 3) A high supply of prey and easy access to young and old individual tapirs might result in predators not needing to utilize bones for nutrients and sustenance (Haynes 1988).
- 4) Bones that were utilized may have been overlooked due to the small size of utilization marks or similarity to other bones damaged by abrasion, trampling, or other causes. As indicated previously, bears often crush bones causing them to appear simply broken and cats may sever the ends of long bones with cheek teeth that leave clean cuts along the remaining piece (Haynes 1983).

The third scenario seems the most likely to have occurred at the GFS as there are remains from large carnivores as well as a stable population of tapirs with juveniles and old adults present.

Spatially, both carnivore utilized bones were recovered from the rhino pit, which, based on TDOT core logs, is located over one of the thickest parts of the deposit, and likely represents a deeper part of the paleo-lake. It is possible that the atlas puncture is a result of predation by an alligator during either the initial takedown or dismemberment. The circular puncture with no bisection suggests this mark was caused by an alligator. Alligators often attack from the water, dragging their prey into deeper water and dismembering large chunks from the carcass (Blumenschine et al. 1996). At this time the cause of such severe pitting on the rib (ETMNH 3808) is unknown. Such heavy utilization is often associated with predator dens and cave sites, but neither of these has been discovered at the GFS.

Weathering

Figures 13-19 indicate a pattern where higher stages of weathering are best represented around the rhino pit, with a few others scattered throughout the site. This pattern, along with the occurrence of bones showing carnivore utilization, appears to correlate with what could be the deeper parts of the paleo-lake. Although the more strongly weathered bones are clustered in one or two specific areas, those with lower weathering levels are dispersed throughout the site creating a homogenized mix of weathering stages. Behrensmeyer (1978) indicates that a homogenous mixed pattern is due to long-term accumulation of fossil material over an area and the differences in weathering stages is the result of micro-environment changes over time. Bunn and Kroll (1986) point out that this pattern measures duration of bone exposure as opposed to the bone accumulation period as bones from the same specimen often exhibit different

weathering stages. However, burial processes seem to dominate at the GFS, while Behrensmeyer's work emphasizes exposed or erosional environments.

The Gray Fossil Site sediments have been interpreted to be of lacustrine origin based on the taxa preserved (Wallace and Wang 2004) and the sediment deposited (Shunk et al. 2006). As Behrensmeyer (1978) shows, it is also possible to use the distribution pattern of weathered bones to indicate the depositional environment they were exposed or buried in. Figure 32 is a comparison of the GFS bone population stage of weathering with that of Behrensmeyer (1978), which documents population of the number of bones for each weathering stage versus each depositional environment. It is clear that the GFS pattern does not resemble any pattern from Behrensmeyer's Amboseli National Park, Kenya studies. This may be due to the GFS occurring in a deposition dominated environment as indicated by the high number of bones that lack any weathering. Assuming that all bone elements of *T. polkensis* weather at the same rate, the GFS pattern from Figure 32 may also indicate the amount of time (in years) each specimen was exposed (Gifford 1981). However, due to the differences in climate between Tennessee and Kenya it is hard to estimate how much longer the bones in Tennessee would need to be exposed in order to attain the same weathering patterns found in Kenya.

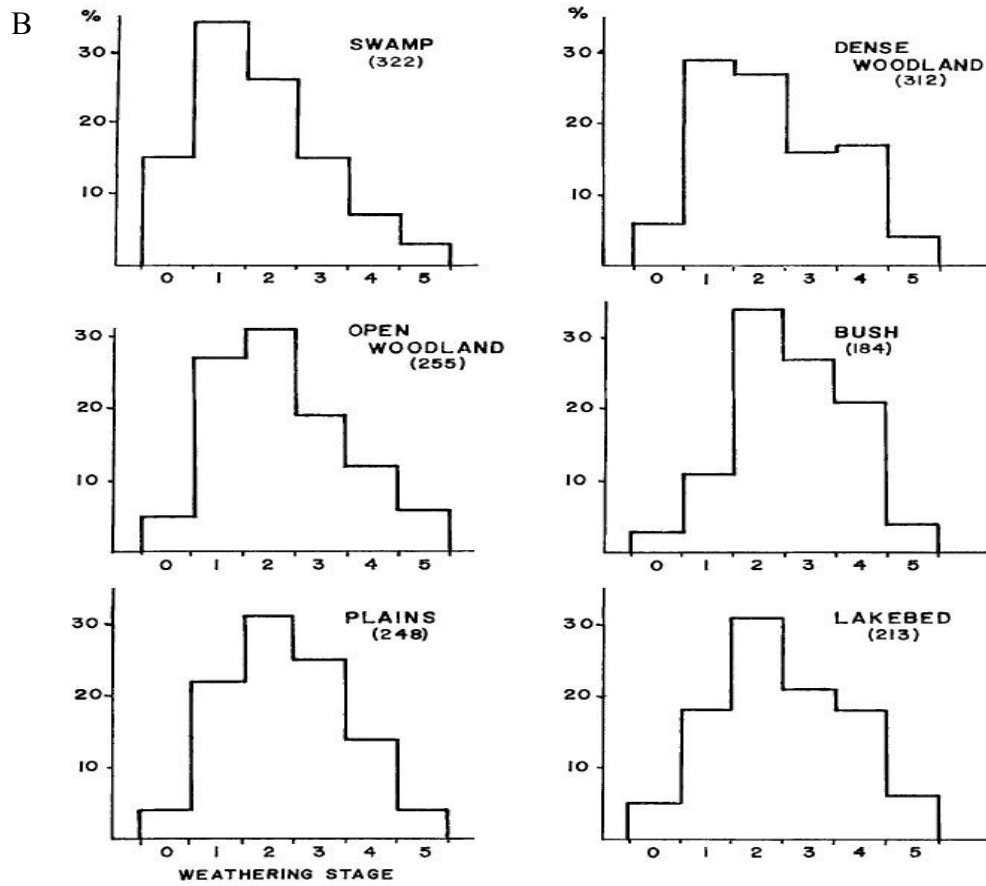
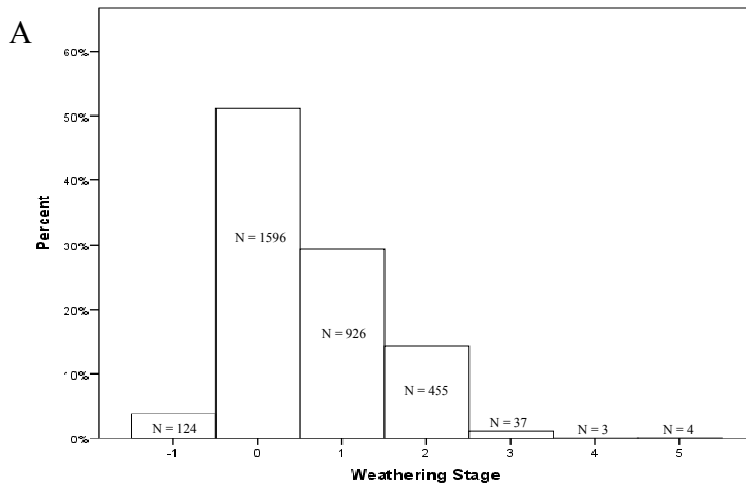


Figure 32: Comparison of A) percentage of bones with the weathering stages defined for the Gray Fossil Site, and B) percentage of weathering stages for each habitat studied in Kenya by Behrensmeyer (1978).

Abrasion

As no tapir bones showed signs of modification by fluvial or eolian processes, abrasion was not considered to be a factor as a taphonomic process at the GFS. This suggests that very little, if any, of the bones were transported, and furthermore that the tapirs represented an autochthonous group, confirming the stable population hypothesis of Gibson (2011). As abrasion due to trampling is hard to discern in the fossil record, it is unclear if trampling was a contributing process or even occurred (and was unlikely to occur in deep water in the paleo-lake). Further research using GIS to map the orientation of fossils at the site could be used to determine whether transportation or trampling did occur, as both processes cause preferred bone orientations (Olsen and Shipman 1988; Bonfiglio 1995). This would be possible if the trend of each bone's orientation was measured and correlated to any identified patterns.

Arthritis

Osteoarthritis or arthritis-like pathologies are not typically considered a taphonomic process and are usually studied within paleoecology; as it often indicates variation of behavior of animal taxa. However, this condition is considered a taphonomic process in the sense that it biases certain specimens to be susceptible to true taphonomic processes. For example, it may cause an individual to become weaker and more susceptible to predation and thus skew number of specimens towards older tapirs (Peterson 1988), loss of bone density could cause more rapid weathering or abrasion (Bartosiewicz 2008), and lipping at articulating surfaces may leave certain specimens more intact or articulated (Greer et al. 1977). At the GFS, tapir specimens with extreme to moderate arthritis (Figures 20-21) appear to be concentrated in four primary areas, (i)

the rhino pit, (ii) the tapir pit, (iii) underneath the ETMNH building, and (iv) the cat pit, while those showing lesser evidence for arthritis (Figures 22-23) are dispersed over the entire site.

It is unclear as to what may have caused this pattern, as the pathology of each specimen is unknown. Only one of these areas has a single carnivore utilized bone and it does not show any sign of arthritis. It is unlikely that this individual died due to predation, although as previously discussed, the lack of material with predation markings does not necessarily mean that predation was not an important process at the site.

Although a few bones with very minor to moderate arthritis also express weathering stages 1-2, there does not seem to be a strong correlation and each attribute's spatial clustering only overlaps around the rhino pit. Also, as no tapir bones with abrasion have been found at the GFS, arthritis does not correlate with that weathering either. Adult tapirs constitute the majority of specimens with moderate to extreme arthritis and most likely correspond with old age; while only two sub-adults have these levels, possibly due to pathological injuries. Of the 611 bones from articulated specimens, only 7 exhibit extreme or moderate arthritis levels, suggesting that arthritis does not appear to influence whether a specimen remains fully articulated after death.

Articulation

Based on Figures 25-27 there appears to be a trend with the majority of articulated and semi-articulated specimens clustered in three areas, the rhino and tapir pits; the cat and elephant pits; and underneath the ETMNH building. It is important to note that the association of bones to a tapir specimen involves a certain degree of error, as the high density of *T. polkensis* specimens sometimes makes association of individual bones to a

specimen difficult. Regardless, the fact that both articulated and semi-articulated specimens are found in three main areas suggests that they are areas of passive deposition with little influence from other taphonomic processes. As only 138 of 1143 bones from articulated or semi-articulated specimens exhibit a weathering stage > 1 , these specimens were most likely buried relatively quickly. Behrensmeyer (1975) indicated that a specimen that resides in water postmortem disarticulates over a period of 1-3 months. This would suggest that specimens recovered from these areas were exposed for at least a few months before burial. The lack of elements with damage due to abrasion or carnivore utilization suggests that these are not important controls on bone element disarticulation although as discussed earlier, trampling as a taphonomic process needs to be analyzed further before it can be discounted.

Age Class

Based on the dispersion of all age classes throughout the deposit (Figures 28-31), there are no identifiable spatial patterns for the tapir specimens found at the GFS. When compared to work done by Haynes (1985) and Lyman (1987), Figure 33 shows that the paleo-environment contained a natural population of tapirs whose remains accumulated due to attrition and not catastrophically. Haynes (1985) points out that if the population was in decline there would be a lack of young. However, as the data show, this is not true. Work done by Gibson (2011) along with remains of a pregnant female tapir (Hulbert et al. 2009), also suggests that the tapirs found at the GFS represented a “viable population” that lived close to the site. However, the discovery by Gibson (2011) that there is a timeline in which the epiphyses of various elements fuse for tapirs needs to be considered in future studies. Because the results here (Figure 33) agree with Gibson’s

studies, inclusion of his timeline may not change the interpretation of how these animals died. However, the spatial patterning of specimen age classes may change as more excavation is carried out at the GFS.

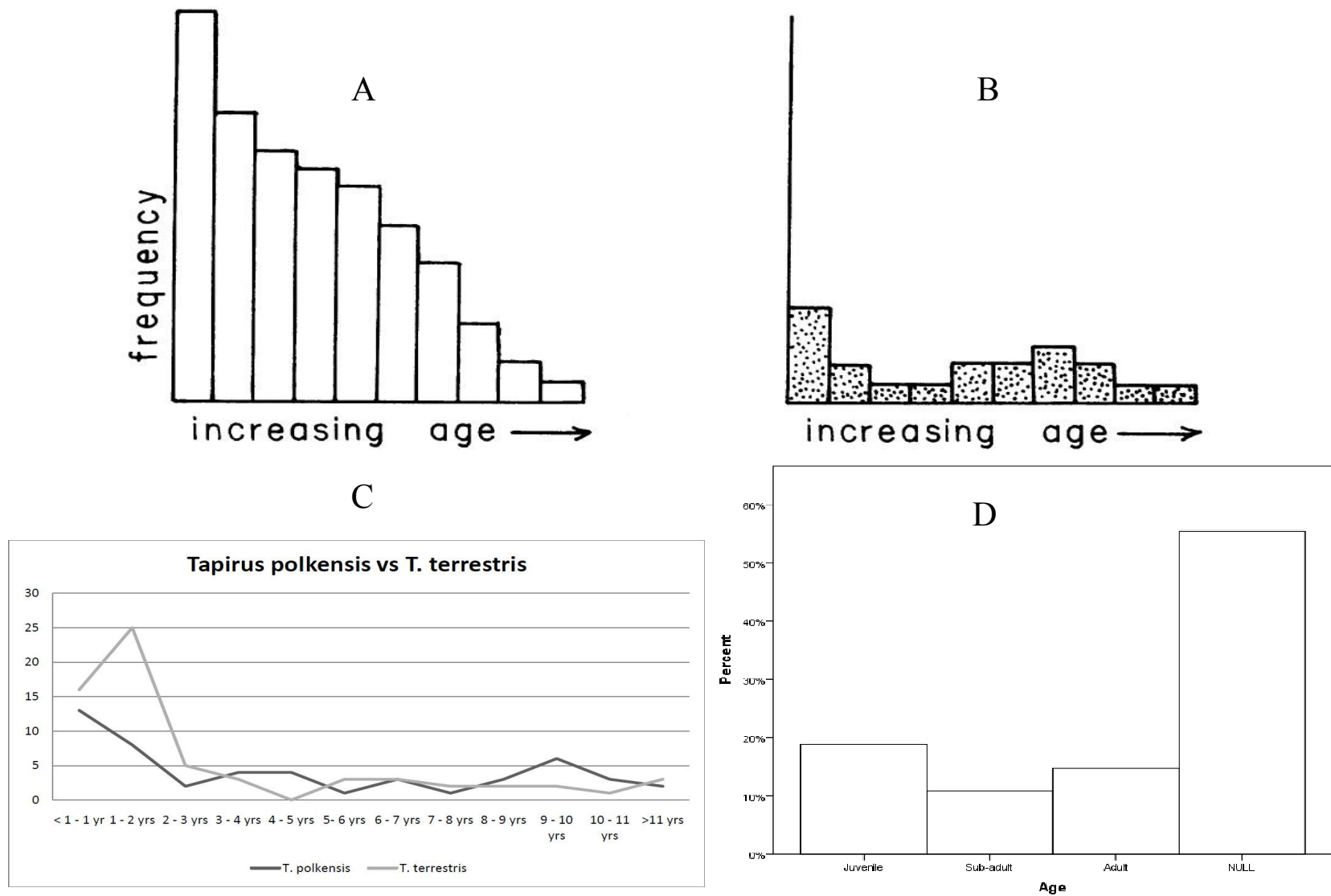


Figure 33: Comparison of age classification for A) catastrophic deposition and B) attritional deposition of carcasses (Lyman 1987) with the C) age profile developed by Gibson (2011) for the Gray Fossil Site and D) the age profile completed in this study.

CHAPTER 6

CONCLUSIONS

Taphonomic Interpretations

Upon completion of spatial analysis and mapping of the tapir bones at the GFS, it was found that 3 of the 6 attributes (weathering, arthritis, and articulation) studied for this project showed clustered patterning. Based on these results, the GFS is interpreted to be a natural ecological environment that hosted a stable population of tapirs, with the fossils being autochthonous or parautochthonous. Little influence from taphonomic processes affected the deposition of the bones, and this supports previous interpretations of the site by Wallace and Wang (2004), Shunk et al. (2006), DeSantis and Wallace (2008), and Gibson (2011). Predation or scavenging did occur at the GFS. Weathering stage patterns represent a series of microenvironments where burial occurred anywhere between a few months and years. None of the tapir bones exhibit signs of abrasion by either eolian or fluvial action, although the possibility of trampling and its effect on bone spatial distribution requires further study.

Although there was a clustered pattern of bones with high levels of arthritis, there does not seem to be any correlation with other taphonomic processes, suggesting that arthritis, in itself, was not a true taphonomic process at the GFS. Future study of arthritis among the tapir population could separate which individuals exhibit arthritis due to aging from those where growth of the bone occurred due to other pathological causes. Grouping of articulated and semi-articulated specimens in three main areas indicates that these were areas of passive deposition with disarticulation due more to decay of soft and connective tissue, as opposed to other processes such as carnivore utilization, scavenging or

transportation. Age class was not an influence on taphonomic processes and the distribution of specimens of differing ages appears to be random. Using the age profile that Gibson (2011) developed to reclassify tapir specimens might reveal a pattern between old aged tapirs and those with extreme or moderate levels of arthritis.

The methodology developed for this project proved adequate for determining spatial patterns for the GFS bones in both 2- and 3-dimensions. By using ESRI ArcGIS, the project was able to be conducted from the initial stages of database management and feature creation, to data analysis and visualization with only one GIS software package required. Although the project database was designed for *T. polkensis*, it can easily be adapted for use with other taxa, not only at the GFS but from other fossil sites. Using preexisting tools in the ESRI ArcToolbox and other pre-built modules, the nearest neighbor script was able to be written using python code. This allowed analysis of patterns to be determined in both 2- and 3-dimensions. However, the NN analysis proved not to be as important as expected due to the clustering bias created by the excavation process and the limited amount of exposed site area. 3D analysis also proved to be difficult as bones at different elevations lack stratigraphic and structural control within the site. Because they were clearly not all buried at the same time within the site they must be analyzed separately.

Future Work

This was the first true GIS analysis to be completed at the GFS using accurate survey data. This study should act as a platform for expansion and a guide to future development of fossil assemblage spatial analysis. The same methodology developed for this study can be used to study other GFS taxa. It could also be used to study

interspecific relationships, such as determining areas of the site where fish, reptiles, or mammals may dominate. However, before 3D analysis can be integrated into future analyses, it will be necessary to develop better stratigraphic controls for the site. Patterns within the database (data mining) and correlations among the various attributes and taphonomic classifications for each bone and specimen should be studied as well. This would provide more insight into how the site was formed.

In terms of spatial analysis, various other methods and spatial statistics could be developed for use with 3-dimensional features and implemented at the site. These include hotspot analysis to identify anomalous bone or specimen features; autocorrelation or Moran's I to indicate whether features within a data set are dependent or independent of each other; and Ripley's K function to allow greater than 1st order patterns (that at which NN operates) to be detected. Integration of the nearest neighbor program within ESRI ArcGIS must also be accomplished. This would improve ease of use, as well as implementation of error handling and minimum convex hull calculations. If this program is to be used with non-GFS data, where the data is not discrete and bounded by the extent of deposit, then edge effects must be accounted for in future use of the NN program. Further, development of a web-based GIS would allow it to be used by researchers with little experience in GIS. This would raise the status of the GFS and make it a showcase of how fossil sites might be studied by paleontologists, paleobotanists, and the public.

Recommendations for the Gray Fossil Site

After completing the database for this study from the collections at the GFS, it has come to the attention of the author that there are many improvements that can be made that would enhance future studies. Firstly, the survey data, once collected, were not

organized in any way except by year, making it difficult to identify which data belonged to which species. This issue could be remedied by linking the spatial data collected during surveying with the collections database, thus allowing quick identification of spatial data relevant to the taxon or specimen a researcher is working with. Secondly, there were many points that once projected and mapped during this study were in the wrong location, usually due to the wrong total station being used or being surveyed from the spoil pile. In order to make sure that these points do not exist among the correct spatial data set, and thus cause errors in analysis, it is important that every other day or maybe at the end of each week, all data collected from the previous time period are projected and mapped, allowing those erroneous points to be identified and corrected or deleted. Thirdly, it was also discovered that some specimens and individual ETMNHs in the collection were in fact composed of multiple specimens, apparent when the bones were classified into multiple age classes. To make attribute collection more accurate, these specimens must be sorted so that one attribute class can be given to each bone or each specimen. Fourthly, the attribute classification schemes created in this study, as well as those that will be developed in the future, should be implemented and used to classify each bone and specimen once they are removed from the sediment and before they are entered into the database. This will allow future research on the spatial patterns to be conducted without having to go through the entire collection and document each bone or specimen, making it easy to conduct the analysis developed here. Finally, this analysis and others that will hopefully be developed in the future should be completed periodically, so that new trends and patterns can be identified and that other problems with data collection can be identified and corrected.

REFERENCES

- Andrews, P. and Cook, J. 1985. Natural modifications to bones in a temperate setting. *Man*, 20:675-691.
- Aslan, A. and Behrensmeyer, A.K. 1996. Taphonomy and time resolution of bone assemblages in a contemporary fluvial system; the East Fork River, Wyoming. *Palaios*, 11:411-421.
- Badgley, C., Bartels, W.S., Morgan, M.E., Behrensmeyer, A.K., and Raza, S.M. 1995. Taphonomy of vertebrate assemblages from the Paleogene of northwestern Wyoming and the Neogene of northern Pakistan. *Palaeogeography, Paleoclimatology, Palaeoecology*, 115:157-180.
- Barber, G.M. 1988. *Elementary Statistics for Geographers*. Guilford Press, New York, New York.
- Barber, C.B., Dobkin, D.P., and Huhdanpaa, H. 1996. The quickhull algorithm for convex hulls. *ACM Transactions on Mathematical Software*, 22:469-483.
- Bartosiewicz, L. 2008. Taphonomy and palaeopathology in archaeozoology. *Geobios*, 41:69-77.
- Behrensmeyer, A.K. 1975. The taphonomy and paleoecology of Plio-Pleistocene vertebrate assemblages east of Lake Rudolf, Kenya. *Bulletin of the Museum of Comparative Zoology*, 146:473-578.
- Behrensmeyer, A.K. 1978. Taphonomic and ecologic information from bone weathering. *Paleobiology*, 4:150-162.
- Behrensmeyer, A.K. 1982. Time resolution in fluvial vertebrate assemblages. *Paleobiology*, 8:211-227.

- Behrensmeyer, A.K. and Hook, R.W. 1992. Paleoenvironmental contexts and taphonomic modes, p. 15-136. *In* Behrensmeyer, A.K., Damuth, J.D., DiMichele, W.A., Potts, R., Sues, H.D., and Wing, S.L. (ed.), *Terrestrial Ecosystems Through Time*. University of Chicago Press, Chicago.
- Behrensmeyer, A.K., Kidwell, S.M., and Gastaldo, R.A. 2000. Taphonomy and paleobiology. *Paleobiology*, 26:103-147.
- Binford, L.R. 1981. *Bones: Ancient Men and Modern Myths*. Academic Press, New York, New York.
- Bishop, M.A. 2010. Nearest neighbor analysis of mega-barchanoid dunes, Ar Rub' al Khali, sand sea: The application of geographical indices to the understanding of dune field self-organization, maturity and environmental change. *Geomorphology*, 120:186-194.
- Blumenschine, R.J., Marean, C.W., and Capaldo, S.D. 1996. Blind tests in inter-analyst correspondence and accuracy in the identification of cut marks, percussion marks, and carnivore tooth marks on bone surfaces. *Journal of Archaeological Science*, 23:493-507.
- Bock, W.J. and Atkins, E.G. 1970. A pseudoarthrosis in the forelimb of a sloth (*Choloepus didactylus*). *American Museum Novitates*, 2439:1-10.
- Bonfiglio, L. 1995. Taphonomy and depositional setting of Pleistocene mammal-bearing deposits from Acquedolci (north-eastern Sicily). *Geobios*, 28:57-68.
- Brain, C.K. 1967. Bone weathering and the problem of bone pseudo-tools. *South African Journal of Science*, 63:97-99.

- Brett, C.E. and Baird, G.C. 1986. Comparative taphonomy: A key to paleoenvironmental interpretation based on fossil preservation. *Palaios*, 1:207-227.
- Bunn, H.T. and Kroll, E.M. 1986. Systematic butchery by Plio-Pleistocene hominids at Olduvai Gorge, Tanzania. *Current Anthropology*, 27:431-452.
- Chew, A. and Oheim, K. 2009. Using GIS to determine the effects of two common taphonomic biases on vertebrate fossil assemblages. *Palaios*, 24:367-376.
- Childs, C. 2009. The top nine reasons to use a file geodatabase. *ArcUser*, Spring 2009:12-15.
- Choi, Y. and Park, H.D. 2006. Integrating GIS and 3D geostatistical methods for geotechnical characterization of soil properties. In Culshaw, M.G., Reeves, H.J., Jefferson, I. and Spink, T.W. (ed.) *Engineering Geology for Tomorrow's Cities*. Geological Society, London.
- Choirat, C. and Seri, R. 2009. Econometrics with python. *Journal of Applied Econometrics*, 24:698-704.
- Clapham, M.E., Narbonne, G.M., and Gehling, J.G. 2003. Paleoecology of the oldest known animal communities: Ediacaran assemblages at Mistaken Point, Newfoundland. *Paleobiology*, 29(4):527-544.
- Clark, P.J., and Evans, F.C. 1954. Distance to nearest neighbor as a measure of spatial relationships in populations. *Ecology*, 35:445-453.
- Clark, P.J. and Evans, F.C. 1979. Generalization of a nearest neighbor measure of dispersion for use in k dimensions. *Ecology*, 60:316-317.
- Coard, R. 1999. One bone, two bones, wet bones, dry bones: transport potentials under experimental conditions. *Journal of Archaeological Science*, 26:1369-1375.

- Colbert, M.W. and Schoch, R.M. 1998. Tapiroidea and other moropomorphs; p. 569-582.
In Janis, C.M., Scott, K.M., and Jacobs, L.L. (ed.), *Evolution of Tertiary Mammals of North America, Volume 1: Terrestrial Carnivores, Ungulates, and Ungulatelike Mammals*. Cambridge University Press, Cambridge.
- Conroy, G.C. 2006. Creating, displaying, and querying interactive paleoanthropological maps using GIS: An example from the Uinta Basin, Utah. *Evolutionary Anthropology*, 15:217-223.
- Cook, J. 1986. The application of scanning electron microscopy to taphonomic and archaeological problems. *In* Roe, D.A. (ed.), *Studies in the Upper Paleolithic of Britain and Northwest Europe. British Archaeological Reports International Series*, 296:143-163.
- Cyran, M., Lane, P., and Polk, J.P. 2010. Oracle database concepts 10g release 2.
http://download.oracle.com/docs/cd/B19306_01/server.102/b14220/toc.htm
- Denys, C. 2002. Taphonomy and experimentation. *Archaeometry*, 44:469-484.
- DeSantis, L.R.G., and Wallace, S.C. 2008. Neogene forests from the Appalachians of Tennessee, USA: Geochemical evidence from fossil mammal teeth.
Palaeogeography, Palaeoclimatology, Palaeoecology, 266:59-68.
- Dodd, J.R. and Stanton, R.J. 1981. *Paleoecology, concepts and applications* (second edition). John Wiley and Sons, New York.
- Downer, C.C. 2001. Observations on the diet and habitat of the mountain tapir (*Tapirus pinchaque*). *Journal of Zoology*, 254:279-291.
- Efremov, I. 1940. Taphonomy: New branch of paleontology. *Pan-American Geologist*, 74:81-93.

- Ellul, C. and Haklay, M. 2006. Requirements for topology in 3D gis. *Transactions in GIS*, 10:157-175.
- Fernandez-Jalvo, Y., Sanchez-Chillon, B., Andrews, P., Fernandez-Lopez, S., and Martinez, L.A. 2002. Morphological taphonomic transformations of fossil bones in continental environments, and repercussions on their chemical composition. *Archaeometry*, 44:353-361.
- Fernandez-Jalvo, Y. and Andrews, P. 2003. Experimental effects of water abrasion on bone fragments. *Journal of Taphonomy*, 1:147-163.
- Fiorillo, A.R. 1989. An experimental study of trampling: Implications for the fossil record, p. 61-72. In Bonnichsen, R. and Sorg, M.H. (ed.), *Bone Modification*. Institute for Quaternary Studies, University of Maine.
- Foerester, C.R. and Vaughan, C. 2002. Home range, habitat use, and activity of Baird's tapir in Costa Rica. *Biotropica*, 34:423-437.
- Froehlich, D.J. 1999. Phylogenetic systematics of basal perissodactyls. *Journal of Vertebrate Paleontology*, 19:140-159.
- Gandhi, V., Kang, J.M., and Shekhar, S. 2008. *Wiley Encyclopedia of Computer Science and Engineering*. John Wiley and Sons, New York.
- Gibson, M.L. 2011. Population structure based on age-class distribution of *Tapirus polkensis* from the Gray Fossil Site, Tennessee. M.S. thesis (unpublished), East Tennessee State University, Johnson City, TN.
- Gifford, D.P. 1981. Taphonomy and paleoecology: A critical review of archaeology's sister disciplines, p. 365-438. In Schiffer, M.B. (ed.), *Advances in Archaeological method and theory*. Academic Press, New York.

- Gold, C. 2008. Working group III position paper: Modelling 3D geo-information, p. 429-433. *In* van Oosterom, P., Zlatanova, S., Penninga, F., and Fendel, E.M. (ed.), *Advances in 3D Geoinformation Systems*. Springer, Berlin, Heidelberg, New York.
- Gray, J.E. 1821. On the natural arrangement of the vertebrate animals. *London Medical Repository*, 15:296-310.
- Greer, M., Greer, J.K., and Gillingham, J. 1977. Osteoarthritis in selected wild mammals. *Proceedings of the Oklahoma Academy of Science*, 57:39-43.
- Grossman, J.D. 1938. *Anatomy of Domestic Animals*. (third edition revised). Philadelphia and London: W. B. Saunders Company.
- Guting, R.H. 1994. An introduction to spatial database systems. *The VLDB Journal*, 3:357-399.
- Haynes, G. 1982. Utilization and skeletal disturbances of North American prey carcasses. *Arctic*, 35:266-281.
- Haynes, G. 1983. A guide for differentiating mammalian carnivore taxa responsible for gnaw damage to herbivore limb bones. *Paleobiology*, 9:164-172.
- Haynes, G. 1985. Age profiles in elephant and mammoth bone assemblages. *Quaternary Research*, 24:333-345.
- Haynes, G. 1988. Mass deaths and serial predation: Comparative taphonomic studies of modern large mammal death sites. *Journal of Archaeological Science*, 15:219-235.
- Hetland, M.L. 2005. *Beginning Python: From Novice to Professional*. Apress, Berkeley, California.

- Hill, A. 1979. Disarticulation and scattering of mammal skeletons. *Paleobiology*, 5:261-274.
- Hill, A. and Behrensmeyer, A.K. 1984. Disarticulation patterns of some modern East African mammals. *Paleobiology*, 10:366-376.
- Hulbert, R.C., Wallace, S.C., Klippel, W.E., and Parmalee, P.W. 2009. Cranial morphology and systematics of an extraordinary sample of the late Neogene dwarf tapir *Tapirus polkensis* (Olsen). *Journal of Paleontology*, 83(2):238-262.
- Jennings, D.S. and Hasiotis, S.T. 2006. Taphonomic analysis of a dinosaur feeding site using geographic information systems (GIS), Morrison Formation, southern Bighorn Basin, Wyoming, USA. *Palaios*, 21:480-492.
- Katsianis, M., Tshipidis, S., Kotsakis, K., and Kousoulakou, A. 2008. A 3D digital workflow for archaeological intra-site research using GIS. *Journal of Archaeological Science*, 35:655-667.
- Kidwell, S.M., Fursich, F.T., and Aigner, T. 1986. Conceptual framework for the analysis and classification of fossil concentration. *Palaios*, 1:228-238.
- Klein, R.G. and Cruz-Urbe, K. 1984. *The Analysis of Animal Bones from Archaeological Sites*. University of Chicago Press, Chicago.
- Knight, J. 2011. An interactive web mapping application for alternative and renewable energies in North Carolina. M.S. thesis (unpublished), North Carolina State University, Raleigh, NC.
- Koller, D., Lindstrom, P., Ribarsky, W., Hodges, L.F., Faust, N., and Turner, G. 1995. Virtual GIS: A real-time 3D geographic information system. *Proceedings of the 6th IEEE Visualization Conference* (Visualization '95):94-100.

- Kvamme, K.L. 1995. A view from across the water: the North American experience in archaeological GIS. In Lock, G. and Stancic, Z. (ed.), *Archaeology and Geographical Information Systems*. Taylor and Francis Ltd., Bristol, Pennsylvania.
- Lawrence, D.R. 1968. Taphonomy and information losses in fossil communities. *Geological Society of America Bulletin*, 79:1315-1330.
- Lee, J. 2008. Working group IV position paper: Spatial data analysis in 3D GIS, p. 435-438. In van Oosterom, P., Zlatanova, S., Penninga, F., and Fendel, E.M. (ed.), *Advances in 3D Geoinformation Systems*. Springer, Berlin, Heidelberg, New York.
- Lizcano, D. J. and Cavelier, J. 2000. Daily and seasonal activity of the mountain tapir (*Tapirus pinchaque*) in the Central Andes of Colombia. *Journal of Zoology*, 252: 429-435.
- Lizcano, D. J., Pizarro, V., Cavelier, J., and Carmona, J. 2002. Geographic distribution and population size of the mountain tapir (*Tapirus pinchaque*) in Colombia. *Journal of Biology*, 29:7-15.
- Lyman, R.L. 1987. On the analysis of vertebrate mortality profiles: Sample size, mortality type, and hunting pressure. *American Antiquity*, 52:125-142.
- Lyman, R.L. 1994. *Vertebrate Taphonomy*. Cambridge University Press, New York.
- Lyman, R.L. and Fox, G.L. 1989. A critical evaluation of bone weathering as an indication of bone assemblage formation. *Journal of Archaeological Science*, 16:293-317.

- Maffei, L. 2003. The age structure of Tapirs (*Tapirus terrestris*) in the Chaco. *Newsletter of the IUCN/SSC Tapir Specialist Group*, 12:18-19.
- Miller, G.J. 1975. A study of cuts, grooves, and other marks on recent and fossil bone: II. Weathering, cracks, fractures, splinters, and other similar natural phenomenon, p. 211-226. In Swanson, E.H. (ed.), *Lithic Technology*. Mouton, Berlin, New York.
- Murray, C., Abugov, D., Alexander, N., Blackwell, B., Chatterjee, R., Geringer, D., Horhammer, M., Hu, Y., Kazar, B., Kothuri, R., Ravada, S., Wang, J., and Yang, J. 2010. Oracle spatial developer's guide 11g release 2. Oracle, Redwood, California.
http://download.oracle.com/docs/cd/E11882_01/appdev.112/e11830/toc.htm
- Nave, J.W., Ali, T.A., and Wallace, S.C. 2005. Developing a GIS database for the Gray Fossil Site, Tennessee, based on modern surveying. *Surveying and Land Information Science*, 65:259-264.
- Nigro, J.D., Ungar, P.S., de Ruiter, D.J., and Berger, L.R. 2003. Developing a geographic information system (GIS) for mapping and analyzing fossil deposits at Swartkrans, Gauteng Province, South Africa. *Journal of Archaeological Science*, 30:317-324.
- Noss, A.J., Cuellar, R.L., Barrientos, J., Maffei, L., Cuellar, E., Arispe, R., Rumiz, D., and Rivero, K. 2003. A camera trapping and radio telemetry study of lowland tapir (*Tapirus terrestris*) in Bolivian dry forests. *Tapir Conservation*, 12:24-32.
- Njau, J.K. and Blumenschine, R.J. 2006. A diagnosis of crocodile feeding traces on larger mammal bone, with fossil examples from the Plio-Pleistocene Olduvai Basin, Tanzania. *Journal of Human Evolution*, 50:142-162.

- Oliphant, T.E. 2007. Python for scientific computing. *Computing in Science and Engineering*, 9:10-20.
- Olsen, S.L. and Shipman, P. 1988. Surface modification on bone: trampling versus butchery. *Journal of Archaeological Science*, 15:535-553.
- Owen, R. 1848. Description of teeth and portions of jaws of two extinct anthracotheroid quadrupeds (*Hyopotamus vectianus* and *Hyopbovinus*) discovered by the Marchioness of Hastings in the Eocene deposits on the north-west coast of the Isle of Wight: with an attempt to develop Cuvier's idea of the classification of pachyderms by the number of their toes. *Quarterly Journal of the Geological Society*, 4:103-141.
- Parmalee, P.W., Klippel, W.E., Meylan, P.A., and Holman, J.A. 2002. A Late Miocene-Early Pliocene population of *Trachemys* (Testudines: Emydidae) from east Tennessee. *Annals of Carnegie Museum of Natural History*, 71:233-239.
- Peterson, R.O. 1988. Increased osteoarthritis in moose from Isle Royale. *Journal of Wildlife Diseases*, 24:461-466.
- Radinsky, L.B. 1966. The adaptive radiation of the phenacodontid condylarths and the origin of the Perissodactyla. *Evolution*, 20:408-417.
- Rothschild, B.M. and Rothschild, C. 1994. No laughing matter: Spondyloarthropathy and osteoarthritis in Hyaenidae. *Journal of Zoo and Wildlife Medicine*, 25:259-263.
- Salas, L.A. 1996. Habitat use by lowland tapirs (*Tapirus terrestris* L.) in the Tabaro River valley, southern Venezuela. *Canadian Journal of Zoology*, 74:1452-1458.

- Schon, B., Laefer, D.F., Morrish, S.W., and Bertolotto, M. 2009. Three-dimensional spatial information systems: State of the art review. *Recent Patents on Computer Science*, 2:21-31.
- Schubert, B.W., and Wallace, S.C. 2006. Amphibians and reptiles of the Mio-Pliocene Gray Fossil Site and their paleoecologic implications. *Journal of Vertebrate Paleontology*, 26:122A.
- Scott, L.M. and Janikas, M.V. 2010. Spatial statistics in ArcGIS, p. 27-41. In Fischer, M.M., and Getis, A. (ed.), *Handbook of Applied Spatial Analysis: Software Tools, Methods and Applications*. Springer, Verlag, Berlin, Heidelberg.
- Shipman, P. and Rose, J. 1983. Bone tools: An experimental approach, p. 303-335. In Olsen, S. (ed.), *Scanning Electron Microscopy in Archaeology*. British Archaeological Reports International Series 452.
- Shunk, A.J., Driese, S.G., and Clark, G.M. 2006. Latest Miocene to earliest Pliocene sedimentation and climate record derived from paleosinkhole fill deposits, Gray Fossil Site, northeastern Tennessee, U.S.A. *Palaeogeography, Palaeoclimatology, Palaeoecology*, 231:265-278.
- Silk, J. 1979. *Statistical Methods in Geography*. Sage Publications, London.
- Sorg, M.H. and Haglund, W.D. 2002. Advancing forensic taphonomy: Purpose, theory, and practice, p. 3-30. In Haglund, W.D., and Sorg, M.H. (ed.), *Advances in Forensic Taphonomy: Method, Theory, and Archaeological Perspectives*. CRC Press, Boca Raton, Florida.
- Tappen, M. 1994. Bone weathering in the tropical rain forest. *Journal of Archaeological Science*, 21:667-673.

- Thompson, C.E., Ball, S., Thompson, T.J., and Gowland, R. 2011. The abrasion of modern and archaeological bones by mobile sediments: the importance of transport modes. *Journal of Archaeological Science*, 38:784-793.
- Tobler, M.W. 2002. Habitat use and diet of Baird's tapirs (*Tapirus bairdii*) in a montane cloud forest of the Cordillera de Talamanca, Costa Rica. *Biotropica*, 34:468-474.
- Tobler, M.W. 2008. The ecology of the lowland tapir in Madre de Dios, Peru: using new technologies to study large rainforest mammals. Ph. D. dissertation, Texas A&M University, College Station, Texas.
- Toots, H. 1965. Sequence of disarticulation in mammalian skeletons. *Rocky Mountain Geology*, 4:37-39.
- Valentine, J.W. and Peddicord, R.G. 1967. Evaluation of fossil assemblages by cluster analysis. *Journal of Paleontology*, 41:502-507.
- van Rossum, G. 1997. *Python Library Reference*. Stichting Mathematisch Centrum, Amsterdam.
- Wallace, S.C. 2004. Reconstructing the past: Applications of surveying and GIS to fossil localities. *Proceedings of the Annual Meeting for the American Congress on Surveying and Mapping, Tennessee Association of Professional Surveyors, Nashville*:1-12.
- Wallace, S.C., and Wang, X. 2004. Two new carnivores from an unusual late Tertiary forest biota in eastern North America. *Nature*, 431:556-559.
- Washburn, D.K. 1974. Nearest neighbor analysis of Pueblo I-III settlement patterns along the Rio Puerco of the East, New Mexico. *American Antiquity*, 39:315-335.

- Whitelaw, J.L., Mickus, K., Whitelaw, M.J., and Nave, J. 2009. High resolution gravity study of the Gray Fossil Site. *Geophysics*, 73:B25-B32.
- Williams, K.D., and Petrides, G.A. 1980. Browse use, feeding behavior, and management of the Malayan tapir. *Journal of Wildlife Management*, 44:489-494.
- Wilson, M.V.H. 1988. Taphonomic processes: Information loss and information gain. *Geoscience Canada*, 15:131-148.
- Wong, D.W.S. and Lee, J. 2005. *Statistical Analysis of Geographic Information with ArcView GIS and ArcGIS*. John Wiley and Sons, New York.
- Worboy, M.F. and Duckham, M. 2004. *GIS: A Computing Perspective* (second edition). CRC Press, Boca Raton, Florida.
- Wu, C.W. and Kalunian, K.C. 2005. New developments in osteoarthritis. *Clinics in Geriatric Medicine*, 21:589-601.
- Zlatanova, S., Rahman, A.A., and Pilouk, M. 2002. Trends in 3D GIS development. *Journal of Geospatial Engineering*, 4:1-10.

APPENDIX

Python Script Used to Calculate Nearest Neighbor Statistic

```
# Nearest Neighbor Statistic
# Created by:
#           Winn Ketchum
#           Department of Geosciences
#           East Tennessee State University
#           Johnson City, TN 37614
# Description: A statistical program that calculates the nearest neighbor
#              statistic for a group of points in both 2- and 3- dimensions.
# Parameters:          NAME          DESCRIPTION
#                    inputfc        Group of points to be analyzed
#                    near           Features nearest to input points
#                    output         CSV file calculations are saved to
#                    area          2D area of study site
#                    volume         3D volume of study site
#-----

# Modules Imported
from __future__ import division
import locale as LOCALE
import arcpy as arc
import SSUtilities as SSU
import csv
import Stats as STATS

# Input Parameters
inputfc = "E:\Analysis of Thesis Extraordinaire\Shapefiles\Specimens\Specimens.shp"
near = "E:\Analysis of Thesis Extraordinaire\Shapefiles\Specimens\Specimens.shp"
area = 7851.0841
volume = 36798.51

# 3D Analyst Function Used
arc.CheckOutExtension("3D")
arc.Near3D_3d(inputfc, near, "", "NO_LOCATION", "NO_ANGLE", "NO_DELTA")

# Observed NN Variables
cnt = SSU.getCount(inputfc)
sumNN = 0
sumTDNN = 0
rows = arc.SearchCursor(inputfc, "", "", "NEAR_DIST;NEAR_DIST3")
for row in rows:
    NN = row.NEAR_DIST
    TDNN = row.NEAR_DIST3
    sumNN += NN
    sumTDNN += TDNN

# Observed NN Calculations
ObsMeanNearDist = sumNN/cnt
ObsMeanNearDist3D = sumTDNN/cnt
```



```

# Expected NN Calculations
ExpMeanNearDist = 1.0 / (2.0 * ((cnt / area)**0.5))
ExpMeanNearDist3D = 0.55396 / (((cnt / volume)**(1/3)))

# Standard Error Calculations
standError = 0.261362 / ((cnt**2 / area)**0.5)
standError3D = (0.201335 * volume**(1/3))/(cnt**(5/6))

# NN Index Calculation
NNratio = ObsMeanNearDist / ExpMeanNearDist
NNratio3D = ObsMeanNearDist3D / ExpMeanNearDist3D

# NN Standard Deviation Calculation
Zvalue = (ObsMeanNearDist - ExpMeanNearDist) / standError
Zvalue3D = (ObsMeanNearDist3D - ExpMeanNearDist3D) / standError3D

# Significance Test
pvalue = STATS.zProb(Zvalue, type = 2)
pvalue3D = STATS.zProb(Zvalue3D, type = 2)

# Output Calculated Value Formatting
ObsOut = LOCALE.format("%0.6f", ObsMeanNearDist)
Obs3dOut = LOCALE.format("%0.6f", ObsMeanNearDist3D)
ExpOut = LOCALE.format("%0.6f", ExpMeanNearDist)
Exp3dOut = LOCALE.format("%0.6f", ExpMeanNearDist3D)
ratOut = LOCALE.format("%0.6f", NNratio)
rat3dOut = LOCALE.format("%0.6f", NNratio3D)
ZvalOut = LOCALE.format("%0.6f", Zvalue)
Zval3dOut = LOCALE.format("%0.6f", Zvalue3D)
pValOut = LOCALE.format("%0.6f", pvalue)
pVal3dOut = LOCALE.format("%0.6f", pvalue3D)

# Output File Creation
outTable = open(output,'w')
outTable.write(["NNValue", "2-Dimensions", "3-Dimensions"])
outTable.writerow("\n["Observed Mean Distance", ObsOut, Obs3dOut])
outTable.writerow("\n["Expected Mean Distance", ExpOut, Exp3dOut])
outTable.writerow("\n["Nearest Neighbor Ratio", ratOut, rat3dOut])
outTable.writerow("\n["Z-Value", ZvalOut, Zval3dOut])
outTable.writerow("\n["P-Value", pValOut, pVal3dOut])
outTable.close()

```

VITA

WINN A. KETCHUM

- Education: B.S. Geology with GIS Emphasis, Northern Arizona University, Flagstaff, Arizona 2008
- M.S. Geosciences, East Tennessee State University, Johnson City, Tennessee 2011
- Professional Experience: Biological Technician, U.S. Fish & Wildlife Service National Elk Refuge, Summers 2009-2010
- Graduate Assistant, East Tennessee State University, College of Arts and Sciences, 2009-2011
- GIS Research Analyst, East Tennessee State University, Department of Geosciences, June 2011 – September 2011
- Publications: Ketchum, W. A. 2011. Using geographical information systems to investigate spatial patterns of the extinct *Tapirus polkensis* at the Gray Fossil Site, Pp. 41-42. In Schubert, B.W. and Mead, J.I. (ed.) *Gray Fossil Site: 10 Years of Research*. West Press, Tucson, Arizona.
- Ketchum, W.A. 2011. Using GIS to analyze spatial distribution and taphonomic processes of the extinct tapir *Tapirus polkensis* at the Gray Fossil Site, Gray, Tennessee. *Geological Society of America Abstracts with Programs*, 43(2):25.
- Conferences: The Role of GIS in Decision Making, Southern Appalachian Conference on GIS, East Tennessee State University: “Applying GIS mapping techniques and analysis to the tapir species, *Tapirus polkensis*, at the Gray Fossil Site, Gray, Tennessee”, September 6, 2011

Association of American Geographers Annual Meeting,
Seattle Washington: Presenter “Developing 3D nearest
neighbor analysis through the study of spatial patterns
inherent to fossils of the extinct species *Tapirus polkensis*
at the Gray Fossil Site, Washington County, Tennessee”
April 15, 2011

Geological Society of America Southeast Section 60th
Annual Meeting, Wilmington North Carolina: Presenter
“Using GIS to analyze spatial distribution and taphonomic
processes of the extinct tapir *Tapirus polkensis* at the Gray
Fossil Site, Gray, Tennessee” March 23-25, 2011

Honors and Awards:

Department of Biological Sciences Travel Grant, 2011

Don Sundquist Center for Excellence in Paleontology
Travel Grant, 2011

Graduate and Professional Student Association Travel
Grant, 2011

Nominated for NAGT/USGS 2009 Cooperative Summer
Field Training Program

Professional Affiliations:

ETSU Graduate and Professional Student Association

Don Sundquist Center for Excellence in Paleontology

Association of American Geographers

Geological Society of America